Progress in Polymer Science 36 (2011) 1443–1498

Contents lists available at ScienceDirect

Progress in Polymer Science

journal homepage: www.elsevier.com/locate/ppolysci

# Sulfonated hydrocarbon membranes for medium-temperature and low-humidity proton exchange membrane fuel cells (PEMFCs)

Chi Hoon Park[a,1], Chang Hyun Lee[b,1], Michael D. Guiver[a,c], Young Moo Lee[a,*]

[a] WCU Department of Energy Engineering, Hanyang University, Seoul 133-791, Republic of Korea
[b] Macromolecules and Interfaces Institute, Virginia Polytechnic Institute and State University, Blacksburg, VA 24061, USA
[c] Institute for Chemical Process & Environmental Technology, National Research Council, Ottawa, Ontario, K1A 0R6, Canada

ARTICLE INFO

*Article history:*
Received 1 February 2011
Received in revised form 27 March 2011
Accepted 27 March 2011
Available online 6 June 2011

*Keywords:*
Proton exchange membrane fuel cell (PEMFC)
Sulfonated hydrocarbon polymers
Sulfonation
Polymer architecture
Physico-chemical tuning technology

ABSTRACT

This review summarizes efforts in developing sulfonated hydrocarbon proton exchange membranes (PEMs) with excellent long-term electrochemical fuel cell performance in medium-temperature and/or low-humidity proton exchange membrane fuel cell (PEMFC) applications. Sulfonated hydrocarbon PEMs are alternatives to commercially available perfluorosulfonic acid ionomers (PFSA, e.g., Nafion®) that inevitably lose proton conductivity when exposed to harsh operating conditions. Over the past few decades, a variety of approaches have been suggested to optimize polymer architectures and define post-synthesis treatments in order to further improve the properties of a specific material. Strategies for copolymer syntheses are summarized and future challenges are identified. Research pertaining to the sulfonation process, which is carried out in the initial hydrocarbon PEM fabrication stages, is first introduced. Recent synthetic approaches are then presented, focusing on the polymer design to enhance PEM performance, such as high proton conductivity even with a low ion exchange capacity (IEC) and high dimensional stability. Polymer chemistry methods for the physico-chemical tuning of sulfonated PEMs are also discussed within the framework of maximizing the electrochemical performance of copolymers in membrane-electrode assemblies (MEAs). The discussion will cover crosslinking, surface fluorination, thermal annealing, and organic–inorganic nanocomposite approaches.

## Contents

---

[*] Corresponding author. Tel.: +82 2 2220 0525; fax: +82 2 2291 5982.
*E-mail address:* ymlee@hanyang.ac.kr (Y.M. Lee).

[1] These authors contributed equally to this work.

0079-6700/$ – see front matter © 2011 Elsevier Ltd. All rights reserved.
doi:10.1016/j.progpolymsci.2011.06.001

**Nomenclature**

| | |
|---|---|
| 6F-BPA | 4,4′-hexafluoroisopropylidene bisphenol |
| 6FCN | disulfonated poly(arylene ether benzonitrile) copolymer containing 6F-BPA |
| AFM | atomic force microscopy |
| BAPFDS | 9,9-bis(4-aminophenyl)fluorene-2,7-disulfonic acid |
| BDSA | 4,4′-diamino-biphenyl 2,2′-disulfonic acid |
| BES | N,N-bis(2-hydroxyethyl)-2-aminoethanesulfonic acid |
| BPS | biphenol-based SPAES copolymer in salt form synthesized by McGrath et al. |
| BPSH | biphenol-based SPAES copolymer in proton form synthesized by McGrath et al. |
| CLPE | cross-linked high-density polyethylene substrate |
| DBSA | 4-dodecylbenzene sulfonic acid |
| DCDPS | 4,4′-dichlorodiphenyl sulfone |
| DMFC | direct methanol fuel cell |
| DOE | Department of Energy |
| DP | diphenol |
| DS | degree of sulfonation or sulfonation degree |
| FDA | 4,4′-(9-fluorenylidene) dianiline |
| FPEB | 4-fluoro-4-phenylethynyl benzophenone |
| HC-MEA | sulfonated hydrocarbon PEM-based MEA |
| HFR | high-frequency resistance |
| IEC | ion exchange capacity |
| IEP | isoelectric point |
| MEA | membrane-electrode assembly |
| NMP | N-methyl-2-pyrrolidinone |
| OBBA | 4,4′-oxybis(benzoic acid) |
| ODADS | 4,4′-diaminodiphenyl ether-2,2′-disulfonic acid |
| PAA | poly(acrylic acid) |
| PAAVS | poly(acrylic acid-co-vinylsulfonic acid) |
| PAE | poly(arylene ether) |
| PAES | poly(arylene ether sulfone) |
| PATBS | poly(acrylamide-*tert*-butylsulfonic acid) |
| PBI | polybenzimidazole |
| PC | polycarbonate |
| PEEK | poly(ether ether ketone) |
| PEFC | polymer electrolyte fuel cell |
| PEK | poly(ether ketone) |
| PEM | proton exchange membrane or polymer electrolyte membrane |
| PEMFC | proton exchange membrane fuel cell |
| PEO | poly(ethylene oxide) |
| PFSA | perfluorosulfonic acid or perfluorinated sulfonic acid |
| PPh | polyphosphazene |
| PPO | poly(phenylene oxide) |
| PS | polystyrene |
| PSf | polysulfone |
| PSK | poly(sulfide ketone) |
| PSSA-MA | poly(styrene sulfonic acid-co-maleic acid) |
| PTFE | polytetrafluoroethylene |
| PVA | poly(vinyl alcohol) |
| PVdF | polyvinylidene fluoride |
| RH | relative humidity |
| SA-DADPS | 3,3′-disulfonic acid-bis [4-(3-aminophenoxy)phenyl]sulfone |
| SEBS | styrene–ethylene–butylene–styrene |
| SPAE | sulfonated poly(arylene ether) |
| SPAEEN | sulfonated poly(arylene ether ether nitrile) |
| SPAEK | sulfonated poly(aryl ether ketone) |
| SPAEN | sulfonated poly(arylene ether nitrile) |
| SPAES | sulfonated poly(arylene ether sulfone) |
| SPAESK | sulfonated poly(arylene ether sulfone ketone) |
| SPEEK | sulfonated poly(ether ether ketone) |
| SPEFC | solid-polymer electrolyte fuel cell |
| SPEK | sulfonated poly(ether ketone) |
| SPI | sulfonated polyimide |
| SPPh | sulfonated polyphosphazene |
| SPPSf | sulfonated poly(phenylene sulfone) |
| SPPSSf | sulfonated poly(phenylene sulfide sulfone) |
| SPPSSfN | sulfonated poly(phenylene sulfide sulfone nitrile) |

| | |
|---|---|
| SPS | sulfonated polystyrene |
| SSA | sulfosuccinic acid |
| TEM | transmission electron microscope |
| $T_g$ | glass transition temperature |
| ZrP | zirconium phosphate |

## 1. Introduction

Many countries are developing eco-friendly energy sources as an alternative to fossil fuels. Such development has been accelerated by the instability of oil prices and frequent natural disasters caused by global climate change [1–3]. Fuel cells are regarded as a promising alternative energy conversion device for both mobile and stationary applications. These cells generate water, heat, and electricity without emitting pollutants via an electrochemical reaction with hydrogen as a fuel and oxygen in the air as an oxidant [4–6]. Although hydrogen is still derived mainly from fossil fuel, energy circulation system with zero pollutant-emission may be accomplished by fuel cell using hydrogen produced from renewable energy sources in the near future. Among the various fuel cell types, proton exchange membrane fuel cells (PEMFCs), also called polymer electrolyte fuel cells (PEFCs) or solid-polymer electrolyte fuel cells (SPEFCs), are a type of fuel cell where proton conductive membranes (i.e., proton exchange membranes (PEMs)) are used as an electrolyte [7,8]. The main advantage of PEMFCs is that they allow for the use of thin polymer electrolytes. Such thin PEMs are effective in providing a short pathway for ion transport from one electrode to the other, which directly improves fuel cell performance by reducing cell resistance. Thin electrolytes can also reduce the total volume and weight of a fuel cell stack system. Polymer electrolytes can be easily utilized because of the absence of leakage problems that are encountered with liquid electrolytes. Due to these advantages, PEMFCs have been widely studied as mobile power sources for transportation applications such as a fuel cell car, and portable electronic devices such as mobile phones and notebook computers.

Despite their limited capacity and need for frequent recharging, lithium ion batteries are currently still the primary power supplies used for small-size portable electronic devices, which only consume a small amount of power. Accordingly, there have been less intensive efforts towards the commercialization of portable PEMFC systems. However, in transportation battery power applications, a recharging time of about 20 min is needed. It is thus impossible to implement the current battery-only-type power sources such as lithium ion batteries in transportation applications because they require charging from an external electric supply source for a long period of time (e.g., a few hours). Direct fueling-type power sources, such as internal combustion engines, are instead needed to reduce recharging or fueling time. Since transportation consumes a large amount of power, power sources should have an adequately long operating time between refueling to allow the current vehicle range of distance. PEMFCs are expected to be desirable transportation power sources due to their high efficiency and energy density per volume and weight. In addition, many countries have encouraged automobile companies to develop eco-friendly fuel cell cars by phasing in environmental regulations related to vehicle emissions and fuel efficiency.

PEMFCs are classified into three categories depending on their operating temperatures: high-temperature PEMFCs over 120 °C, medium-temperature PEMFCs from 70 °C to 120 °C, and low-temperature PEMFCs below 70 °C. High-temperature PEMFCs are generally operated under non-humidified conditions because water boils at 100 °C. Low-mid temperature PEMFCs are operated either under fully humidified conditions below 100 °C or under reduced humidity conditions over 100 °C. Under high-temperature/non-humidified conditions, catalyst poisoning from carbon monoxide (CO) impurities in fuels becomes less serious because catalyst activity is improved at elevated temperatures. This enables the use of fuels with less stringent purity requirements. Furthermore, the complexity and overall size of PEMFC systems can be reduced due to the absence of large humidifiers and the adoption of smaller cooling systems [9]. However, high operating temperatures can lead to the thermal degradation of PEMFC components. In addition, the electrochemical performance of high-temperature PEMFCs is currently too low for their adoption in commercially available transportation systems. In contrast, conventional PEMFCs operated under low temperature/fully humidified conditions exhibit high electrochemical performance. Unfortunately, PEMFCs operating at low temperature and high humidity require high-quality CO-free fuels and additional water management systems, including humidifiers. Therefore, PEMFC systems operating in the medium temperature range and at reduced humidity are being extensively studied, particularly in the field of transportation [10].

To select appropriate PEMs for use in PEMFCs, it is necessary to understand the proton transport mechanisms in PEMs. In general, protons within PEMs are transported through water channels in complex forms associated with water molecules such as $H_3O^+$, $H_5O_2{}^+$, and $H_9O_4{}^+$ (i.e., the vehicle mechanism [11]). The protons are transferred by "forming and breaking hydrogen bonds with proton accepting media such as water or phosphoric acid" and by "inter molecular proton transfer" (i.e., the Grotthuss mechanism or hopping mechanism) [12–19]. The vehicle mechanism is believed to be the dominant proton transport mechanism in low-mid temperature PEMs at low degrees of hydration. The Grotthuss mechanism can also be present in low-mid temperature PEMs at high levels of hydration since water molecules can act as proton accepting media. The Grotthuss mechanism also provides insight on proton transport through PEMs operating at high temperatures and under non-humidified conditions, because some liquids with hydrogen bonding sites (such as phosphoric acid, imidazole and triazole) can act as proton accepting media with high degree of self dissociation [9,20–23]. PEMs for each operating condition have thus been developed by considering both transport mechanisms. The focus of this review is medium-temperature PEMs, which are

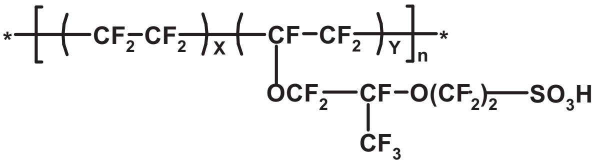

Fig. 1. Chemical structure of Nafion®.

generally designed to have water channels that are formed by the hydrophilic characteristics of polymer matrices. Hydrophilicity in polymers can generally be achieved by introducing acid functionalities such as sulfonic acid, carboxylic acid, and phosphoric acid in polymer backbones. Among the acid candidates, sulfonic acid groups are by far most commonly employed [24–29]. In addition, due to their low p*K*a values (i.e., high acidity), sulfonic acid groups are most widely used in PEMs. There are two methods of introducing sulfonic acid groups into polymer matrices: direct copolymerization of sulfonated monomers (the monomer sulfonation method) and the polymer sulfonation method (or post-sulfonation method). In this review, both methods will be discussed and progress in PEM materials development will be detailed. In addition to sulfonic acid groups, other acid functional groups such as phophophonic acid [29–31] and sulfonamide [32,33] have been used to impart hydrophilicity in polymers.

Nafion®, manufactured by DuPont™ (see Fig. 1) is the most well-known PEM with acid functional groups. Research regarding PEMFCs began with the Gemini space program in the 1960s. The first membrane was a sulfonated polymer based on polystyrene-divinylbenzene, which exhibited a very short lifetime due to the susceptibility of its backbone to radical attack (i.e., poor oxidative stability). Nafion®, a perfluorinated sulfonic acid (PFSA) membrane, was utilized in PEMFC to overcome such a weakness. While Nafion® membranes were originally developed for the chloroalkali permselective membranes, they have been widely used in PEMFCs because of their excellent chemical and oxidative stability derived from their perfluorinated backbone [27,34]. Despite the low ion exchange capacity (e.g., IEC of Nafion® 112 = 0.9 mequiv. $g^{-1}$), Nafion® PFSA membranes have a high acidity due to the electron-withdrawing characteristics of fluorine atoms around the terminal sulfonic acid groups on the side chains [16,35–38]. PFSA membranes also form water channels effectively, despite the low water uptake, as a result of the strong phase separation between extremely hydrophobic backbones and hydrophilic side chains (Fig. 2(a)) [12,16,38–40]. In particular, the flexibility of the acidic side chains allows the ready formation of water channel [38]. Consequently, PFSA membranes display high proton conductivity and dimensional stability [16,38,39,41]. However, a number of issues such as cost, safety, the dehydration and consequent loss of conductivity at elevated temperature hinder the widespread commercialization of PEMFCs that use PFSA membranes. Such issues arise due to the complex nature of fluorine chemistry and environmental pollution associated with toxic fluorinated exhaust fumes that are emitted during the incinerating process. Furthermore, the low glass transition temperatures ($T_g$) of PFSA membranes (e.g., broad $T_g$ from ~55 °C to ~130 °C [42]) reduce their mechanical strength.

Given the above issues, extensive research has been devoted to developing alternatives to PFSA PEMs, particularly for PEMFCs as transportation power sources. Note that PEMs must satisfy tough criteria; they should possess high dimensional stability, excellent physico-chemical durability, low frequency resistance with electrodes, and high proton conductivity even at low relative humidity (RH) and high temperature (e.g., US Department of Energy (DOE) target >0.1 S $cm^{-1}$ at 50% RH and 80 °C). These properties are required so as to achieve high electrochemical fuel cell performance over a long period time (current DOE target >5000 h).

The most promising PEM candidates are sulfonated hydrocarbon PEMs. As shown in Fig. 3, sulfonated hydrocarbon PEMs can be classified as sulfonated polystyrene copolymers (SPSs), sulfonated polyimides (SPIs), sulfonated poly(phenylene)s, sulfonated poly(arylene)-type polymers, or sulfonated poly(phosphazene)s (SPPhs) according to their backbone structures [5,24,25,27,28,43–47]. The major advantage of these hydrocarbon PEMs is that it is possible to design tailored polymer structures with desired properties using various monomers. When compared to PFSAs, sulfonated hydrocarbon PEMs are generally easy to produce and recycle, relatively free from environmental pollution problems, and can be synthesized with relatively cheap monomers. In particular, since many sulfonated hydrocarbon PEMs have high thermal and mechanical stabilities, they can maintain their mechanical properties and have high water uptakes over a wide temperature range [27,28,34]. Sulfonated hydrocarbon PEMs also have significantly lower gas permeability than PSFA membranes. For these reasons, sulfonated hydrocarbon PEMs have been recognized as promising electrolyte materials, especially for medium-temperature and low-temperature PEMFCs.

Despite their high water uptake, poor water channel formation has frequently been observed in sulfonated hydrocarbon PEMs due to weak phase separation between hydrophilic and hydrophobic moieties (Fig. 2(b)) [12,16,38–40]. Consequently, sulfonated hydrocarbon PEMs exhibit relatively low proton conductivities even at high ion exchange capacities (IECs) and excessive swelling behavior under hydrated conditions (i.e., low dimensional stability) [16,38]. Furthermore, sulfonated hydrocarbon polymers generally exhibit lower chemical and oxidative stability when compared to hydrocarbon polymers without sulfonic acid groups. Such behavior arises from the susceptibility of the sulfonated polymer backbones (such as in polyimides) to chemial attack [26], or their low molecular weight due to the low reactivity of sulfonated monomers [27]. While sulfonated hydrocarbon PEMs generally have a high water uptake, a reduction in their proton conductivity is inevitable over 100 °C due to the evaporation of water molecules.

Many attempts have been made to overcome the aforementioned issues via the synthesis of copolymers with desirable polymer architectures (e.g., block copolymers, high-free volume copolymers, grafted/branched copolymers, and highly sulfonatable monomer-based

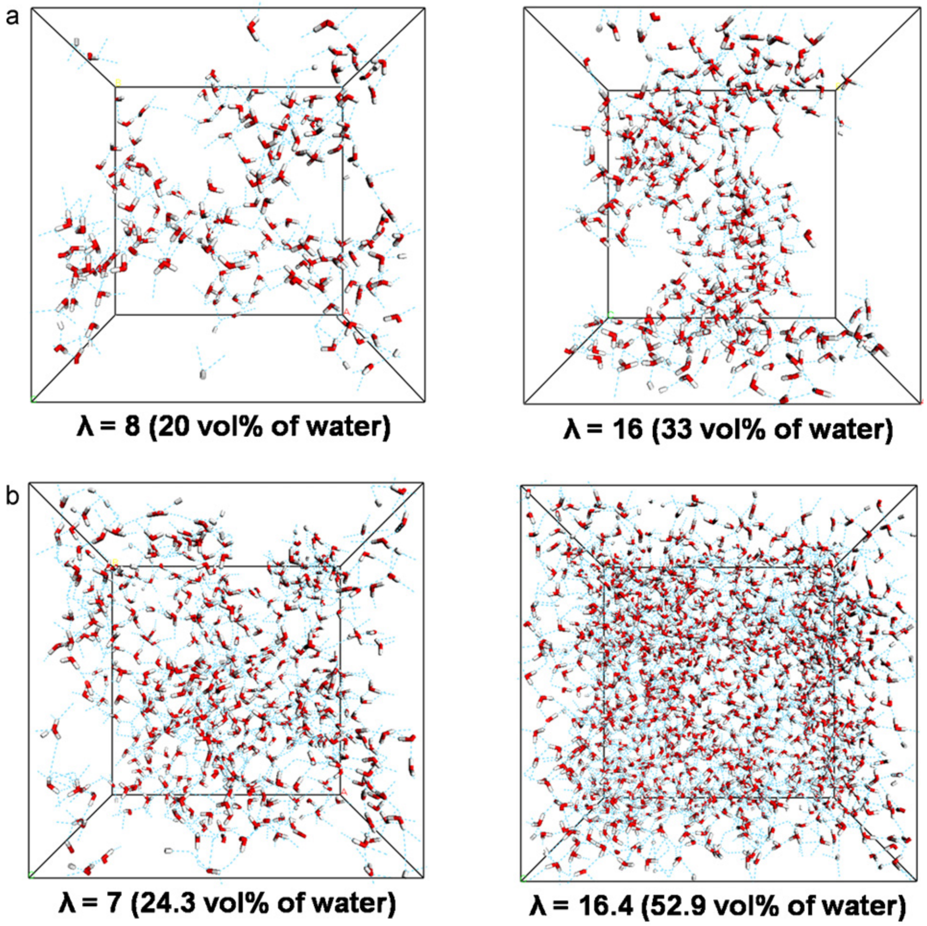

**Fig. 2.** Comparison of simulated water molecules distribution in (a) Nafion® and (b) sulfonated block copolyimides (DS = 80) having the similar λ values. *Colors*: red (O), white (H), blue line (hydrogen bonding) [38]. (For interpretation of the references to color in this figure legend, the reader is referred to the web version of the article.)

[38] Copyright 2010, American Chemical Society.

copolymers) or through polymer chemistry approaches for the physico-chemical tuning of sulfonated PEMs (e.g., crosslinking, surface fluorination, thermal annealing, and organic–inorganic nanocomposites). This review summarizes efforts in developing sulfonated hydrocarbon PEMs with properties that make them attractive for durable medium-temperature and/or low-humidity PEMFC applications.

## 2. Synthesis of sulfonated hydrocarbon PEMs

### 2.1. Sulfonation

Sulfonation is an electrophilic substitution reaction where a sulfonation agent reacts on the aromatic rings and their protons are substituted by sulfonic acid. Here, the reaction site selectively occurs on the electron-rich site of benzene rings, such as the ortho-position to the electron-donating groups. Electron-withdrawing groups deactivate benzene rings to electrophilic sulfonation. As such, the position of sulfonic acid groups can be controlled by the choice of the monomer or the polymer structure. Sulfonation methods are mainly categorized by the host materials into two groups, which are discussed below.

### 2.1.1. Polymer sulfonation

The post-polymerization sulfonation method has long been used for the sulfonation of natural materials in cationic exchange resins for water softening and demineralization [48]. Due to its convenience, this method has often been employed for PEMs in order to introduce sulfonic acid groups into various types of aromatic polymers. However, polymer chain degradation and/or undesirable side reactions may occur during the sulfonation process without adequate attention to suitable sulfonation agents, reaction temperature, and reaction time. In addition, it is sometimes difficult to precisely control the degree of sulfonation (DS) and the site of sulfonic acid groups in the polymer.

Sulfonation agents for polymers should be carefully chosen according to the structure of the host polymer, due to degradation and solubility problems [24,27]. For example, Smitha et al. reported that poly(phenylene oxide) (PPO) and polysulfone (PSf) were sulfonated with chlorosulfonic acid, whereas acetyl sulfate was appropriate for the sulfonation of polystyrene (PS) and polycarbonate (PC) [29]. The concentration of the sulfonation agent and the reaction time and temperature are generally the primary factors that determine the DS of the resulting sulfonated polymers. Representative sulfonation agents include:

(1) Strong agents: concentrated sulfuric acid, fuming sulfuric acid, chlorosulfonic acid.

(2) Mild agents: acetyl sulfate, sulfur trioxide complexes, trimethylsilyl chlorosulfonate ($(CH_3)_3SiSO_3Cl$).

Strong sulfonation agents may result in an inhomogeneous reaction or chain degradation due to their high reactivity, and excessive sulfonation can render the host polymer water soluble. While mild sulfonation agents can lead to a more homogeneous reaction, with no degradation, and less side reactions occurring, it is often difficult to achieve a sufficiently high DS with these agents [29,49].

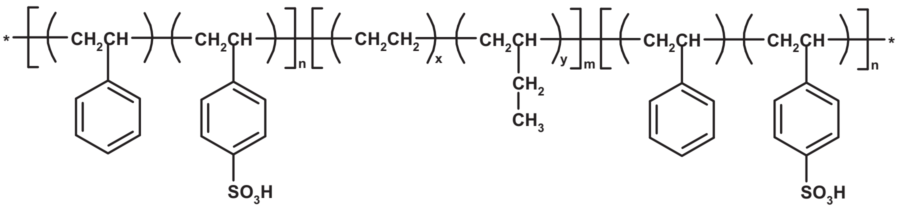

(a) Sulfonated styrene copolymers (SPSs) [50, 51].

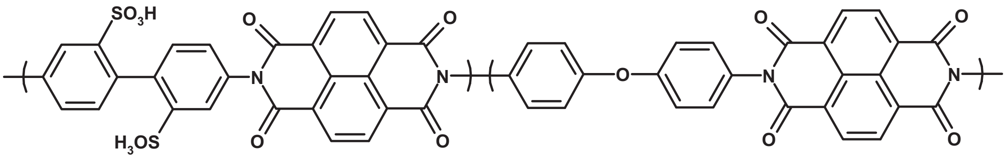

(b) Sulfonated polyimides (SPIs) [92].

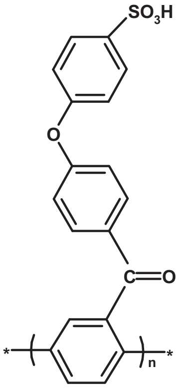

(c) Sulfonated poly(phenylene)s [45].

**Fig. 3.** Various types of sulfonated hydrocarbon proton exchange membranes (PEMs): (a) sulfonated styrene copolymers (SPSs) [50,51]; (b) sulfonated polyimides (SPIs) [92]; (c) sulfonated poly(phenylene)s [45]; (d) sulfonated poly(arylene) types polymers [27]; and (e) sulfonated poly(phosphazene)s [46,47].

[50] Copyright 2002, American Chemical Society; [27] Copyright 2004, American Chemical Society.

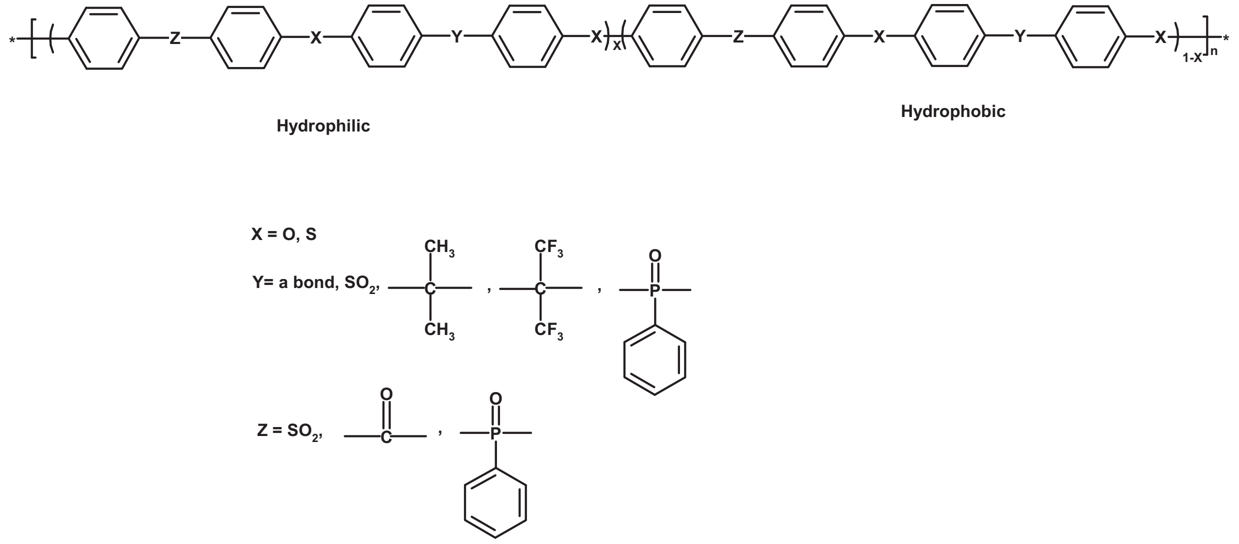

(d) Sulfonated poly(arylene) types polymers [27].

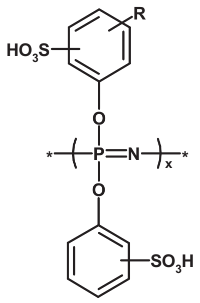

(e) Sulfonated poly(phosphazene)s [46, 47].

Fig. 3. (*Continued*).

Since the post-sulfonation method requires aromatic rings for the electrophilic substitution reaction, it has been widely used for polymers containing styrene units. A representative PEM based on polystyrenes is the sulfonated styrene–ethylene–butylene–styrene (SEBS) membrane (Fig. 3(a)), such as that manufactured by Dais Analytic. For the sulfonation of SEBS polymers, a sulfur trioxide/triethyl phosphate complex solution at low tem-

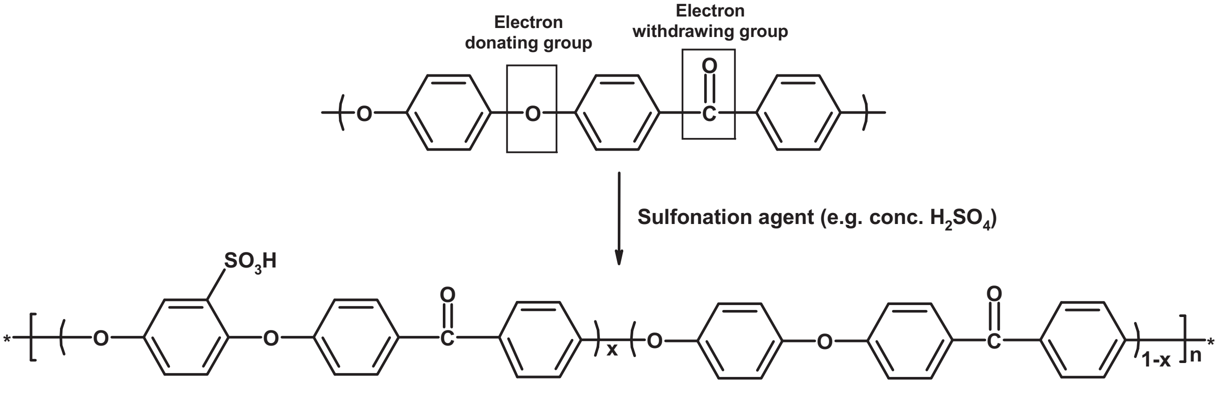

**Fig. 4.** Sulfonation of poly(ether ether ketone) (PEEK).

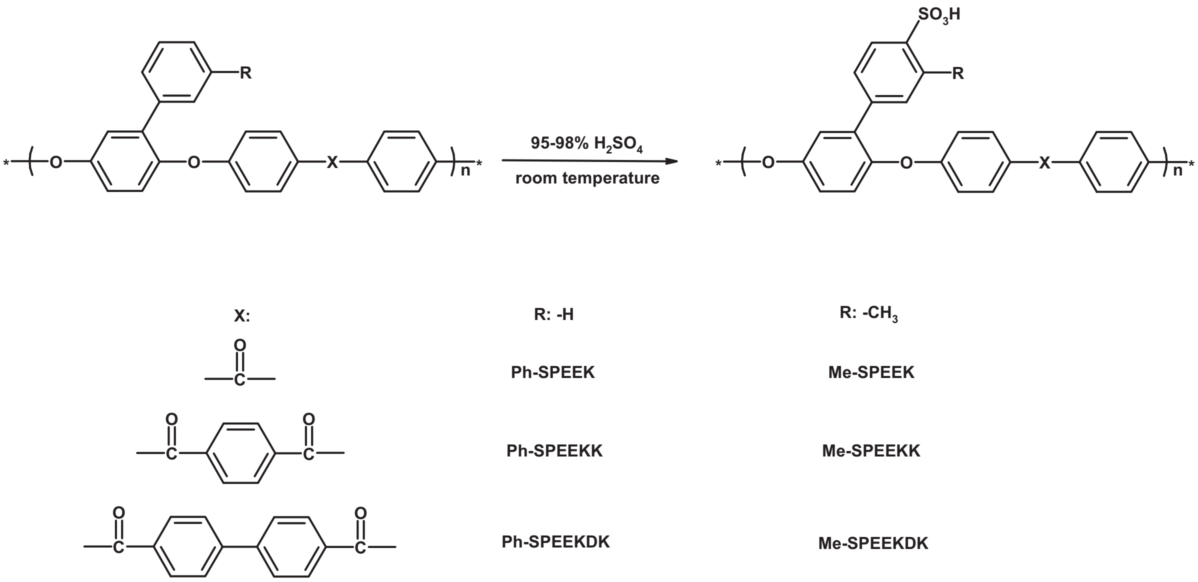

(a) Homopolymer-type sulfonated poly(ether ketone)s (SPEKs)

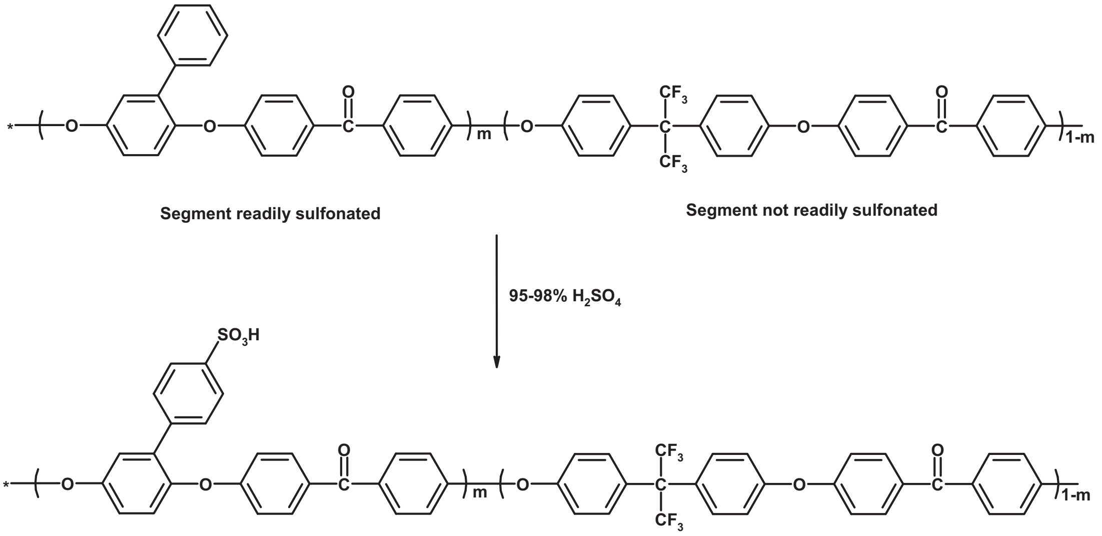

(b) Copolymer-type sulfonated poly(ether ketone)s (SPEKs)

**Fig. 5.** Sulfonation of poly(ether ketone)s (PEKs) having various pendant phenyl groups: (a) homopolymer-type sulfonated poly(ether ketone)s (SPEKs), and (b) copolymer-type sulfonated poly(ether ketone)s (SPEKs) [59].
[59] Copyright 2007, American Chemical Society.

peratures between −5 °C and 0 °C or acetyl sulfate at 50 °C is used as a sulfonation agent [50,51]. However, the applicability of SEBS polymers in PEMFCs is limited due to the poor oxidative stability of sulfonated aliphatic polystyrene units [52]. Sulfonated polystyrenes have thus been studied as a grafted side chain so as to introduce sulfonic acid groups onto a non-sulfonated polymer main-chain [53,54].

Noshay and Robeson originally reported on the polymer sulfonation of bisphenol A polysulfone [55]. This work was followed by many studies where other poly(arylene ether)-type polymers were employed. Among these polymers, poly(ether ether ketone) (PEEK), such as commercial Victrex®, is most extensively used as a host polymer. In PEEK, the sulfonic acid group is introduced to the ring located between ether linkages due to their electron-

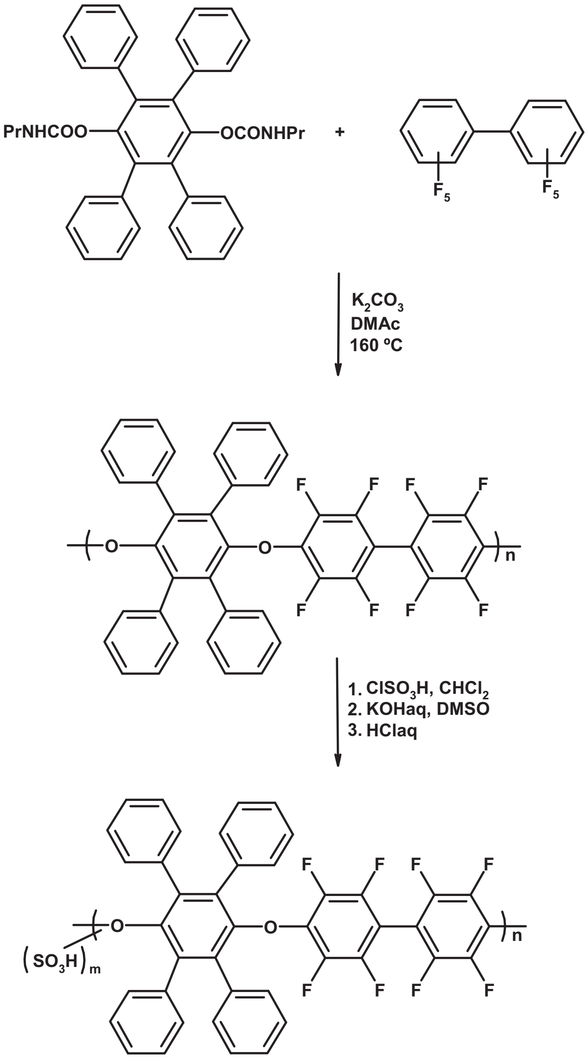

**Fig. 6.** Synthesis and sulfonation process of sulfonated poly(arylene ether)s composed of tetraphenylphenylene ether and perfluorobiphenylene units [60].

donating character. Concentrated sulfuric acid is more appropriate as a sulfonation agent than chlorosulfonic acid or fuming sulfuric acid due to polymer chain degradation issues (Fig. 4) [56–58].

Guiver and co-workers reported on a method to control the sulfonation sites by adjusting the molecular structures of the host polymers [59]. PEEK with the various side substituents, such as phenyl, methylphenyl, trifluoromethylphenyl, and phenoxyphenyl groups, was sulfonated under rapid and mild reaction conditions using concentrated sulfuric acid (95–98%) at room temperature. It was observed that while PEEKs with selected pendant groups, such as phenyl and 4-methylphenyl, had dramatically shorter sulfonation times than commercial PEEK under mild reaction conditions, other pendant groups could not be readily sulfonated. In addition, a series of sulfonated poly(ether ketone)s (SPEKs) with different DS was prepared by controlling the length of the ketone monomers in the homopolymer (Fig. 5(a)) and the composition of sulfonatable/non-sulfonatable segments (Fig. 5(b)). Homopolymer-type SPEKs were found to exhibit a lower dimensional swelling ratio than copolymer-type SPEKs with similar IEC values.

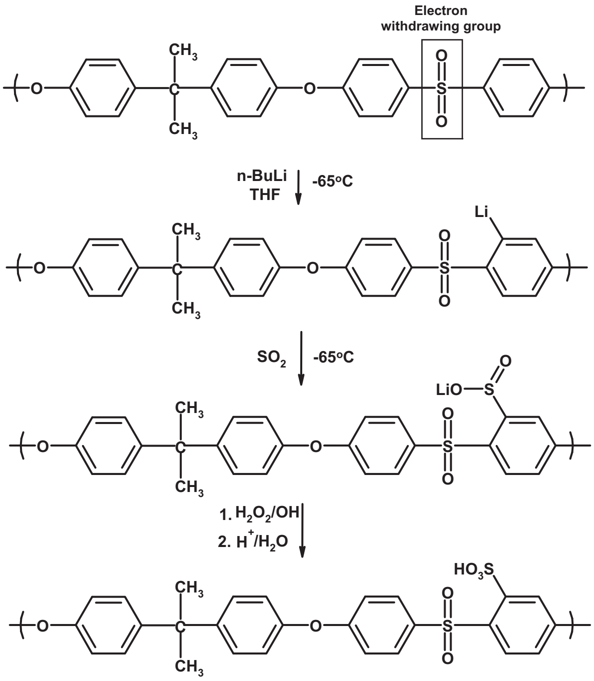

**Fig. 7.** Sulfonation process via lithiation of sulfonated poly(sulfone)s [62].

In 2001, Hay et al. suggested interesting PEM designs that included highly sulfonatable monomers with many pendant phenyl rings, where a hydrophilic segment could

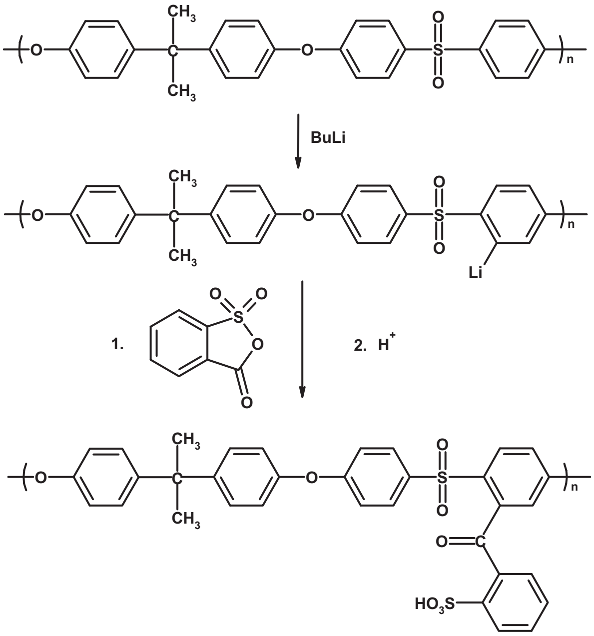

**Fig. 8.** Process for sulfophenylated poly(sulfone)s via lithiation [66].

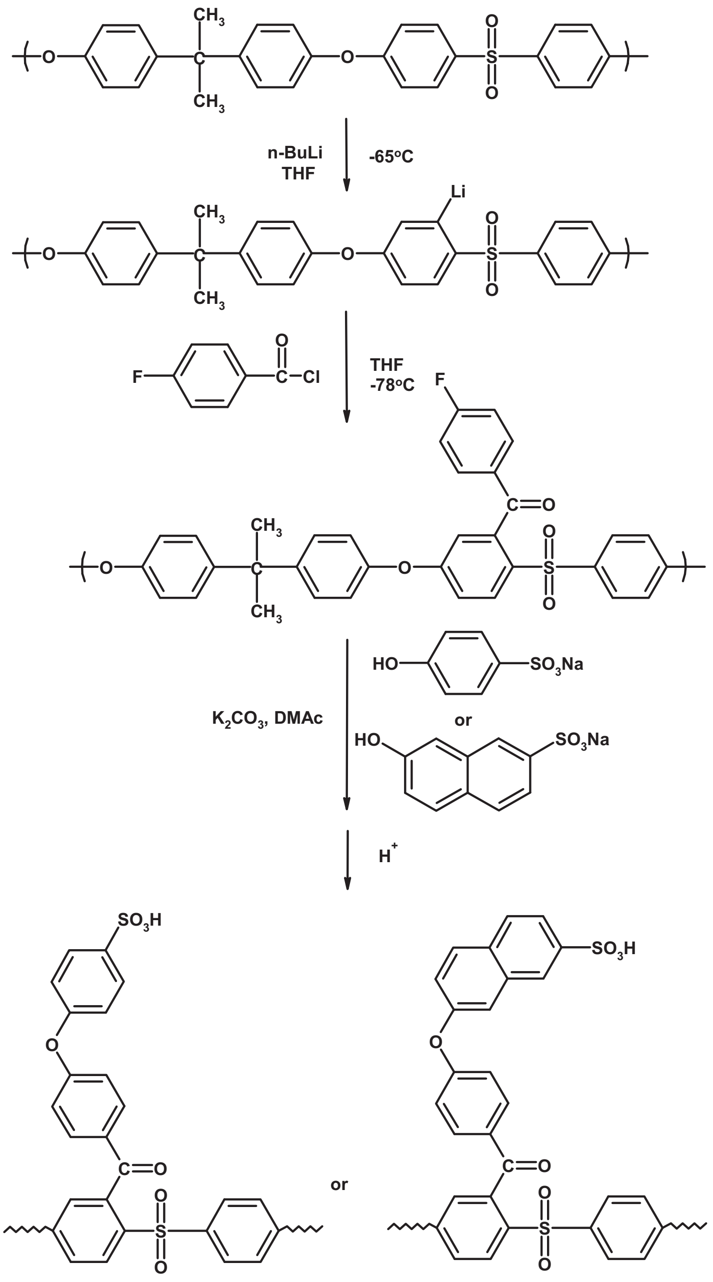

**Fig. 9.** Synthesis of sulfophenoxybenzoyl polysulfone and sulfonaphthoxybenzoyl polysulfone [67].

have more than three sulfonic acid groups after sulfonation [60,61]. Fig. 6 shows the synthesis and sulfonation processes for sulfonated poly(arylene ether)s (SPAEs) composed of tetraphenylphenylene ether and perfluorobiphenylene units [60]. After sulfonation, sulfonic acid groups were located at the para position of the pendant phenyl ring; their DS per repeat unit ($m$) could be controlled by the reaction stoichiometry. However, since the resulting highly sulfonated polymers with $m = 3$ were soluble in methanol, copolymers with non-sulfonatable bis(3,5-dimethylphenyl) sulfone monomers were also synthesized. The results attained by the Hay research group were later applied to the concept of PEMs with highly sulfonatable monomers, which will be discussed later in Section 2.2.6.

Another approach to polymer sulfonation is metalation, or lithiation, without the use of conventional sulfonation agents. This approach was first reported by Kerres et al., who applied a three-step reaction process of lithiation, sulfonation, and oxidation to commercial polysulfone Udel®, as shown in Fig. 7 [62]. In a conventional sulfonation reaction, sulfonic acid groups are introduced onto the ortho-position of electron-rich benzene rings activated by electron-donating groups such as ether linkages, which can give rise to instability due to the low reaction energy barrier

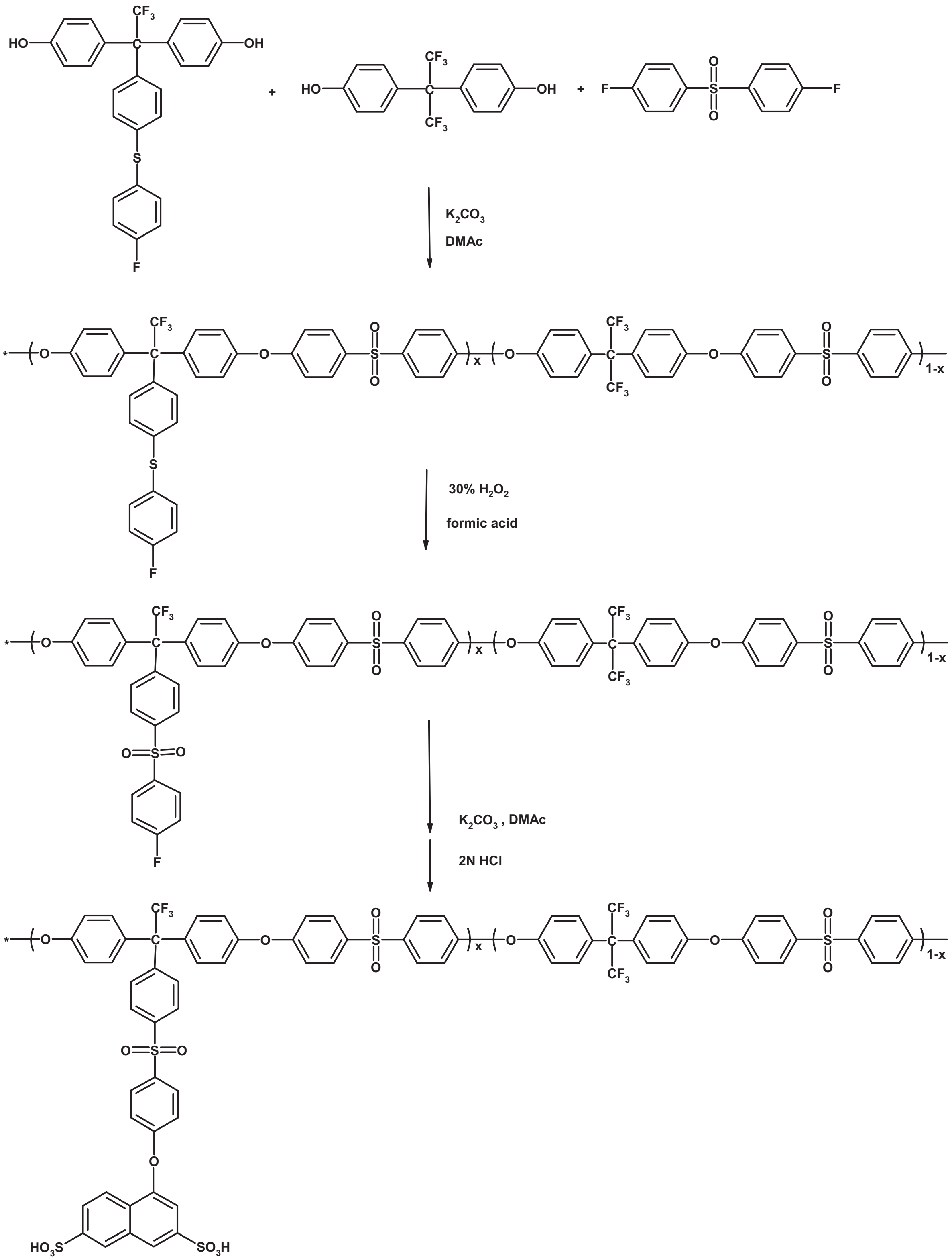

**Fig. 10.** Synthetic route of poly(arylene ether sulfone)s with grafting capability [68].

[68] Copyright 2006, American Chemical Society.

[63]. However, sulfonic acid groups introduced by lithiation are potentially more stable and exhibit a higher acidity because lithiation occurs on electron-poor benzene rings that are deactivated by the electron-withdrawing group such as a sulfone group [34,64,65]. Despite this potential advantage, the final oxidation step that follows lithiation and sulfination can result in a reduction in the expected IEC, and chain degradation [62].

The grafting of sulfonation groups onto polymer side chains is also an attractive method to prepare novel flexible PEMs. As demonstrated with Nafion®, sulfonated groups at the end of a side chain induce strong phase separation between the hydrophobic main chain and the hydrophilic side chain. This phase separated morphology can decelerate polymer main chain degradation by radical species that are present in the water channel [38]. In previous research by the Jannasch group, a sulfophenyl ring was introduced to polysulfone using the above lithiation process developed by Guiver et al. [65], followed by subsequent anionic reaction with sulfobenzoic acid cyclic anhydride, as shown in Fig. 8 [66]. The same group also synthesized novel poly(sulfone)s with pendant sulfonated aromatic side chains; the DS was conveniently controlled by the degree of lithiation in the first step, because the second step proceeded with full conversion (Fig. 9) [67]. Despite their novel synthetic approach and grafting structure, unfavorable transetherification reactions limited an increase in the DS. Zhao et al. reported on poly(ether sulfone)s with a grafted sulfonated group, where reagents with two sulfonic acid groups were attached at the end of a 4-fluorophenyl sulfide pendant group via a nucleophilic substitution reaction [68]. In the study, the authors suggested a novel grafting strategy to introduce disulfonated phenolates into the pendant side chain. The strategy involved the activation of para fluorine on a pendant group via the oxidation of sulfide to sulfone (see Fig. 10).

### 2.1.2. Direct copolymerization of sulfonated monomers

Various approaches have been proposed to overcome the issues of polymer chain degradation and sulfonic acid group instability that are inherent in the polymer sulfonation method. One approach is to introduce sulfonic acid groups into monomers and then copolymerize non-sulfonated monomers with sulfonated monomers to control IEC. This monomer sulfonation method avoids the polymer chain degradation during the sulfonation process and enables the introduction of sulfonic acid groups into a variety of polymer backbones that have sensitivity to strong acidic conditions. For example, while many studies have been carried out to prepare sulfonated polyimides (SPIs), there are few reports on the fabrication of SPIs via polymer sulfonation because the PI backbones are susceptible to decomposition during sulfonation process [69,70]. Furthermore, the use of sulfonated monomers allows the design of the polymer to be easily tailored for desirable properties such as the DS and the choice of sulfonated sites (e.g., inactivated sites for high stability and acidity, as shown in Fig. 11 [71]). In particular, special architecture for sulfonated polymers (e.g., multi block copolymers) can be designed by controlling the topology and/or molecular weight of sulfonated and non-sulfonated oligomers and/or polymers [72–75]. However, there are relatively few commercially available sulfonated monomers [34]. Another factor is that the steric hindrance of sulfonated monomers may decrease the reactivity and limit the high molecular weight of the resulting sulfonated polymers [27].

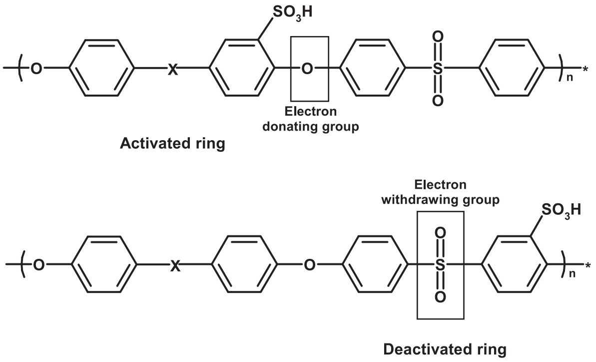

**Fig. 11.** Introduction of sulfonic acid groups via post-sulfonation (upper) and monomer sulfonation (below).

A list of widely used sulfonated monomers is shown in Fig. 12. Sulfonated dihalo monomers, which are mainly utilized for polyarylene-type polymers, were first reported on by Robesen and Matzner. The monomers were not initially used for fuel cell membranes, but for flame retarding materials [76]. Ten years later, sulfonated 4,4′-dichlorodiphenyl sulfone was synthesized and purified by Ueda et al. for aromatic poly(ether sulfone)s [77]. Wang et al. reported on the use of 3,3′-disulfonated 4,4′-difluorodiphenyl ketone monomer for poly(arylene ether ketone)s (Fig. 13) [78]. However, research on fuel cell applications using sulfonated dihalo monomers began when the McGrath research group synthesized 3,3′-disulfonated 4,4′-dichlorodiphenyl sulfone monomers and prepared a BPSH series based on sulfonated poly(arylene ether sulfone) (SPAES) copolymers (Fig. 14) [79,80]. The same group and coworkers also studied structure–property relationships using various monomers [81–84], which will be discussed in Section 2.2.1. Na and co-workers detailed the use of 1,4-bi(3-sodium sulfonated-4-fluorobenzoyl) benzene as a sulfonated monomer for sulfonated poly(ether ether ketone ketone)s (SPEEKs) [85,86]. Various types of SPAEs are listed in Fig. 3(d). Sulfonated commercial monomers (Fig. 12(b)) were also examined for the polymerization of PEMs due to their availability and low price. Guiver and co-workers used commercial sulfonated bisphenol monomers to prepare SPAE-type polymers. The researchers also performed a comparative study of sulfonated poly(arylene ether ether nitrile) (SPAEEN) copolymers with different sulfonic acid bonding sites (Fig. 15) [87–90], which will be further discussed in Section 2.2.1.

For SPIs, a sulfonated commercial monomer, 4,4′-diamino-biphenyl 2,2′-disulphonic acid (BDSA) was used in early research by Mercier and Pineri's group (Fig. 16) [72,75,91,92]. However, BDSA-based SPIs have exhibited a relatively low hydrolytic stability despite attempts to improve this through the introduction of a six-membered ring of naphthalenic anhydride [93]. To overcome this problem, Okamoto and co-workers synthesized two types of sulfonated diamines, 4,4′-diaminodiphenyl ether-2,2′-disulfonic acid (ODADS) with a flexible structure [94] and 9,9-bis(4-aminophenyl)fluorene-2,7-disulfonic acid (BAPFDS) with a rigid and bulky structure [95], as shown in Fig. 17. When compared to BDSA-based SPIs, SPIs incorporating ODADS exhibited much better hydrolytic stability due to their flexibility. This finding was further supported by the reduced stability of SPIs when flexible non-sulfonated diamines were replaced with rigid diamines. However, despite their rigidity, SPIs with BAPFDS displayed a hydrolytic stability that was similar to that exhibited by ODADS-based SPIs. Such stability was due to the high basicity of BAPFDS, which favors imido ring stability. The Okamoto group also attempted to impart intrinsic hydrolytic stability to SPIs by incorporating various types of monomers [26]. In particular, SPIs with sulfonic acid groups on the side chains (grafted sulfonic acid groups) exhibited a significant improvement in their hydrolytic stability due to the higher basicity of the diamine moieties and their microphase-separated structure [96,97]. Using a similar concept, Asano et al. synthesized highly stable sulfonated copolyimides with aliphatic groups in both the main chains and the side chains. The structures did not display a significant open circuit voltage (OCV) drop during 5000 h of operation (Fig. 18) [98]. The McGrath group researched a novel sulfonated diamine monomer, 3,3′-disulfonic acid-bis [4-(3-aminophenoxy)phenyl]sulfone (SA-DADPS), where sulfonated groups were introduced to aromatic rings other than the amino-phenyl ring in order to reduce

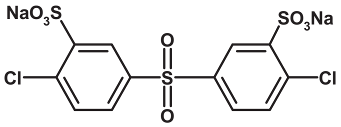

3,3′-disulfonated 4,4′-dichlorodiphenyl sulfone

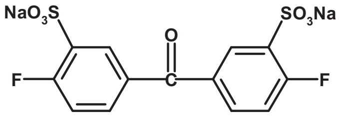

3,3′-disulfonated 4,4′-difluorodiphenyl ketone

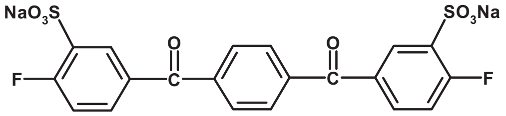

1,4-bi(3-sodium sulfonated-4-fluorobenzoyl) benzene

(a)

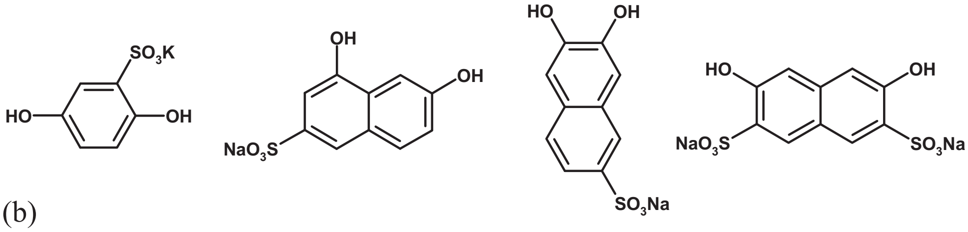

(b)

**Fig. 12.** (a) Sulfonated dihalo monomers, (b) sulfonated bisphenol monomers, and (c) sulfonated diamine monomers.

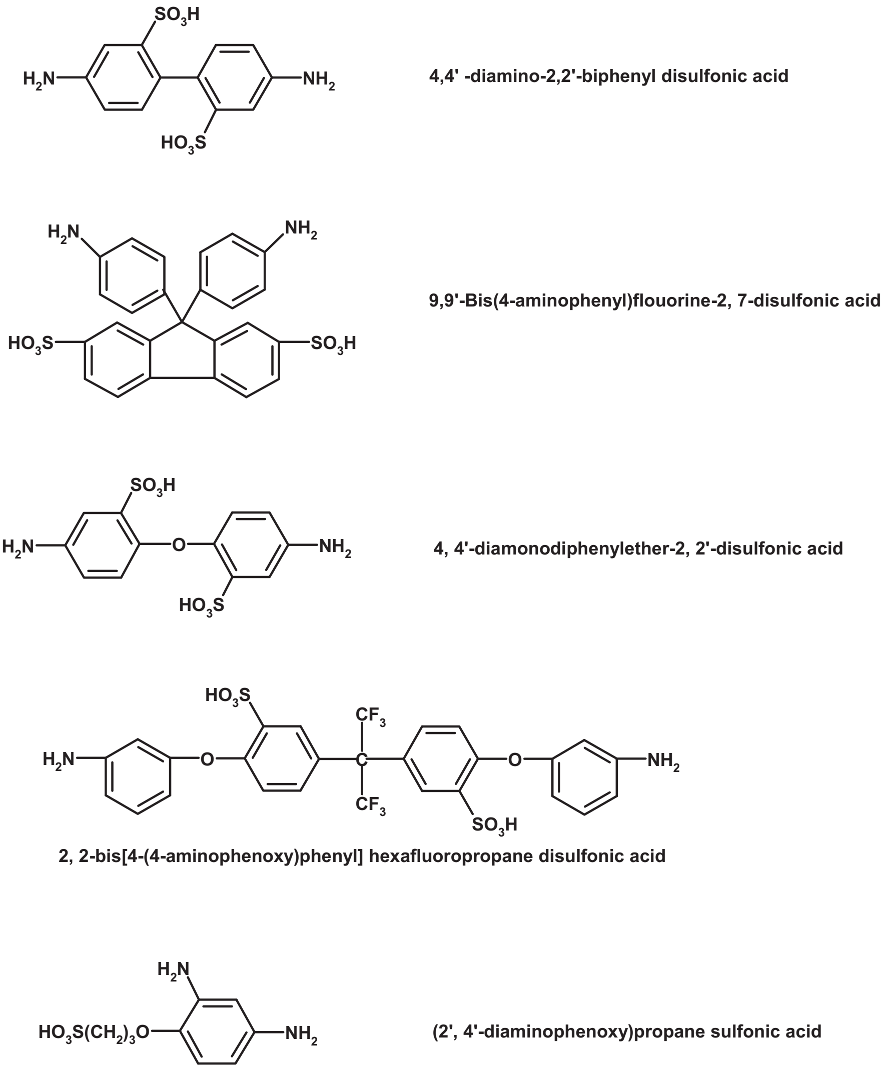

**Fig. 12.** (*Continued*).

the electron-withdrawing effect of sulfonic acid groups that cause poor hydrolytic stability (Fig. 19) [99,100]. Pertaining to this stability issue, Li et al. suggested an interesting design of a novel sulfonated monomer, where sulfonic acid groups were introduced on the dianhydride monomer rather than the diamine monomer [101]. In this study, 4,4′-binaphthyl-1,1′,8,8′-tetracarboxylic dianhydride (BTDA) was sulfonated using fuming sulfuric

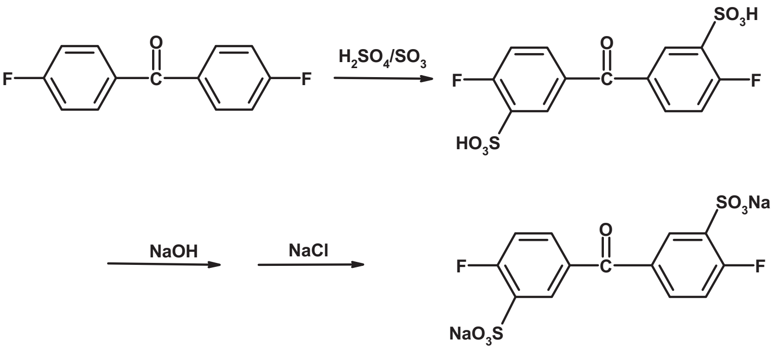

**Fig. 13.** Synthetic route of sulfonated 3,3′-disulfonated 4,4′-difluorodiphenyl ketone monomer [78].

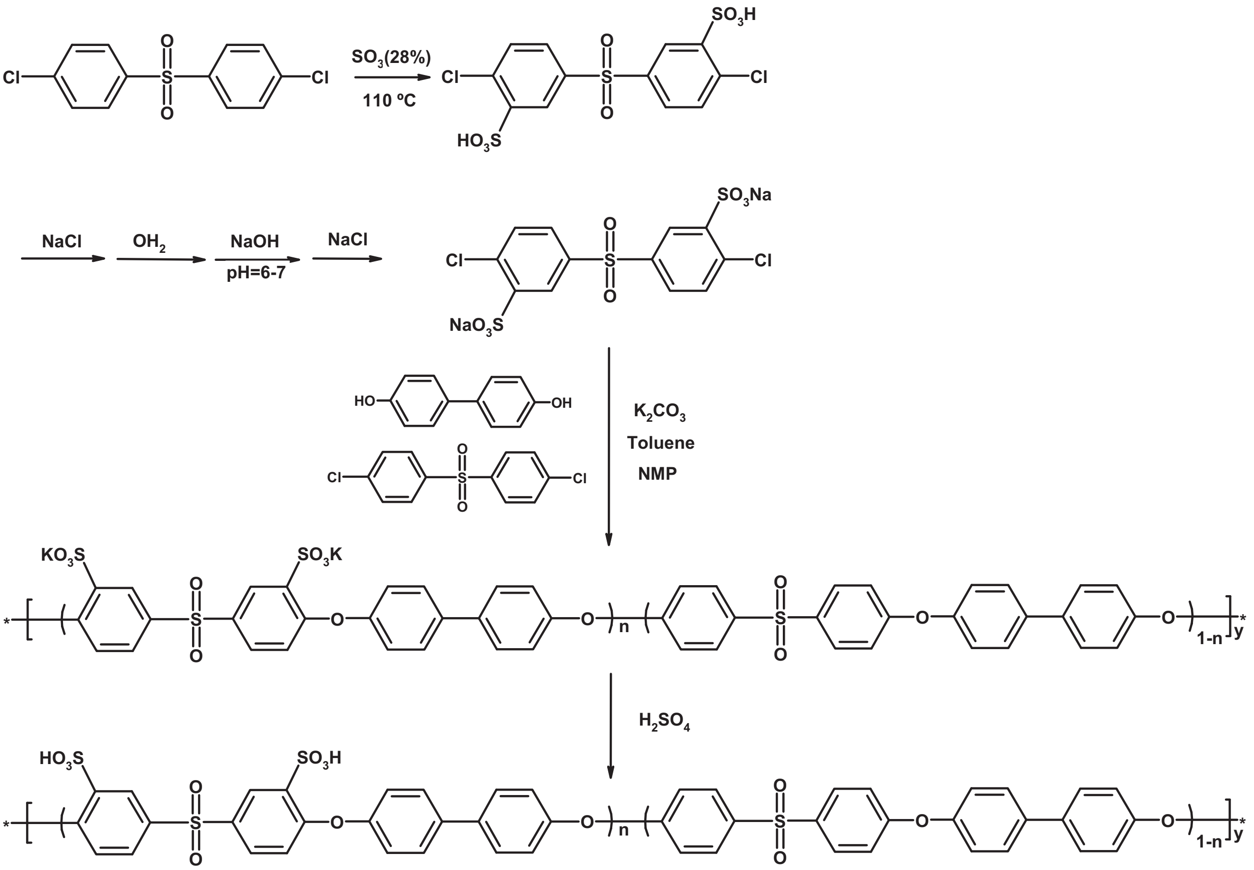

**Fig. 14.** Synthetic route of 3,3′-disulfonated 4,4′-dichlorodiphenyl sulfone monomer and sulfonated poly(arylene ether sulfone) [79,80].

acid, and then polymerized with various non-sulfonated diamines. Since the resulting sulfonated PIs had sulfonic acid groups on the deactivated positions of the aryl backbone rings and high DS, they showed very high proton conductivities. In particular, sulfonated copolyimide polymerized with hexane-1,6-diamine, SBTDA, and BTDA had excellent water stability at 90 °C without sacrificing proton conductivity.

## 2.2. Recent high-performance sulfonated hydrocarbon PEMs

In the mid-2000s, as knowledge regarding the synthesis of new sulfonated hydrocarbon PEMs progressed and the well-ordered hydrophilic channel structure in Nafion® had been disclosed, the importance of new polymer designs having high proton conductivities even at low IECs was addressed. This issue was expanded to high IEC PEMs without sacrificing mechanical stability. Earlier PEMs exhibited relatively low proton conductivity and high water swelling due to poor water channel formation (as mentioned in Section 1). Particular attention was paid to controlling the nano (or micro)-structure of these PEMs through polymer topology.

In this section, recent trends in high-performance sulfonated hydrocarbon PEMs will be discussed.

### 2.2.1. Introduction of functional groups

In the initial development stages of fuel cells based on sulfonated hydrocarbon PEMs, their MEAs suffered from poor adhesion and delamination between the Nafion® ionomer binder in the catalyst layers and the hydrocarbon PEMs due to differences in chemical properties. However, extensive research has been devoted to improving MEA fabrication methods for hydrocarbon PEMs and enhancing membrane properties such as the balance between proton conductivity and water uptake. The incorporation of functional groups into sulfonated PEMs is an effective way to improve PEM performance (including the electrochemical performance) without sacrificing membrane properties such as the IEC value.

The McGrath group first introduced fluorine groups into hydrocarbon PEMs using 4,4′-hexafluoroisopropylidene bisphenol (6F-BPA) monomers for SPAES copolymers [81]. The authors studied the effect of bisphenol monomers with various chemical structures on the properties of the resulting SPAES copolymers, as shown in Fig. 20(a). 6F-BPA copolymer systems exhibited the lowest water sorption due to the hydrophobicity of the fluorine groups. A disulfonated poly(arylene ether benzonitrile) copolymer containing 6F-BPA (6FCN, see Fig. 20(b)) had much less water uptake than both the copolymer without benzonitrile groups and the copolymer without fluorine and nitrile

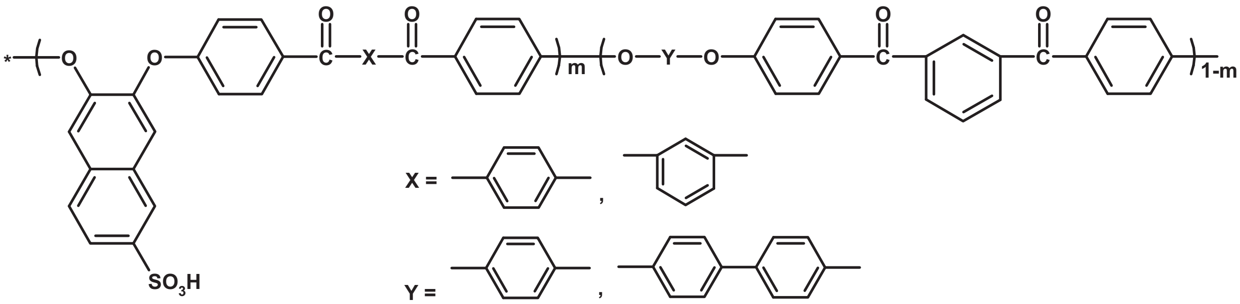

(a) SPAEEKK

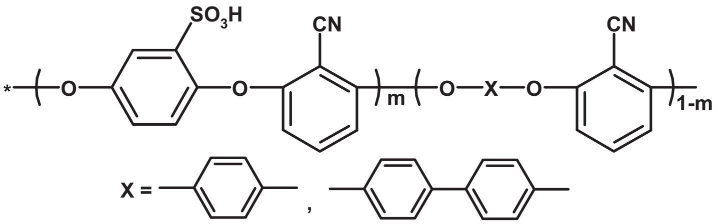

(b) SPAEEN

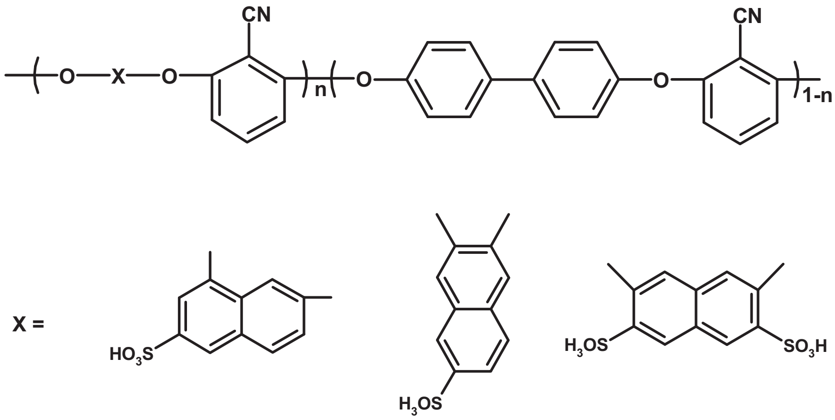

(c) m-SPAEEN P-SPAEEN D-SPAEEN

**Fig. 15.** Chemical structure of poly(arylene ether ether nitrile) copolymer having different sulfonic acid bonding site from commercial sulfonated bisphenol monomers [87–90].
[89] Copyright 2006, Elsevier Ltd.; [90] Copyright 2007, American Chemical Society.

groups at equivalent IECs; the proton conductivities of the structures were all comparable [102]. In particular, Kim et al. reported that the 6FCN copolymer displayed the highest fuel cell performance [103]. Such performance was due to two factors: a low water uptake that resulted from the interaction between nitrile groups and sulfonic acid and the reduced interfacial resistance from the improved adhesion between fluorine groups in the copolymer and the Nafion®-bonded electrodes [83,103].

Guiver and co-workers expanded the above concept to sulfonated poly(aryl ether ketone)s (SPAEKs) containing hexafluoroisopropylidene diphenyl moieties, as shown in Fig. 21 [104,105]. Various sulfonated poly(arylene ether nitrile)s (SPAENs) were synthesized as explained in Section 2.1.2 and shown in Fig. 15(b) and (c) [88–90]. The introduction of nitrile groups into the PEMs was expected to promote adhesion onto either the catalyst or carbon particles in the catalyst layers [88]. SPAENs con-

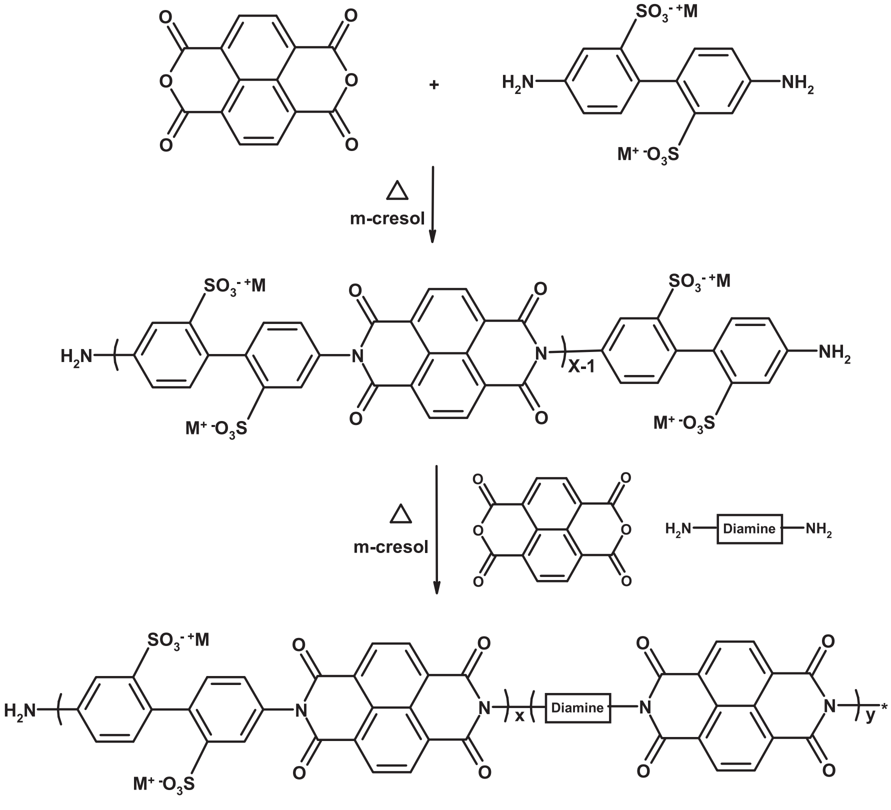

Fig. 16. Synthetic route of sulfonated poly(imide)s based on BDSA [92].

taining a naphthalene structure with the sulfonic acid groups shown in Fig. 15(c) exhibited much lower water uptakes and swelling ratios than previous SPAENs with hydroxyquinone monomers. Such behavior was due to the synergistic effect of inter-chain attraction between polymer chains via the strong polar interaction between nitrile groups, and to the hydrophobicity of the naphthalene structure [89,90]. Furthermore, SPAEEN with sulfonic acid groups meta to the ether linkage (m-SPAEEN) and those with sulfonic acid groups located pendant on a phenyl ring (P-SPAEEN) exhibited much higher proton conductivities because the meta linkage and the long-distance connectivity of their sulfonic acid groups, could eliminate deactivation of the sulfonic acid groups, respectively [90]. As a result, m-SPAEEN membranes showed high performance in both PEMFC and DMFC fuel cell applications

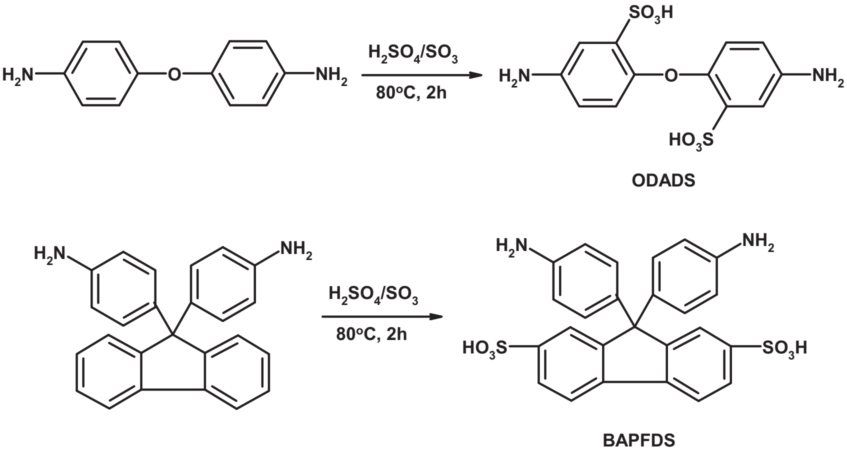

Fig. 17. Sulfonation of 4,4′-diaminodiphenyl ether-2,2′-disulfonic acid (ODADS) [94] and 9,9-bis(4-aminophenyl)fluorene-2,7-disulfonic acid (BAPFDS) [95].
[94] Copyright 2002, American Chemical Society; [95] Copyright 2002, American Chemical Society.

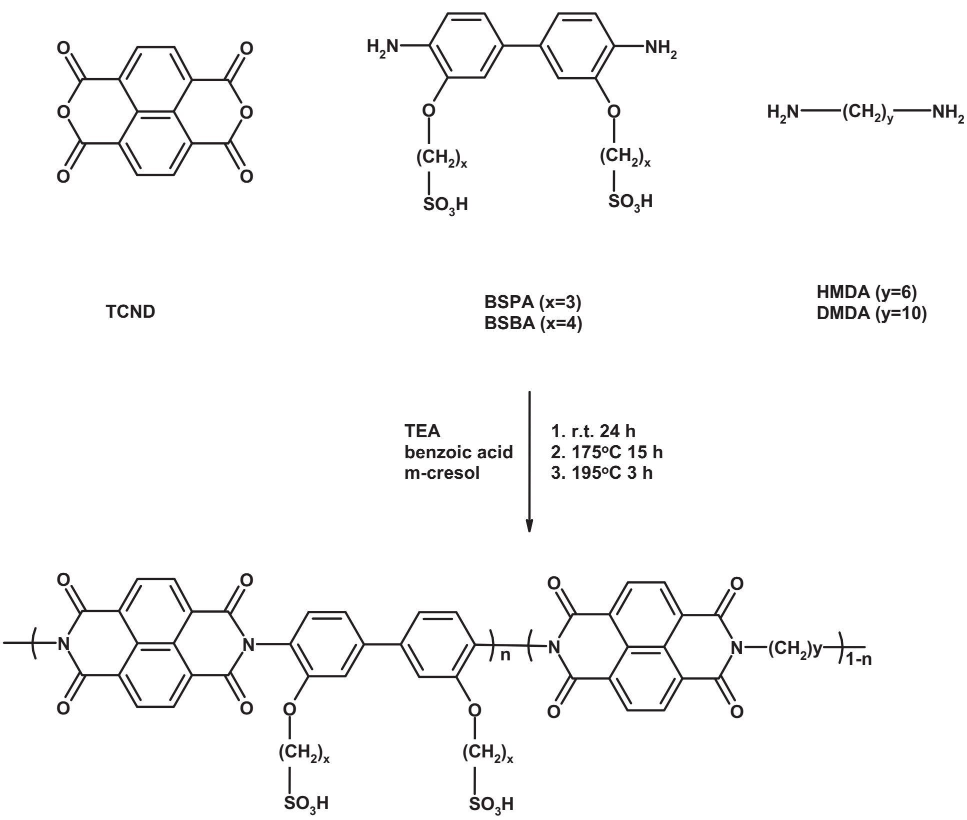

**Fig. 18.** Synthetic route of sulfonated aliphatic/aromatic poly(imide)s [98].
[98] Copyright 2006, American Chemical Society.

[106,107]. The authors also explained the effect of the angled structure, which increased the interchain spacing and created pores with sulfonic acid groups within. As the pores effectively confined water molecules via hydrogen bonds, the proton conductivity could be improved and be less sensitive to temperature. This is a very important concept for sulfonated PEMs with a high free volume and it will be further discussed in the next section. In another paper, Guiver and co-workers synthesized SPAE with a high fluorine content and SPAEN with a high nitrile content; each contained pendant phenyl sulfonic acids, as shown in Fig. 22 [108]. The sulfonic acid groups could be introduced exclusively on the para-position of the pendant phenyl ring with chlorosulfuric acid under relatively mild conditions. The SPAE and SPAEN with DS values of 1.0 exhibited high IECs of 1.75 and 2.71 mequiv. g$^{-1}$, high proton conductivities of 0.135 and 0.140 S cm$^{-1}$ at 80 °C in water, and low water uptakes of 32 and 39.6%, respectively. On a tradeoff plot of proton conductivity versus water uptake, the PEMs exhibited high proton conductivity and low water uptake in comparison with Nafion®.

### 2.2.2. Sulfonated hydrocarbon PEMs with high free volume

One of the most important issues for sulfonated PEMs in fuel cells is water management within the structures. If PEMs swell excessively with water under humidified operating conditions, they can be delaminated from the catalyst layer which has a relatively lower degree of water swelling,

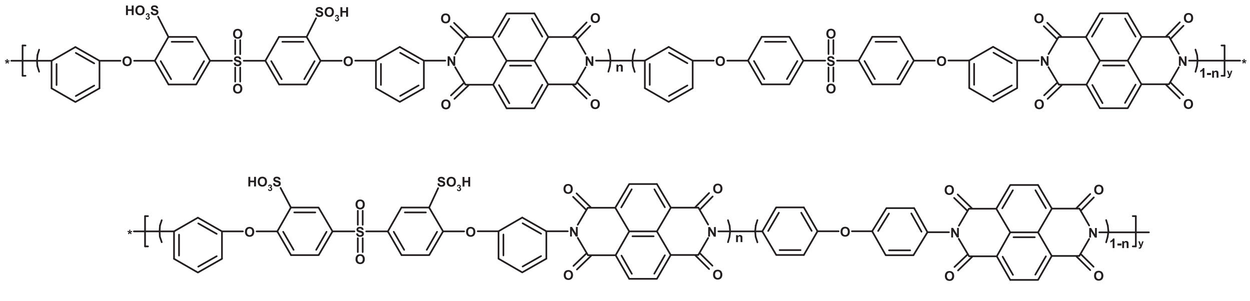

**Fig. 19.** Chemical structure of sulfonated poly(imide)s based on 3,3′-disulfonic acid-bis [4-(3-aminophenoxy)phenyl]sulfone (SA-DADPS) [99,100].

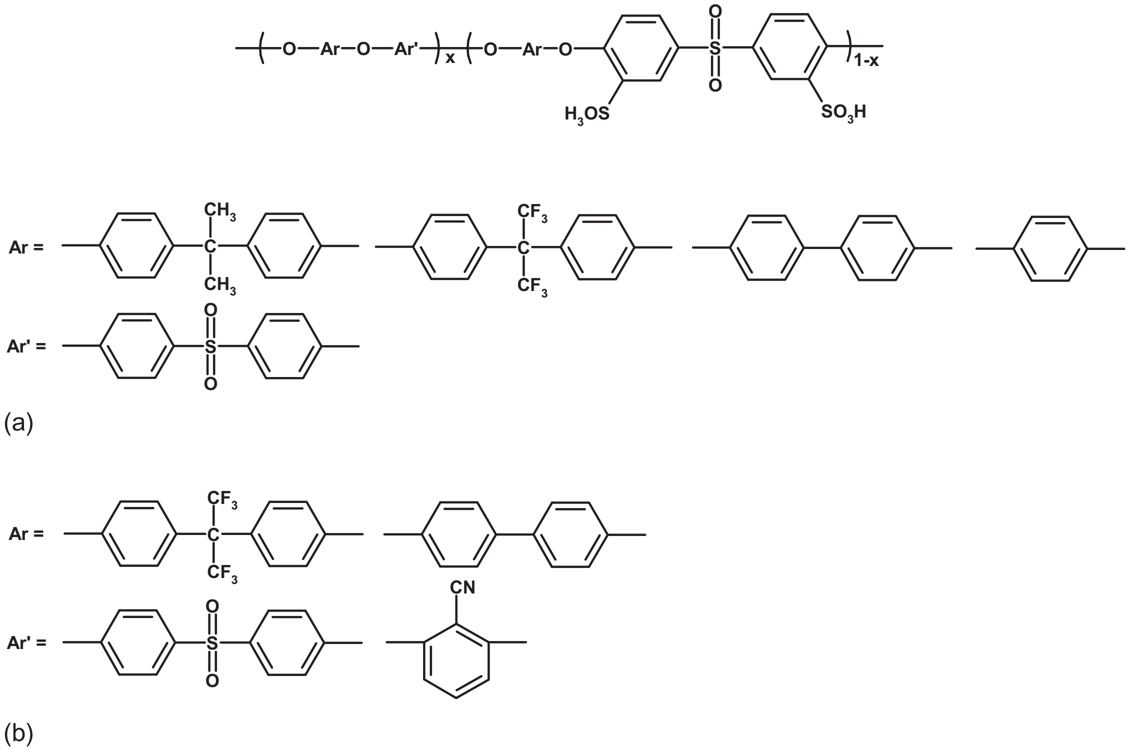

**Fig. 20.** Sulfonated poly(arylene ether sulfone) copolymers having various bisphenol and functional groups [81,102].

due to differences in dimensional swelling ratio between the hydrocarbon PEM and the PFSA ionomer-catalyst. This dimensional miss-match phenomenon has been reported as one of the major reasons for low durability in fuel cell systems [109]. However, since fuel cell systems are operated under reduced humidity with increasing temperature (as mentioned in Section 1), PEMs should be designed to retain water even under a low RH, to ensure high proton conductivity. Consequently, PEMs that are able to maintain water content and have high proton conductivity when operated in a range of RH (40–100%) must be developed.

A possible way to solve this is to utilize polymer having a high free volume imparted through the introduction of bulky monomers. In general, the sorption of small molecules, such as gas molecules in a polymer host material, is affected by the amount of free volume of the polymer

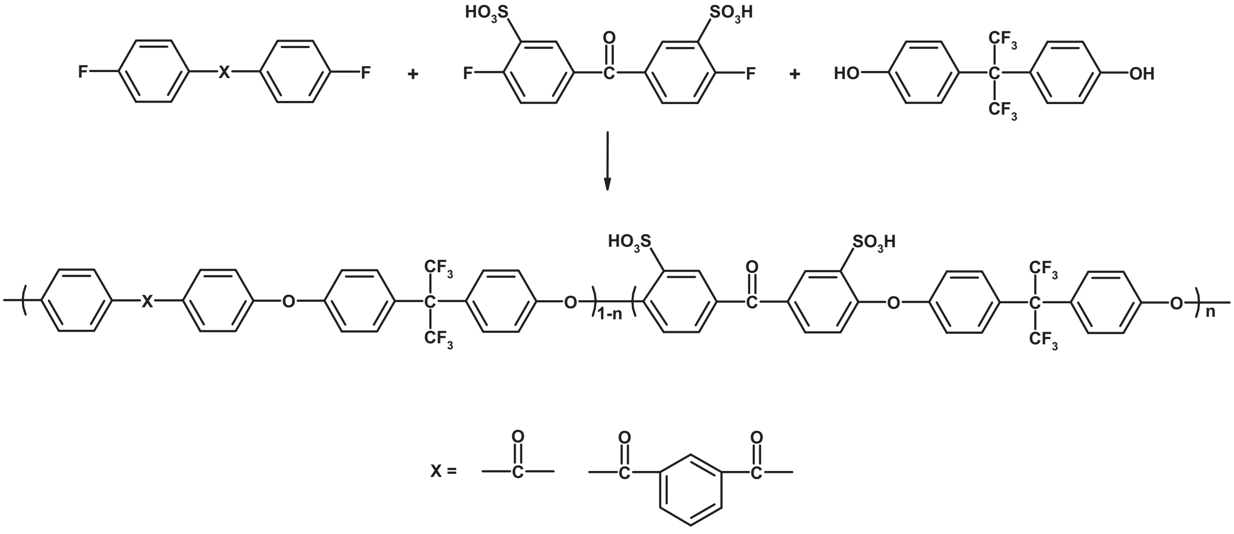

**Fig. 21.** Sulfonated poly(aryl ether ketone)s containing hexafluoroisopropylidene diphenyl moiety [104,105].
[104] Copyright 2004, American Chemical Society.

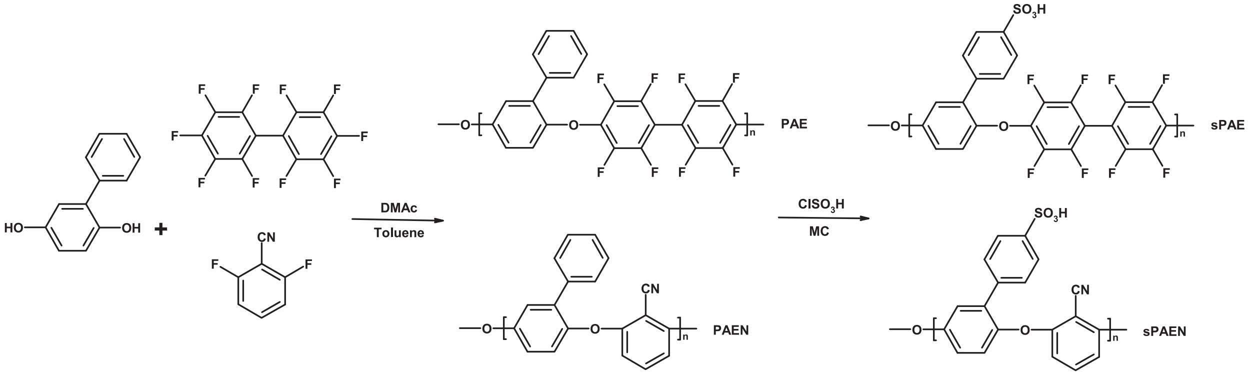

**Fig. 22.** Copoly(arylene ether)s containing pendant sulfonic acid groups and other functional groups [108].

which the absorbed molecules have access to. This behavior can be likened to sulfonated PEMs which absorb water molecules. Using this concept, PEMs with a high free volume have been investigated to absorb a large amount of water molecules and to retain them even under low humidified conditions. Of course, water swelling in sulfonated PEMs is different from and more complex than gas sorption behavior due to the much higher solvation effect of water molecules and the resulting structural change of sulfonated PEMs. As a result, most researches have demonstrated the effect of high free volume in sulfonated PEMs with phenomenological experimental results such as high water uptake. Also, the distribution of sulfonic acid groups in the vicinity of the free volume affects the absorption of water in sulfonated polymers. In particular, little attention has been paid to the latter point, despite the many trials to prepare PEMs with high free volume.

In the early stages of PEM research in 1999 and 2000, Litt and co-workers used the above concept for a series of highly proton conductive SPIs with high chemical and mechanical stabilities [110,111]. The incorporated angular and rigid rod-like bulky comonomers and the resulting polymer structures from this work are shown in Fig. 23. Sulfonated polyimides with comonomers in categories (b) and (c) exhibited a higher *d*-spacing than those with a linear comonomer from (a) and a homopolymer because the bulky or angular comonomers could prevent polymer chain packing. The structures also displayed higher water uptake and proton conductivities at high and low humidities. The authors explained that, with larger interchain spacings, more free volume could be available for water molecules to occupy (i.e., high water uptake) and thus, a high conductivity could be maintained even at low humidity. However, the importance of connectivity of free volume was not considered in this study.

Watanabe and co-workers studied various types of sulfonated PEMs with bulky fluorenyl groups such as SPIs [112], SPAES [113–116], and sulfonated poly(arylene ether sulfone ketone)s (SPAESKs) [117,118]. Based on the findings from the Litt group, SPIs with 4,4′-(9-fluorenylidene) dianiline (FDA) were synthesized with increasing FDA compositions up to 60 mol%. The incorporation of bulky fluorenyl groups over 30 mol% caused the confinement of water molecules. As a result, the proton conductivity did not decrease even above 100 °C and high proton conductivity (1.67 S cm$^{-1}$) was attained at 120 °C and 100% RH [112]. In the following studies, Watanabe and co-workers introduced sulfonic acid groups to bulky fluorenyl groups so as to obtain the synergistic effect of a high water affinity via the formation of high free volume and high hydrolysis stability via the introduction of acidic groups on the pendant phenyl groups [113,114]. This idea was later expanded to the concept of PEMs with high IECs (detailed in Section 2.2.4) and PEMs with highly sulfonatable monomers (discussed in Section 2.2.5). Both homopolymers and copolymers of sulfonated poly(arylene ether sulfone)s (SPAESs) were prepared via the polymer sulfonation method (Fig. 24), where regioselective substitution of the 2,7-positions of the pendant fluorenyl groups (not on the main chain) with sulfonic acid groups was performed using a careful sulfonation reaction. The sulfonation reaction was successfully carried out with a low concentration of chlorosulfuric acid. The resulting PEMs, especially the homopolymer PEM with an IEC of 1.80 mequiv. g$^{-1}$, exhibited very high oxidative stability in hot Fenton's reagent and high hydrolytic stabilities at 140 °C and 100% RH due to the location of the sulfonic acid groups on the pendant groups [114]. One of the homopolymer-type PEMs with an IEC of 1.14 mequiv. g$^{-1}$ exhibited a proton conductivity that was comparable to Nafion® 112 and displayed the highest maximum proton conductivity at 140 °C. However, in contrast to the results attained by the Litt group, most of the membranes showed a much higher dependence on humidity than Nafion® 112.

### 2.2.3. Hydrophilic–hydrophobic multiblock copolymers

An attractive way to obtain distinct phase separation is to fabricate multiblock copolymers composed of hydrophilic and hydrophobic blocks. Highly phase-separated hydrophilic blocks can form well-defined nano-sized water channels for proton conduction, which result in less dependence of humidity and temperature on proton conductivity, as well as an overall reduction in both the water uptake and dimensional changes compared with random copolymer of the same IEC.

McGrath and co-workers first adapted the concept of distinct phase separation in block copolymers to sulfonated aromatic PEMs, such as SPAESs and SPIs, and extensively

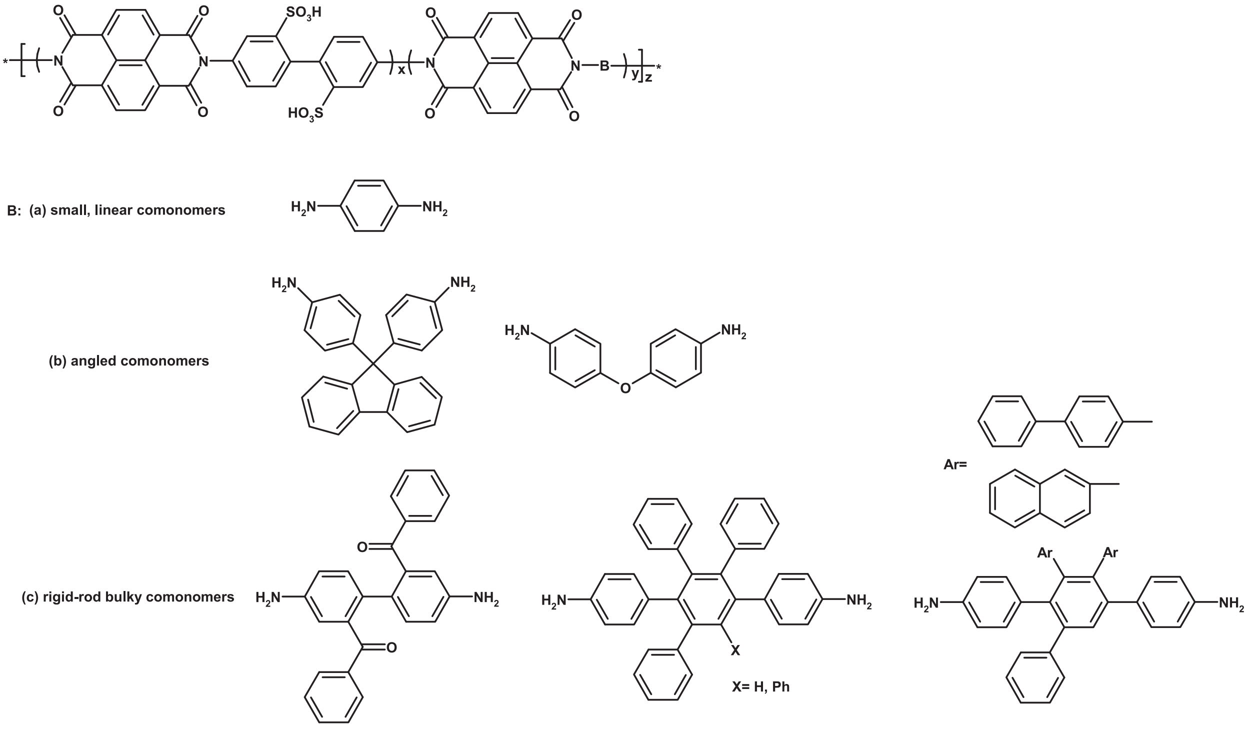

**Fig. 23.** Chemical structure of a series of rigid-rod sulfonated polyimides [110].
[110] Copyright 1999, American Chemical Society.

studied novel sulfonated multiblock copolymers using various sulfonated monomers [73,74,119–123]. Images of well-defined nano-phase separation were obtained for sulfonated multiblock SPAES copolymers, and the PEMs had high proton conductivity even under low humidity conditions below 40% RH. The first report pertaining to multiblock copolymers from this group detailed the use of multiblock copolymers with sulfonated poly(4′-phenyl-2,5-benzophenone) as the hydrophilic block and poly(arylene ether sulfone) (PAES) as the hydrophobic block [119]. The multiblock copolymers did not exhibit characteristic nano-phase separation described above, probably due to their low IECs. In subsequent research using highly activated fluorine-terminated telechelics and hydroxyl-terminated telechelics, sulfonated-fluorinated PAE multiblocks were successfully synthesized with high IECs up to 2.2 mequiv. $g^{-1}$ (Fig. 25). The multiblock copolymers exhibited proton conductivities that were higher than that of Nafion®, particularly under low humidity conditions [73]. The authors concluded that well-defined phase separation in their multiblock copolymers, which was confirmed by AFM images, resulted in high proton conductivity. The McGrath group used AFM imaging to show nano-phase separation in their membranes because, unlike TEM images, AFM images can be obtained under hydrated conditions. The same group also studied the effect of block length on morphology and PEM performance. Fig. 26 shows the chemical structure and the AFM images of a segmented sulfonated poly(arylene ether sulfone)-*b*-polyimide copolymer [74]. In related studies, well-defined nano-phase separated morphologies were attained for multiblock copolymers as the block length was increased. This in turn improved the proton conductivity and water uptake of the structures [74,121]. In particular, multiblock copolymers based on sulfonated and non-sulfonated poly(arylene ether sulfone) oligomers exhibited anisotropic swelling behavior (i.e., a lower in-plane swelling, but higher through-plane swelling than a random copolymer and Nafion® with isotropic swelling behaviors). This could be advantageous in actual fuel cell systems operated under low humidified conditions by reducing the effect of dimensional miss-match between hydrocarbon PEM and PFSA ionomer-catalyst [121]. Multiblock copolymers exhibit proton conductivities that are less RH-dependent and higher than that of Nafion® [124].

Ueda and co-workers suggested new approaches to synthesize sulfonated multiblock copoly(ether sulfone)s via the nucleophilic aromatic substitution of hydroxyl-terminated oligomers with a chain extender for PEMFC (see Fig. 27(a)) [125,126]. Decafluorobiphenyl (DFB) was used as a chain extender, due to its high reactivity, which could prevent the ether–ether interchange reaction and the resulting randomized polymer architecture. Accordingly, their multiblock copolymers were obtained with high molecular weights, and the hydrophilic and hydrophobic block lengths could be controlled. The resulting PEMs had high oxidative stability and low dimensional swelling ratio. In particular, they showed higher proton conductivity than random copolymers, and could maintain comparatively high proton conductivity even under 50% RH [125]. These properties were further investigated with multiblock copolymers having various block lengths [126]. The

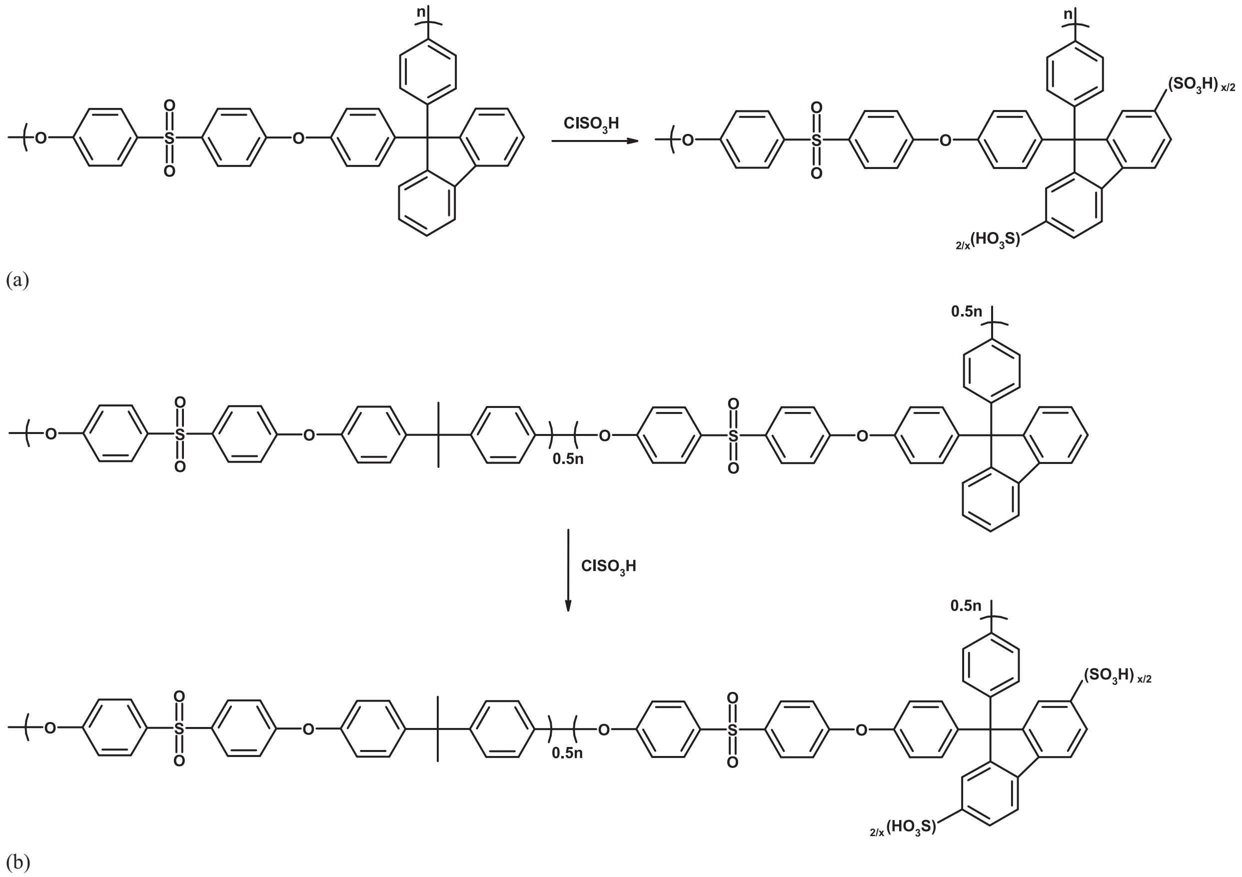

**Fig. 24.** Chemical structure of sulfonated poly(arylene ether sulfone)s having sulfofluorenyl groups: (a) homopolymer type and (b) copolymer type [113,114].
[114] Copyright 2005, American Chemical Society.

resulting membranes also had high oxidative stability and maintained high water uptake (7.3–18.7 wt%) even under 50% RH. Their proton conductivities with the optimized oligomer lengths were higher than that of Nafion® 117 at 80 °C and 95% RH, and showed a high value of 0.007 S cm$^{-1}$ even under 50% RH. Fig. 27(b) shows the cross-sectional morphology of multiblock copolymer with block lengths of 14,000/14,000 ($M_n$ of hydrophilic/hydrophobic oligomers), which showed a clear hydrophilic/hydrophobic-separated structure and contributed to effective proton conduction.

### 2.2.4. Grafted or branched sulfonated hydrocarbon copolymers

In 2002, Ding et al. performed a pioneering model study where a sulfonated graft polymer composed of a polystyrene backbone and a poly(sodium styrene

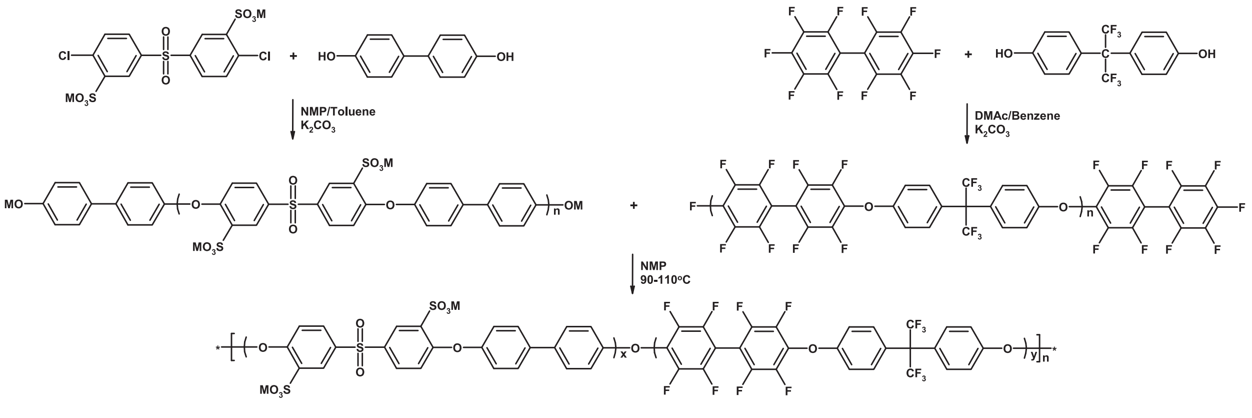

**Fig. 25.** Multiblock sulfonated-fluorinated poly(arylene ether)s [73].

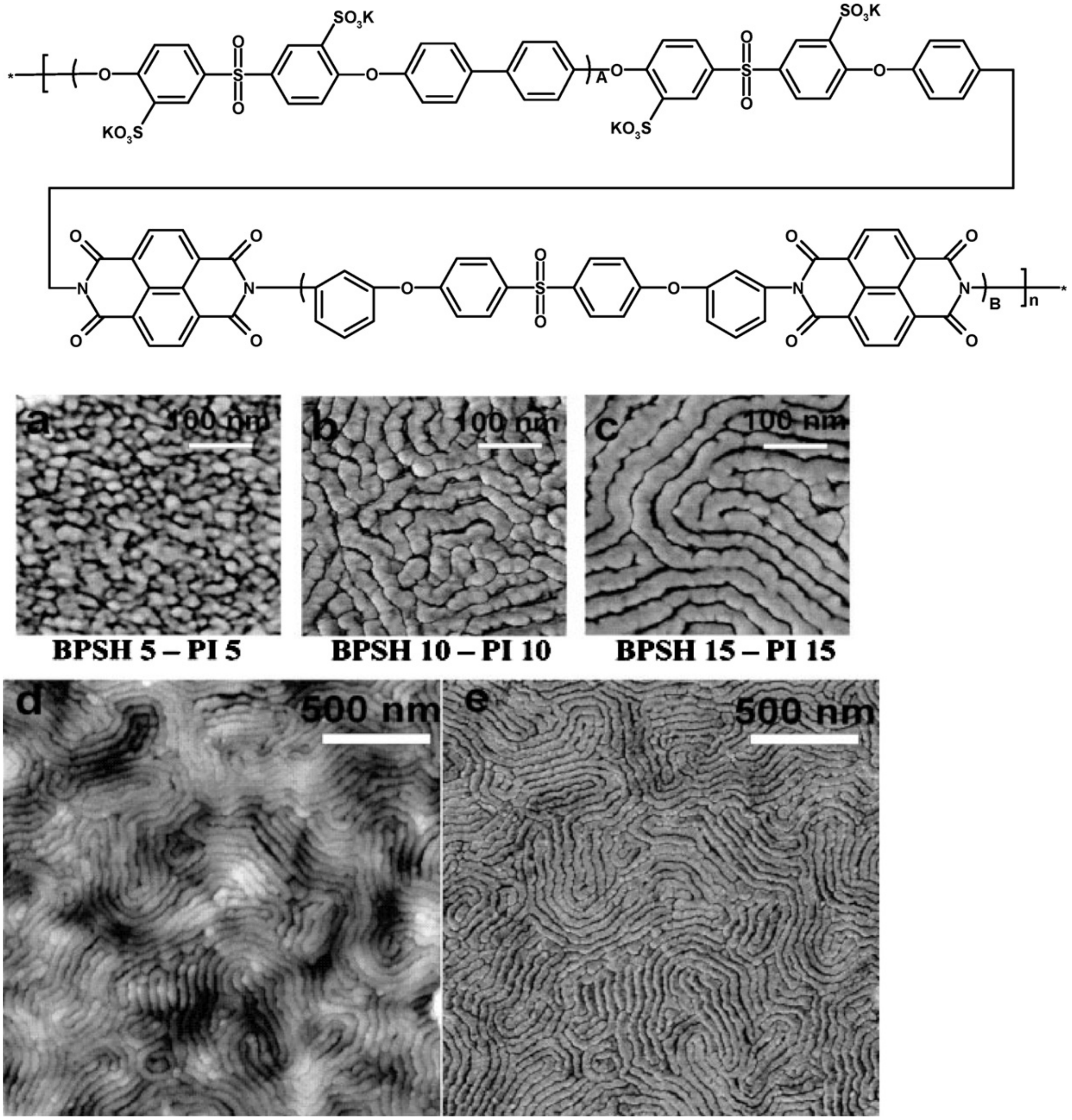

**Fig. 26.** Chemical structure of sulfonated poly(imide)s based on 3,3′-disulfonic acid-bis [4-(3-aminophenoxy)phenyl]sulfone (SA-DADPS) and their AFM images [74].

sulfonate) side chain was synthesized via free-radical polymerization [53]. Phase separation of ionic aggregates was shown to be controlled by the chain length of the graft chains, which had a direct effect on the proton conductivity. As expected, the copolymer with the longer graft chain exhibited higher proton conductivity. However, the authors stated that the commercial applicability of the fabricated grafted copolymers was limited, probably due to the poor stability of the styrene-based backbone and side chain. Ding and co-workers expanded the above concept to a much more stable highly fluorinated backbone and successfully fabricated novel comb-shaped copolymers (see Fig. 28). In particular, the $\alpha$-methyl polystyrene hydrophilic side chain of the structures induced strong phase separation in the hydrophobic fluorinated main-chain, which was confirmed by TEM and SAXS [54]. However, while the initial performance of the structures was superior to that of Nafion® and BPSH-35 in a DMFC, the current density was reduced due to the instability of the side chain [127].

Guiver and co-workers designed comb-shaped SPAES with a new sulfonated side-chain grafting unit containing two or four sulfonic acid groups, as shown in Fig. 29 [128]. PAES containing a methoxy group was first synthesized via a conventional aromatic nucleophilic substitution. The methoxy groups were then converted to a reactive hydroxyl group suitable for grafting. Finally,

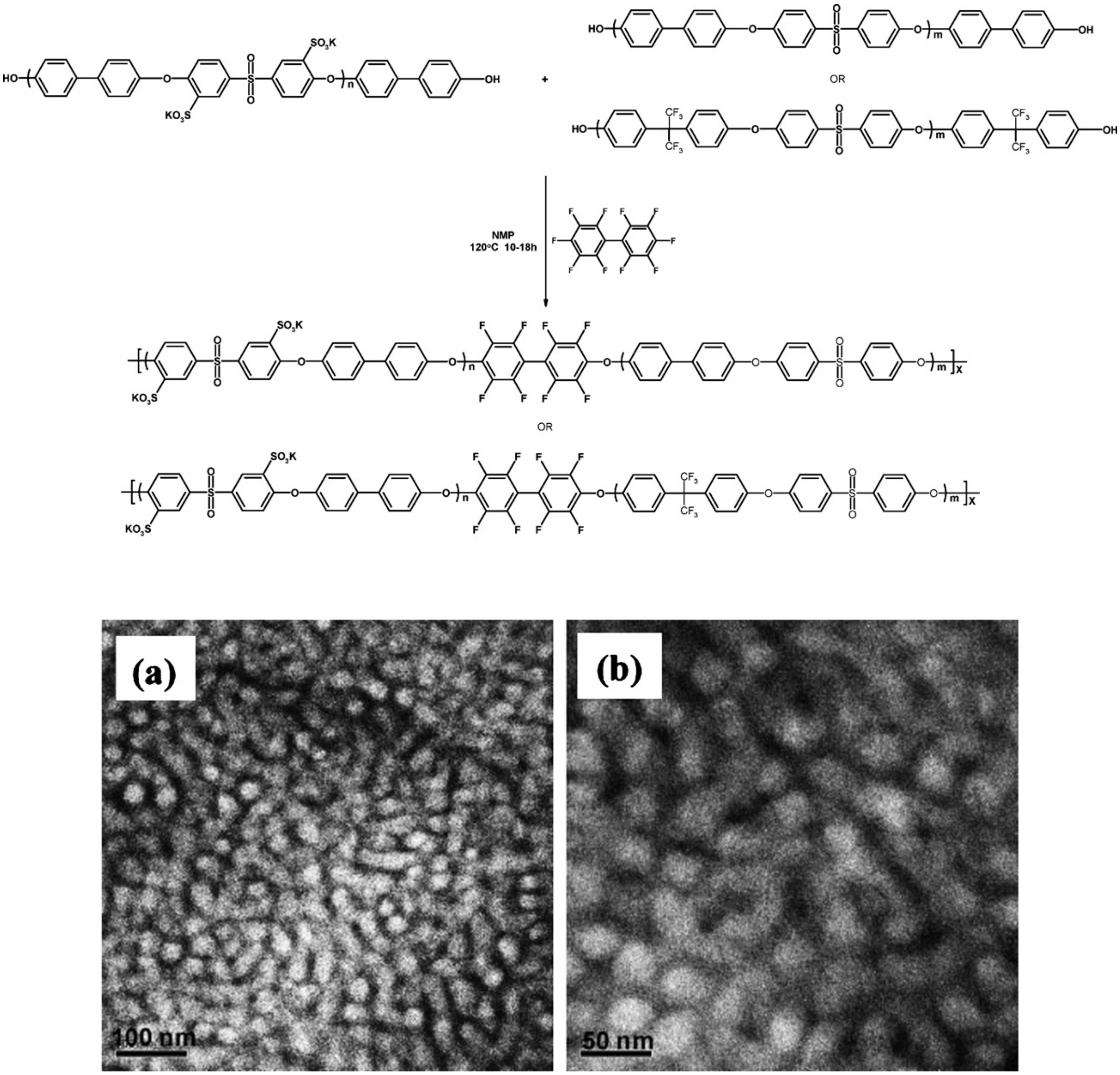

**Fig. 27.** Synthetic route of sulfonated multiblock copoly(ether sulfone)s and the TEM images showing the cross-sectional morphology of multiblock copolymer with bock lengths of 14,000/14,000 ($M_n$ of hydrophilic/hydrophobic oligomers) with (a) low resolution and (b) high resolution [125,126].

the functional copolymer was grafted with previously synthesized sulfonated side chains. The resulting comb-shaped copolymers with two or four sulfonic acid groups exhibited high proton conductivities (0.034–0.147 and 0.063–0.125 S cm$^{-1}$, respectively) and low water uptakes (18–60 and 27–53%, respectively).

The Ueda research group expanded the above strategy to star-shaped block copolymers (Fig. 30) [129]. Star-shaped sulfonated block copoly(ether ketone) with hydrophilic and hydrophobic blocks as arms was synthesized via a Friedel–Crafts reaction of a tri-functional core. The structure was subsequently sulfonated with concentrated sulfuric acid. The hydrophilic block with sulfonated sites was attached directly to the core and the hydrophobic block was placed at the end of each arm. The resulting sulfonated polymers were soluble in common polar aprotic solvents and the solvent-cast membranes were tough and flexible. Due to their structural characteristics, the membranes exhibited relatively good dimensional stability despite their high water uptake. In particular, the proton conductivities of the membranes were comparable and/or higher than those of Nafion® at 80 °C and 50–95% RH.

Lee et al. reported on grafted SPI membranes that were prepared through thermal-solution imidization and the subsequent incorporation of sulfoalkylated grafting agents with different alkyl chain lengths, as shown in Fig. 31 [130]. The additional sulfonic acid (–$SO_3H$) groups at the end of the sulfoalkylated side chains significantly contributed to

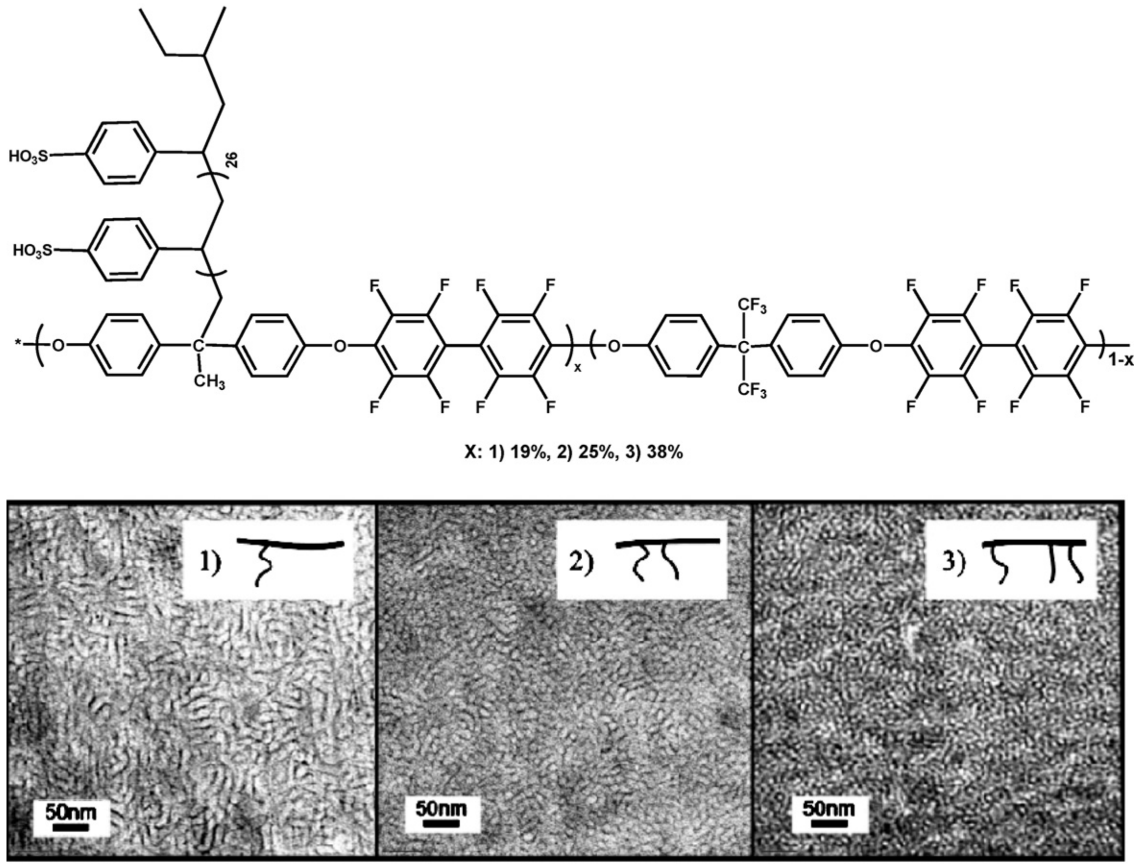

**Fig. 28.** Chemical structure of highly fluorinated comb-shaped copolymers and their TEM images; their side chain monomer contents and IECs are (1) 19 wt%, 0.87 mequiv. $g^{-1}$, (2) 25 wt%, 1.40 mequiv. $g^{-1}$, and (3) 38 wt%, 1.75 mequiv. $g^{-1}$, respectively [54].

enhancements in both the IEC and proton conductivity. Furthermore, the resulting PEMs displayed a much improved level of ductility when compared to pristine SPI due to the internal plasticizing effect of the alkyl side chain. While grafted SPIs with long graft chains exhibited lower IECs than those with short side chains, they had a relatively higher number of water molecules per $-SO_3H$ group and a large amount of bound water, which resulted in their higher proton conductivity. In addition, the low acidity of the resulting PEMs with long graft chains improved their durability to chemical attack, such as in hydrolysis and radical-induced decomposition.

### 2.2.5. Sulfonated hydrocarbon PEMs with high IEC

Kreuer and co-workers recently suggested a very promising strategy involving the formation of extremely electron-deficient poly(arylene) with a high IEC. A series of sulfonated poly(phenylene sulfone)s (SPPSfs) containing only sulfone units ($-SO_2-$; electron-withdrawing group) connecting the phenyl rings was prepared via a two-step process consisting of a nucleophilic aromatic polycondensation reaction to prepare sulfonated poly(phenylene sulfide sulfone)s (SPPSSfs) and their subsequent oxidation to SPPSfs (see Fig. 32) [63,131,132]. These ionomers exhibited increased acidity and higher hydrolytic stability of the sulfonic acid groups due to the absence of electron-donating groups, such as ether linkages, in their backbone structure. High thermo-oxidative stability and water insolubility was observed even at high IECs, due to the crystallinity (physical crosslinking) of the ionomers. The crystallinity resulted from the rigidity of the diarylsulfone unit and a high degree of intermolecular interaction. The copolymer-type ionomers (Fig. 32(a)) displayed IEC values in the range of 1.29–2.64 mequiv. $g^{-1}$, were still insoluble in water, and exhibited higher proton conductivities than that of Nafion® [63]. However, the degree of sulfonation (i.e., the ratio of sulfonated phenyl rings to unsulfonated rings) of the copolymer-type ionomers was limited to less than 50% due to their structural limitations. Through modifying the preparation route using $Na_2S$ as the sulfide, Kreuer et al. obtained SPPSf that was monosulfonated (100% DS) on each phenyl ring ($sPSO_2$-220, see Fig. 32(b)) and had an extremely high IEC (4.3–4.5 mequiv. $g^{-1}$) [131]. In its dry state, the polymer also possessed a remarkably high density (1.75 g $cm^{-3}$) that was nearly as high as the density of pure sulfuric acid ($H_2SO_4$; 1.83 g $cm^{-3}$). Kreuer et al. stated that the density of $sPSO_2$-220 appeared to be the highest among all of the reported aromatic non-fluorinated polymers. The $sPSO_2$-220 also exhibited very high thermo-oxidative and hydrothermal stability, but unfortunately, it was soluble in water due to its high IEC. With regards to the hydra-

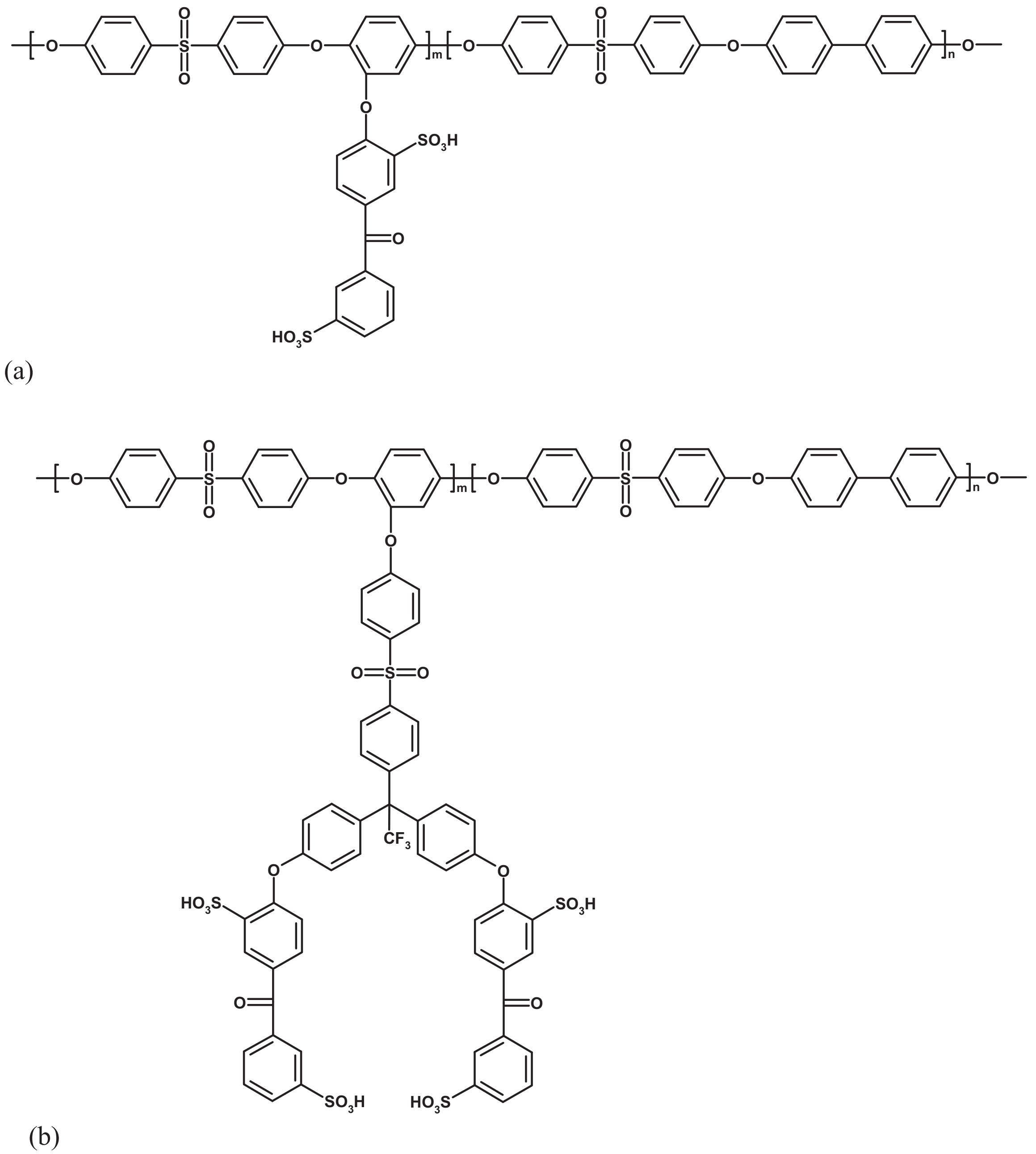

**Fig. 29.** Chemical structure of the comb-shaped sulfonated poly(arylene ether sulfone) having a sulfonated side-chain grafting unit containing (a) two or (b) four sulfonic acid groups [128].
[128] Copyright 2008, American Chemical Society.

tion behavior and proton conductivity of $sPSO_2$-220, Kreuer and co-workers cited its unique microstructural and transport features [132]. A high DS leads to the development of a microstructure characterized by narrow, hydrated, and hydrophilic domains that are highly connected on a longer scale. For $sPSO_2$-220, its high absolute water uptake at given relative humidities and its high charge carrier concentration corresponding to a high IEC ($\sim$4.5 mequiv. $g^{-1}$) resulted in very high proton conductivities, but a low water transport coefficient. In particular, these trends became more evident at higher water contents and temperatures. As a result, the proton conductivity of $sPSO_2$-220 was seven times higher than that of Nafion® under low humidity (30% RH) and high temperature (135 °C) conditions.

The above concept (i.e., well-connected but narrow hydrophilic domains) is somewhat different from the main idea of this review on how to establish distinct phase separation between hydrophobic and hydrophilic moieties (i.e., well-connected and wider hydrophilic domains). As mentioned previously, since hydrocarbon PEMs have func-

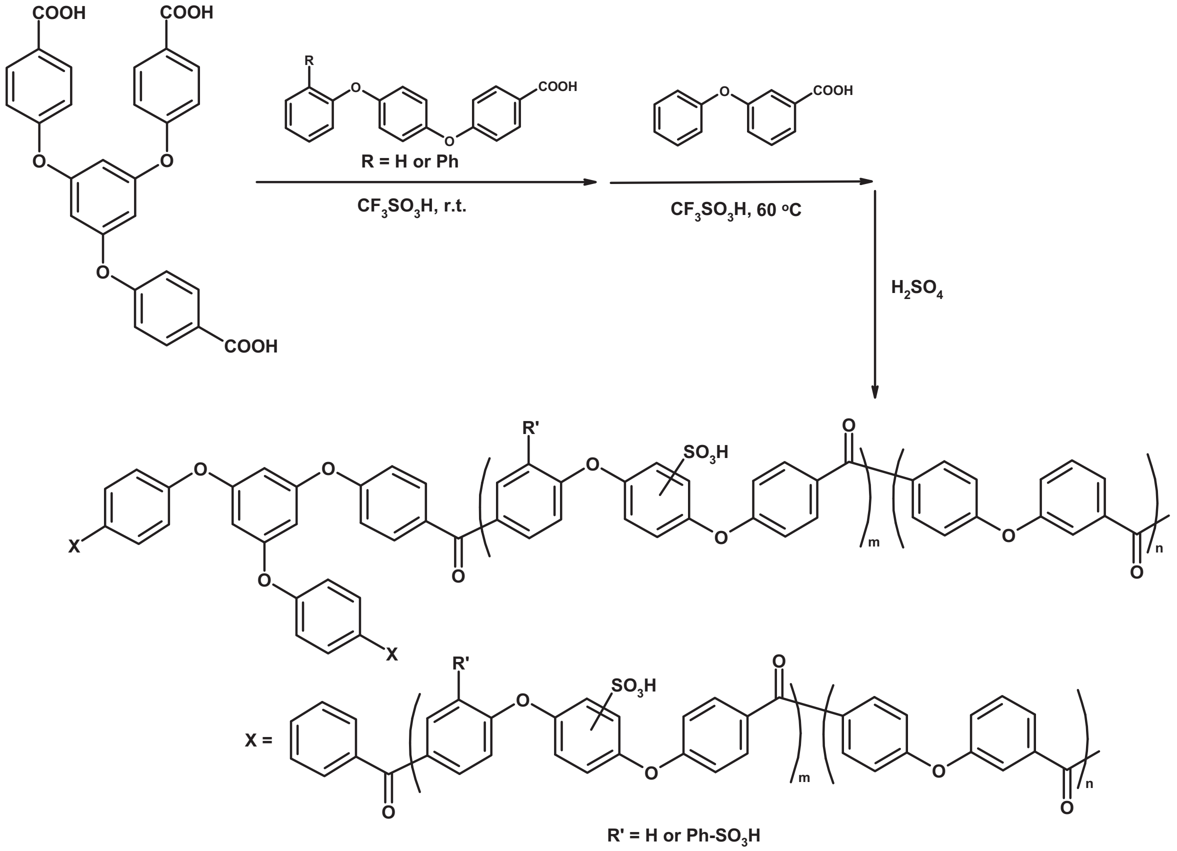

**Fig. 30.** Synthetic route of star-shaped sulfonated block copoly(ether ketone)s [129].
[129] Copyright 2008, American Chemical Society.

tional groups that can interact with water molecules even in hydrophobic moieties, water molecules are distributed through the whole PEM matrix and thus, cannot form a distinct water channel, as shown in Fig. 2. This scenario results in decreased proton conductivity for hydrocarbon PEMs [38]. Consequently, most research on hydrocarbon PEMs to date has focused on how to make well-connected and wider water channels by concentrating proton-conductive sulfonic acid groups onto the hydrophilic block. As suggested in these studies, dispersing a large amount of sulfonic acid groups throughout PEMs (i.e., high IECs) to increase the water content (which can play a role in transporting protons) can lead to the formation of well-connected but narrow water channels. These channels can in turn decrease the water osmotic drag coefficient, which is a potential problem in wider water channels, without sacrificing proton conductivity. Considering the advantages of this approach, such as high proton conductivity and a low water osmotic drag coefficient, the concept of well-connected but narrow water channels (e.g. sPSO$_2$-220) appears to be highly innovative and promising.

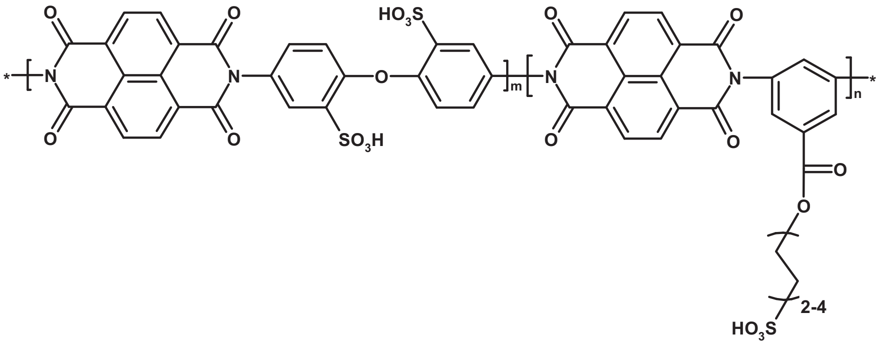

**Fig. 31.** Chemical structure of grafted sulfonated polyimide (SPI) membranes with different alkyl side-chain chain lengths [130].

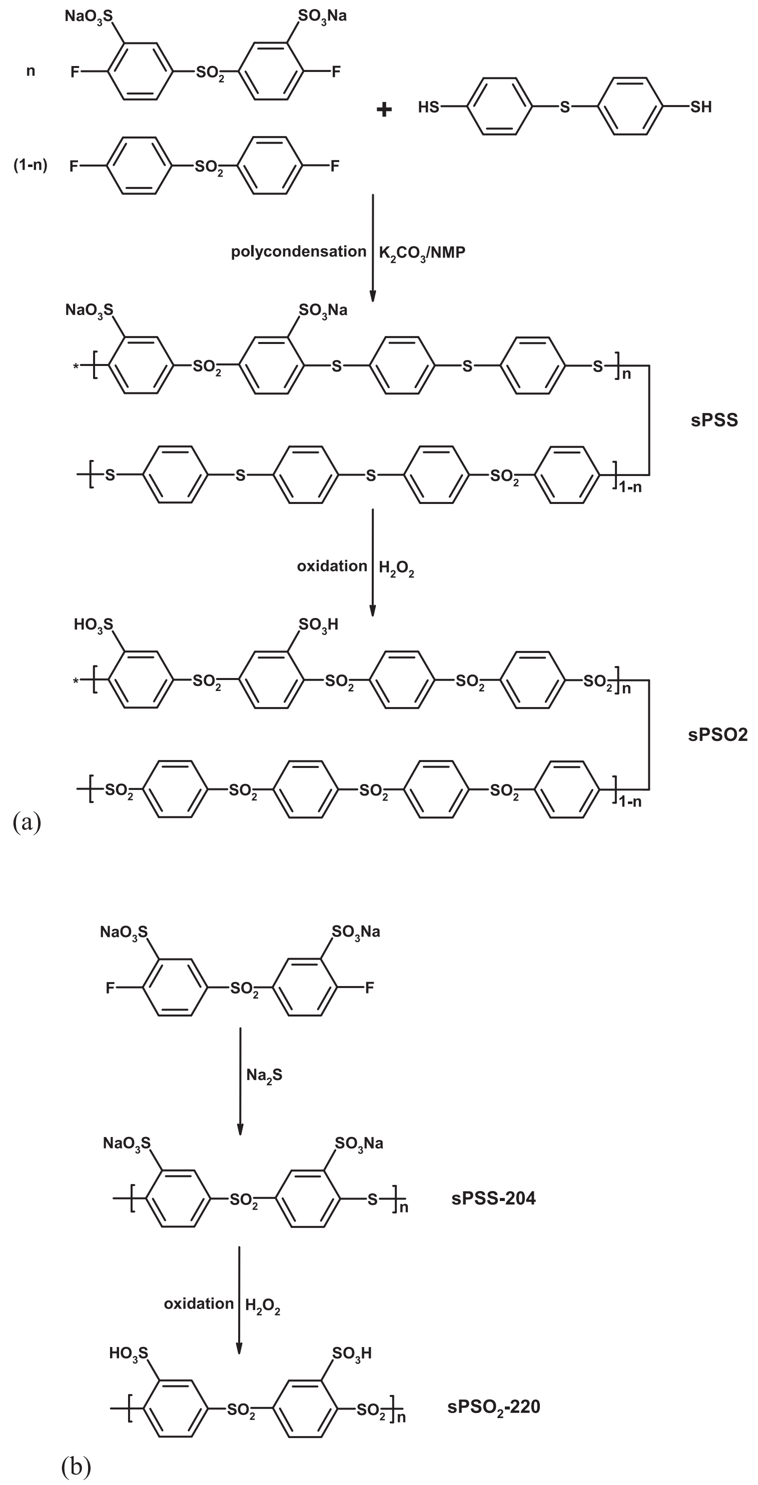

**Fig. 32.** Synthetic route of sulfonated poly(phenylene sulfone)s with high IECs: (a) copolymer type [63] and (b) homopolymer type [131,132]. [63] Copyright 2007, American Chemical Society; [131] Copyright 2009, American Chemical Society; [132] Copyright 2009, Royal Society of Chemistry.

Watanabe et al. used the concept of sulfonated PEMs with high IEC to overcome the high humidity dependency in proton conductivity in their sulfonated PEMs discussed in Section 2.2.2. The introduction of methyl groups enabled the SPAESs to have high IECs in the range of 1.32–3.26 mequiv. $g^{-1}$ (Fig. 33) without sacrificing hydrolytic, oxidative, dimensional, and mechanical stability [115]. The researchers used a flow reactor for sul-

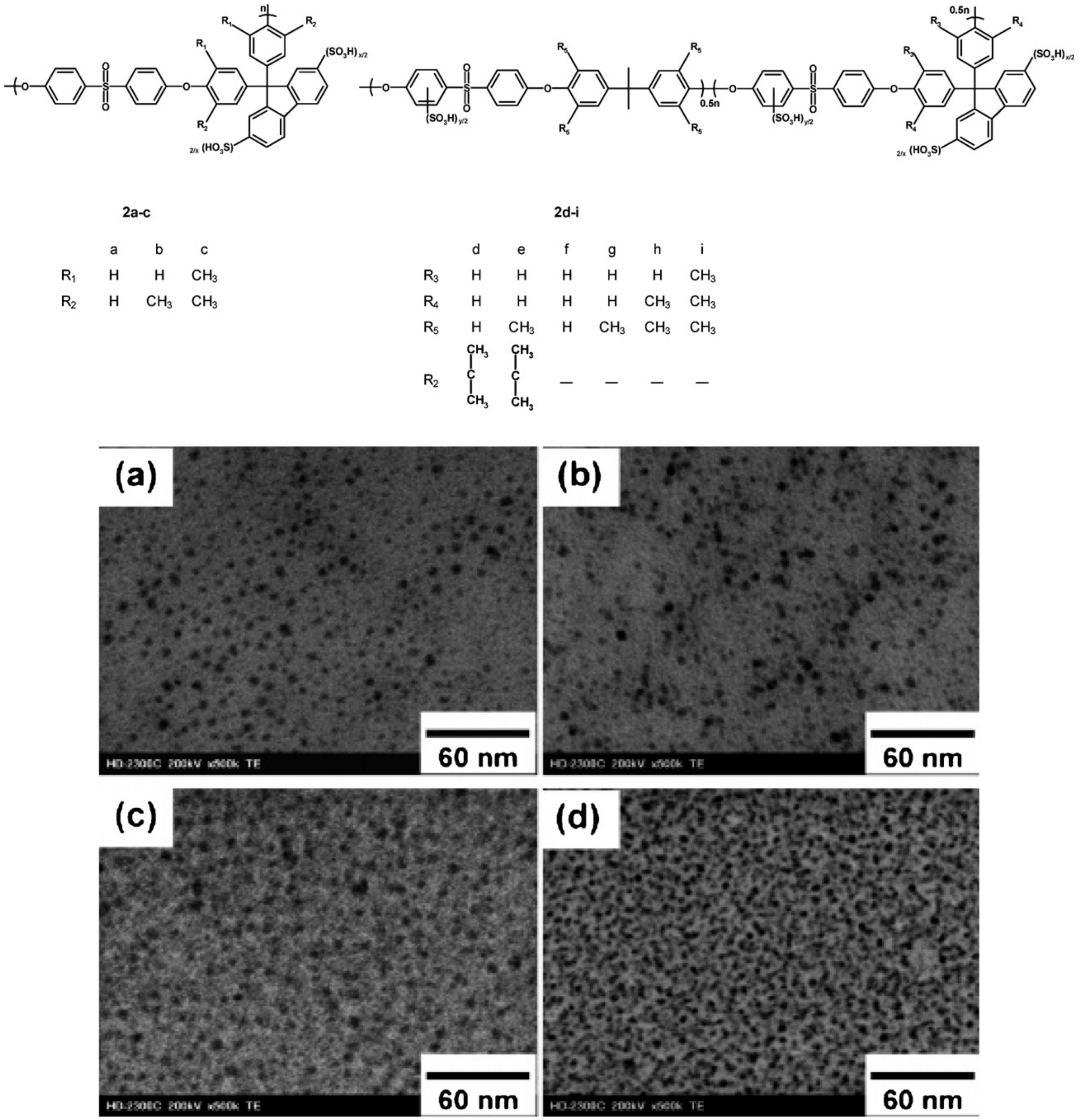

|  | a | b | c |
|---|---|---|---|
| $R_1$ | H | H | $CH_3$ |
| $R_2$ | H | $CH_3$ | $CH_3$ |

|  | d | e | f | g | h | i |
|---|---|---|---|---|---|---|
| $R_3$ | H | H | H | H | H | $CH_3$ |
| $R_4$ | H | H | H | H | $CH_3$ | $CH_3$ |
| $R_5$ | H | $CH_3$ | H | $CH_3$ | $CH_3$ | $CH_3$ |
| $R_2$ | $C(CH_3)_2$ | $C(CH_3)_2$ | – | – | – | – |

**Fig. 33.** Chemical structure of methyl-substituted sulfonated poly(arylene ether sulfone)s having sulfofluorenyl groups and their STEM images: (a) 2a (IEC = 1.58 mequiv. g$^{-1}$); (b) 2a (IEC = 2.51 mequiv. g$^{-1}$); (c) 2e (IEC = 3.26 mequiv. g$^{-1}$); and (d) Nafion® 112 [115].
[115] Copyright 2007, American Chemical Society.

fonation in order to overcome the poor solubility of the resulting sulfonated polymers. The reactor allowed for sulfonic acid groups to be introduced to the main chain under more severe conditions, such as a higher concentration of chlorosulfuric acid. Methyl groups on the isopropylidene biphenyl segment (R5 positions) were more effective than methylation on fluorenyl units in imparting high mechanical stability, hydrolytic stability, and dimensional stability. In particular, membrane 2e in Fig. 33 with the highest IEC (3.36 mequiv. g$^{-1}$) exhibited very low dimensional swelling in the area and thickness directions, despite having the highest water uptake. Membrane 2e also had proton conductivities that were comparable to, or even higher, than Nafion® 112 at 80–120 °C and 20–93% RH. The authors explained that the desirable properties of membrane 2e were the result of well-connected ionic clusters, as shown in Fig. 33.

Ueda and co-workers extended their multiblock copolymer structures to the concept of sulfonated hydrocarbon PEMs with high IEC [133]. In their study, using additional post-sulfonation reaction with concentrated sulfuric acid to the multiblock copolymer structure in Fig. 27(a), highly sulfonated multiblock copolymers were successfully obtained with the IEC range of 1.90–2.75 mequiv. $g^{-1}$. In particular, their multiblock copolymer with IEC of 2.75 mequiv. $g^{-1}$ showed high proton conductivity, comparable with Nafion® 117 in the range of 50–95% RH, and maintained its high proton conductivity of 0.0023 S $cm^{-1}$ even under 30% RH. Using the resulting highly sulfonated multiblock copolymers, crosslink reaction between sulfonic acid groups in their main chains were also tried in the presence of the condensation agent [134].

Ueda and co-workers also fabricated stable PEMs by incorporating binaphthalenyl groups in SPAES [135]. Highly sulfonated PAES (SPAES) with binaphthyl units and a very high IEC (3.01 mequiv. $g^{-1}$) was synthesized via nucleophilic aromatic polymerization, as shown in Fig. 34(a). Despite its high IEC, the resulting membrane (BNSH-100) exhibited high mechanical stability in the dry state and controlled dimensional changes in its hydrated state (80 °C and 95% RH). In particular, BNSH-100 had a high water uptake of 18.7 and 11.6 wt% at 50 and 30% RH, respectively. The proton conductivity of BNSH-100 at 80 °C was higher than that of Nafion® 117 in the range of 30–95% RH. Ueda et al. stated that the high IEC value of BNSH-100 resulted in excellent proton conductivity over a wide range of relative humidities. In addition, the high hydrophobicity of the binaphthyl units contributed to good dimensional stability, which was confirmed by a phase-separated image taken with an AFM in tapping mode (Fig. 34(b)).

### *2.2.6. Sulfonated hydrocarbon PEMs based on highly sulfonatable monomers*

After introducing the concept of using tetraphenylphenylene ether with up to four sulfonic acid groups clustered on pendant phenyl rings via the polymer sulfonation method (as discussed in Section 2.1.1) [60,61], the Hay research group studied various other PEM designs with highly sulfonatable monomers. These designs included linear [136], branched [137,138], and dendritic multiblock [139,140] structures. Since the authors used the post-polymerization sulfonation method, electron-withdrawing groups, such as ketone and/or sulfone groups, were introduced onto the PEM backbone to avoid main chain sulfonation and enhance the solubility of the resulting polymers. Fig. 35(a) shows sulfonated linear aromatic poly(sulfide ketone)s (PSK) with six sulfonic acid groups on each hexaphenylbenzene end group [136]. When using the analogous aromatic dithiol monomers, the resulting non-sulfonated polymer was insoluble in any organic solvent due to its rigidity and regularity. With a large excess of chlorosulfuric acid in dichloromethane at room temperature, the selective and quantitative introduction of sulfonic acid groups successfully occurred only on the end groups. The resulting PEMs exhibited relatively high proton conductivities of 0.069 and 0.037 S $cm^{-1}$ when considering their very low IECs of 0.48 and 0.47 mequiv. $g^{-1}$, respectively. The author concluded that these results could be accounted for by significant phase separation in the PEMs. However, since the proton conductivity of the PEMs was insufficient for effective fuel cell operation, the Hay group used other strategies to increase the IEC of the PEMs. When using the polymer sulfonation method to fabricate sulfonated PEMs, there are two ways to increase the IEC: increase the number of sulfonatable monomers or increase the number of sulfonatable sites in the monomers. For the former strategy, sulfonated branched PEKs were synthesized in accordance with the concept of PEMs with sulfonatable end groups, as shown in Fig. 35(b) [137,138]. Hexaphenylbenzene moieties and 3,6-ditrityl-9*H*-carbazole moieties were used as end groups for sulfonation, where six and eight sulfonic acid groups, respectively, were successfully introduced. However, due to the lower reactivity of 3,6-ditrityl-9*H*-carbazole, a two-step polymerization method that was different from the one-step polymerization process for 1-(4-hydroxyphenyl)-2,3,4,5,6-pentaphenylbenzene was carried out. After sulfonation, the resulting PEMs exhibited IECs (0.76–1.09 mequiv. $g^{-1}$ and 0.99–1.25 mequiv. $g^{-1}$) and proton conductivities (0.04–0.091 S $cm^{-1}$ and 0.066–0.095 S $cm^{-1}$) that were comparable to those of Nafion® (0.91 mequiv. $g^{-1}$ and 0.098 S $cm^{-1}$). It was stated that the high proton conductivities were due to the existence of significantly phase-separated and highly interconnected ionic channels, as observed in the TEM images of Fig. 35(e). Sulfonated dendritic multiblock co-PAESs were also fabricated with hexakis(4-(4-fluorophenylsulfonyl)phenyl)benzene having 15 pendant phenyl rings as sulfonatable sites, as shown in Fig. 35(c) [139]. However, the resulting PEMs were too brittle for a proton conductivity measurement, because the introduction of bulky dendritic blocks and the use of relatively short average blocks prevented intermolecular chain entanglement. To avoid this problem, longer block lengths enabled the introduction of a much larger number (up to 13) of sulfonic acid groups and thus, improved mechanical properties were obtained (Fig. 35(d)) [140]. The proton conductivities of the resulting structures (0.058–0.067 S $cm^{-1}$) at IEC levels in the range of 0.92–1.26 mequiv. $g^{-1}$ were similar to that of Nafion® 117 (0.098 S $cm^{-1}$) at an IEC of 0.91 mequiv. $g^{-1}$ at room temperature and 100% RH condition.

Tian et al. synthesized PAEs with randomly distributed nanoclusters of 6, 12, and 18 sulfonic acid groups, as shown in Fig. 36 [141,142]. The researchers developed a monomer design based on work performed by the Hay group, as discussed in Section 2.2.1 and shown in Fig. 6. As the IECs of the resulting PEMs increased from 1.16 to 1.69 mequiv. $g^{-1}$, water uptake increased from 20%, 29%, and 35% to 60%, 88%, and 125% at 35 °C, respectively. In addition, the proton conductivities of the structures increased from 0.021 S $cm^{-1}$, 0.040 S $cm^{-1}$, and 0.039 S $cm^{-1}$ to 0.099 S $cm^{-1}$, 0.123 S $cm^{-1}$, and 0.137 S $cm^{-1}$ at 75 °C and 100% RH condition, respectively. From an analysis of TEM images, it was confirmed that spherical ionic clusters with a relatively uniform size were well-dispersed throughout the resulting membranes. PEM with monomer (c) (see Fig. 36) was found to have a larger ionic domain size (15 nm) than PEMs with monomer (a) (3 nm) and monomer (b) (12 nm) (see Fig. 36) due to its longer hydrophilic block segments.

Ueda and co-workers reported on locally and densely sulfonated PAESs [143,144]. SPAESs with eight sulfonic acid groups (Fig. 37(a)) were synthesized by the nucle-

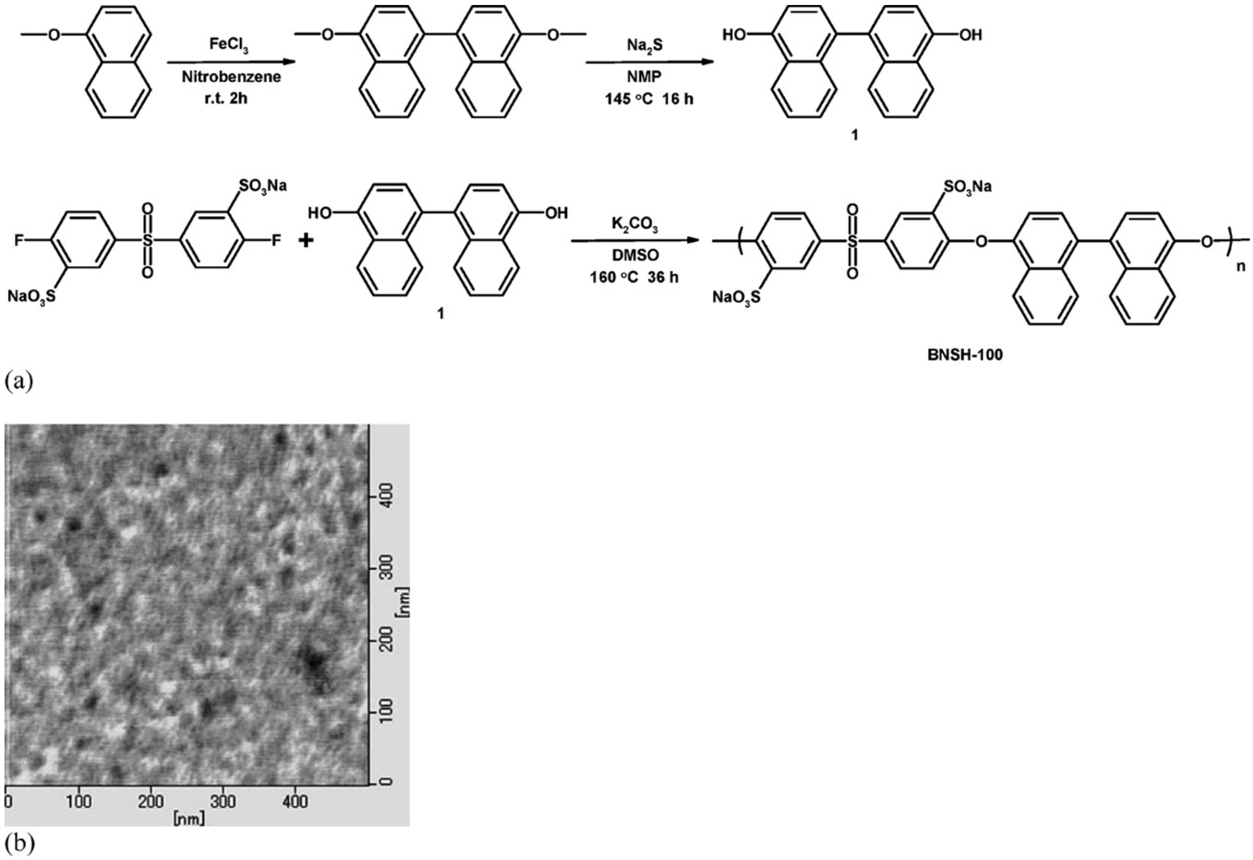

**Fig. 34.** (a) Chemical structure of a highly sulfonated poly(ether sulfone) with binaphthyl units and (b) its AFM tapping mode phase image [135]. [135] Copyright 2010, Royal Society of Chemistry.

ophilic substitution of 4,4′-dichlorodiphenylsulfone with 1,2,4,5-tetrakis([1,1′-biphenyl]-2-oxy)-3,6-bis(4-hydroxyphenoxy)benzene and 2,2-bis(4-hydroxyphenyl) hexafluoropropane, followed by sulfonation using chlorosulfonic acid [143]. However, SPAESs with ten sulfonic acid groups (Fig. 37(b)) required an additional oxidation step when compared to those with eight. Ueda and co-workers also synthesized PAESs by the nucleophilic substitution of bis(4-fluorophenyl) sulfone with 1,2,4,5-tetrakis([1,1′-biphenyl]-2-oxy)-3,6-bis(4-hydroxyphenoxy) benzene and bis(4-hydroxyphenyl) sulfide that was oxidized using m-chloroperoxybenzoic acid; the structures were sulfonated using sulfuric acid [144]. The resulting PEMs exhibited excellent proton conductivity over a wide range of relative humidities due to their well-defined phase-separated structure. The phase separation was the result of the large difference in polarity between the hydrophilic and hydrophobic segments of the polymer backbone. In particular, the PEM with an IEC of 2.38 mequiv. $g^{-1}$ exhibited proton conductivity that was comparable to that of Nafion® 117 at 30% RH.

The Watanabe research group reported sulfonated block copolymers having highly sulfonatable fluorenyl groups. The researchers combined three concepts in their work: PEMs with a high free volume, multiblock PEMs, and the introduction of highly sulfonatable monomers as discussed in Sections 2.2.2, 2.2.3, and 2.2.6, respectively [116–118]. In particular, SPAESKs containing a hydrophobic sulfone-ketone block structure were fabricated via the polymer sulfonation method, with 100% selective sulfonation of all phenyl rings of the fluorenyl moieties occurring, without sulfonation of the hydrophobic block (see Fig. 38) [117,118]. STEM images revealed rod-like and well-interconnected aggregation of the hydrophilic block. According to the authors, the aggregation was the result of the high local concentration of sulfonic acid groups within the hydrophilic blocks, which enhanced phase separation between the hydrophilic and hydrophobic blocks. The aggregation of hydrophilic blocks was more distinct with increases in the IEC and the hydrophilic block length. X30Y8 with an IEC = 1.62 mequiv. $g^{-1}$ and well-defined phase separation (see images in Fig. 38(c) and (d)) exhibited a similar or higher proton conductivity than Nafion® over a wide humidity range. The structure also retained its high proton conductivity at 110 °C, which could enable successful fuel cell operation even under harsh conditions (100 °C and 53 or 30% RH). The sulfonated PEMs in this study exhibited anisotropic swelling behavior with larger dimensional changes in the through-plane direction than in the in-plane direction. The PEMs also displayed very high hydrolytic stability and moderate oxidative stability.

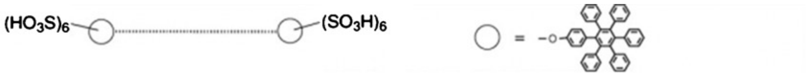

(a) Sulfonated linear **PSK**, $(PhCOPhCOPhSPhCOPhCOPhS)_n$ or $(PhCOMe_4PhCOPhSPhCOPhCOPhS)_n$

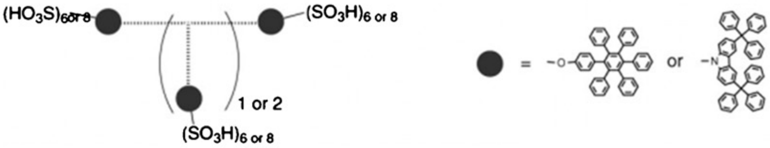

(b) Sulfonated branched **PEK**, $(PhSO2PhOPhCOPhO)_n$ or $(PhCOMe_3PhCOPhOPhCOPhO)_n$

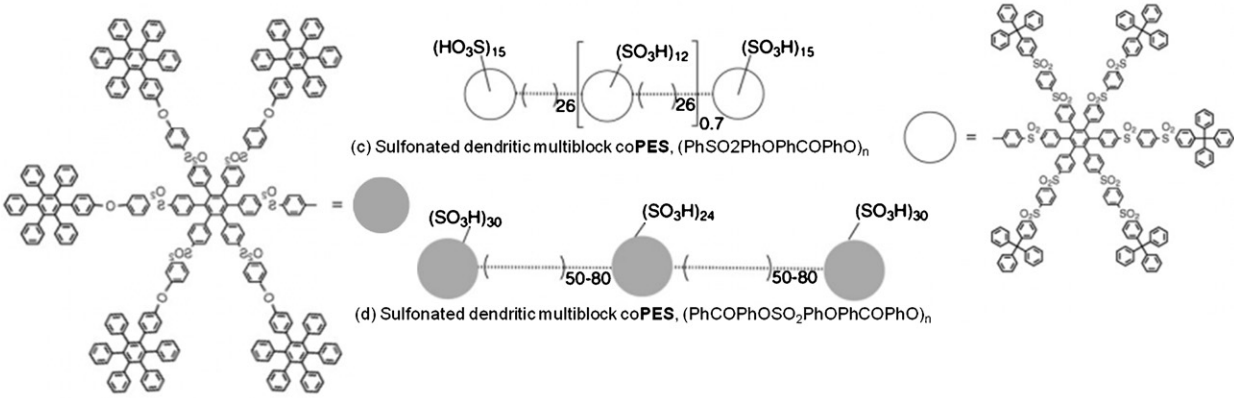

(c) Sulfonated dendritic multiblock co**PES**, $(PhSO2PhOPhCOPhO)_n$

(d) Sulfonated dendritic multiblock co**PES**, $(PhCOPhOSO_2PhOPhCOPhO)_n$

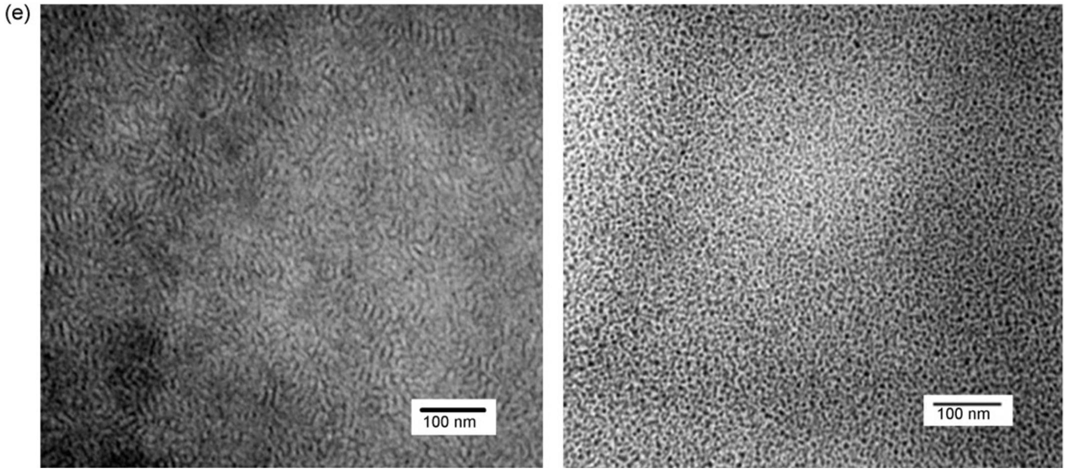

**Fig. 35.** Chemical structure of sulfonated PEMs having highly sulfonatable end groups by Hay's group: (a) sulfonated linear PSK [136]; (b) sulfonated branched PEK [137,138]; (c) sulfonated dendritic multiblock coPES [139]; (d) sulfonated dendritic multiblock coPES [140]; and (e) TEM micrographs of sulfonated branched PEK and Nafion® [137].
[136] Copyright 2008, American Chemical Society; [137] Copyright 2008, American Chemical Society.

Li et al. utilized this concept to synthesize SPAES copolymers having two or four sulfonated pendant phenyl rings using monomer sulfonation method as well as post-polymerization sulfonation method, as shown in Fig. 39 [145]. Monomer sulfonation led to sulfonated monomers having two or four pendent sulfonic acid groups at the p-phenyl position. In particular, SPAES with four sulfonic acid groups exhibited high proton conductivity and lower water uptake. The high performance was attributed to the more blocky and locally concentrated sulfonic acid groups in the SPAES.

### 2.2.7. *Properties of sulfonated hydrocarbon PEMs*

In this section, major properties of PEMs (i.e., water uptake and proton conductivity) that determine PEMs performance and stability will be discussed focusing on the recent trends in sulfonated hydrocarbon PEMs. Most literature discussed in this review used Nafion® (particularly

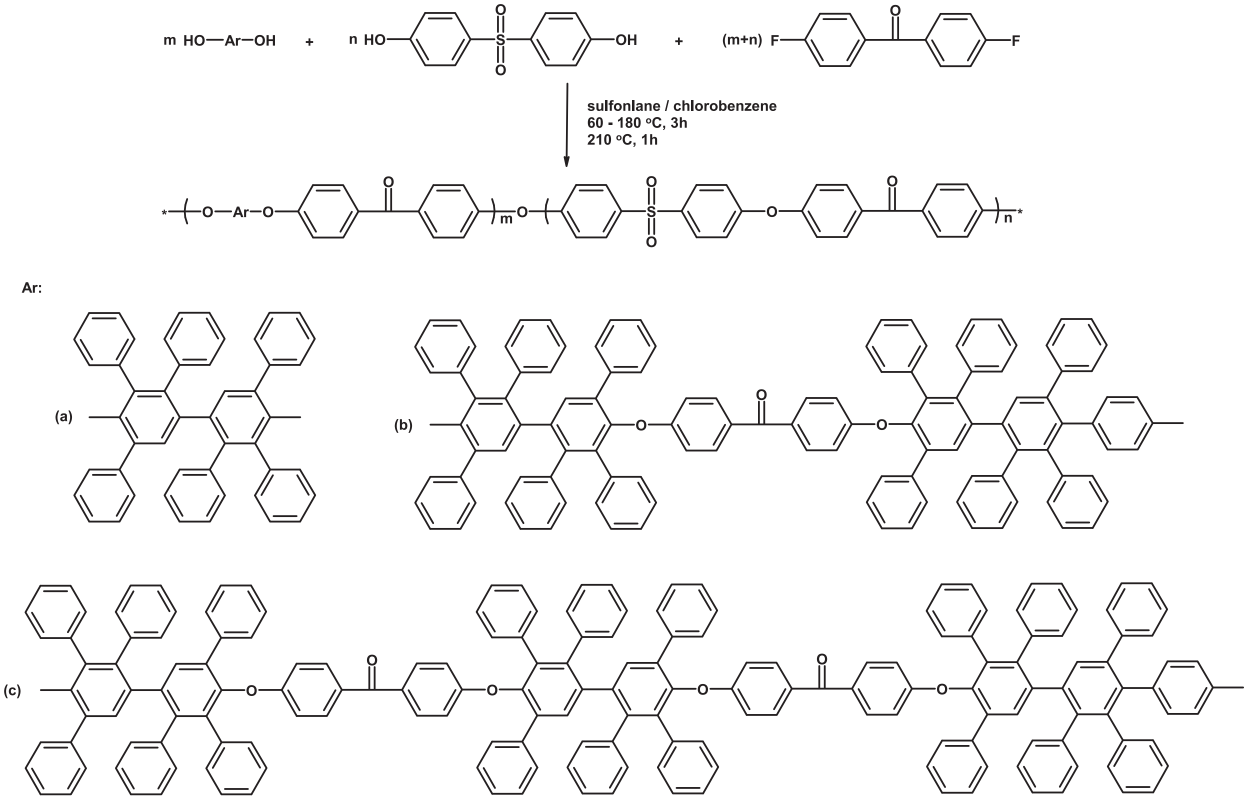

**Fig. 36.** Chemical structure of poly(aryl ether)s having 6, 12 and 18 sulfonatable pendant phenyl groups [141,142].
[141] Copyright 2009, American Chemical Society.

Nafion® 112) with IEC of about 0.91 mequiv. $g^{-1}$ as a reference sample for medium-temperature PEMFC. However, as shown in Fig. 40, the water uptake and proton conductivity of Nafion® (black stars) were differently reported by different research groups, although they used the same membrane and measurement method. Accordingly, an absolute comparison of the values in PEMs property and performance seems to be meaningless in this review. Instead, we will try to demonstrate the characteristics of each design strategy in Section 2.2 by analyzing the trend in water uptake and proton conductivity, and then suggest a solution to overcome their general disadvantages without unduly sacrificing their advantages. In this section, the reference samples (red stars in Fig. 40) represent hydrocarbon random copolymers without specific functionality or side chain, obtained via conventional polycondensation. In addition, some papers did not report water uptake and/or proton conductivity under the conditions discussed in this section (about 25 °C and/or 80 °C), and therefore will not be considered in this section (e.g., sulfonated hydrocarbon PEMs with high free volume in Section 2.2.2).

Fig. 40(a) and (b) shows the relationship of weight-based water uptake (wt%) and proton conductivity to IEC for various types of sulfonated hydrocarbon PEMs at 25 °C, respectively. In addition, to enhance readers' understanding of Fig. 40, the same data are listed in Table S1 in the Appendix. A correlation graph between water uptake and proton conductivity is also drawn in Fig. 40(c) to compare the characteristics of various types of PEMs. Nafion® (black stars in Fig. 40(a)) shows similar or somewhat higher water uptake values than sulfonated hydrocarbon PEMs with the similar IECs at 25 °C. However, note that the density of Nafion® (about 1.98 g $cm^{-3}$) is higher than those of sulfonated hydrocarbon PEMs (about 1.2–1.6 g $cm^{-3}$). Nevertheless, much of the literature reports water uptake as wt% rather than vol%. Accordingly, it is difficult to directly compare the water uptakes between Nafion® and hydrocarbon sulfonated PEMs on a wt% basis. Considering the practical IEC range of sulfonated hydrocarbon PEMs (over 1.25 mequiv. $g^{-1}$), the water uptake in Nafion® can be regarded as relatively low, which can be more clearly seen in Fig. 40. Proton conductivities of Nafion® at 25 °C (black stars in Fig. 40(b)) are much higher than sulfonated hydrocarbon PEMs with the similar IECs. Hydrocarbon PEMs, can attain the same level of proton conductivity as Nafion® at 25 °C when they have much higher IEC values (over 1.5 mequiv. $g^{-1}$). Consequently, Nafion® exhibits high proton conductivity even with low water uptake and at low temperature, as shown in Fig. 40(c), which demonstrates the effective formation of well-connected water channels for proton transport in Nafion®. As discussed in Section 1, the high proton conductivity (i.e., well-connected water channel) of Nafion® mainly results from three factors: (1) high acidity of the sulfonic acid groups, (2) mobility of sulfonic acid groups, and (3) large differences between the hydrophobicity of

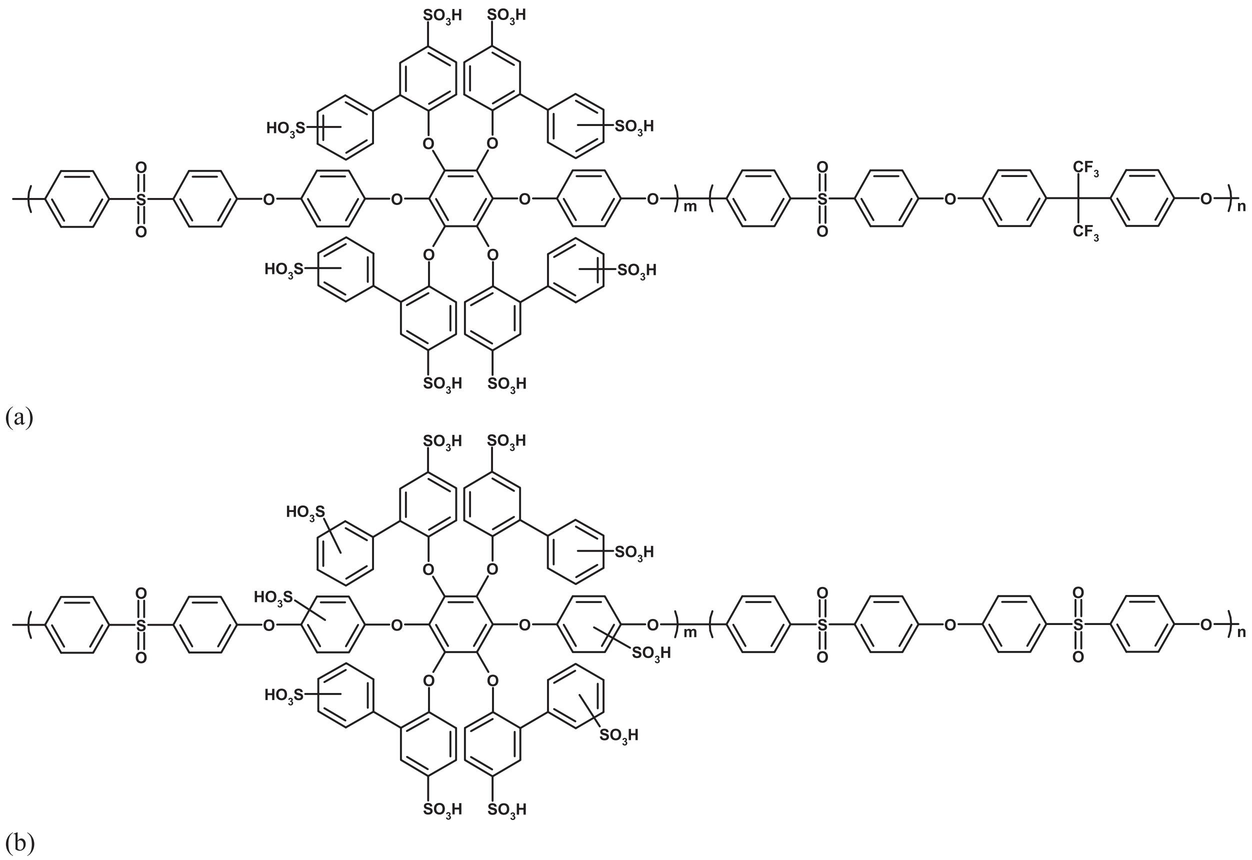

**Fig. 37.** Chemical structure of sulfonated poly(ether sulfone)s with (a) 8 sulfonic acid groups [143] and (b) 10 sulfonic acid groups [144]. [143] Copyright 2009, American Chemical Society.

non-sulfonated moiety and the hydrophilicity of sulfonated moiety in the PEM structure. These factors are also helpful to understand the properties of sulfonated hydrocarbon PEMs which will be discussed below.

Kim and Pivovar introduced the concept of categorizing PEMs into broad characteristics such as those with functional groups [146,147]. Sulfonated hydrocarbon PEMs with functional groups (blue circles in Fig. 40(a)) have comparably low water uptake 25 °C for given IEC values. This suggests that the introduction of functional groups (e.g., nitrile groups) and/or control of their connectivity (e.g., connectivity of sulfonic acids to naphthalene monomers) can control excessive swelling of the membranes even for those with high IECs under hydrated condition. On the other hand, this class of PEMs (blue circles) shows relatively low proton conductivity and a scattered trend at 25 °C according to their backbone chemical structure and functional group type, as shown in Fig. 40(b). Moreover, in order to obtain high proton conductivity, very high IECs are necessary but this may cause poor mechanical stability. Note that most sulfonated hydrocarbon PEMs with functional groups tend to have low proton conductivities (below 0.1 S $cm^{-1}$). In certain cases, functional groups can increase acidity, such as in the case of electronegative and electron withdrawing fluorine, which results in a PEM with higher proton conductivity than the reference (non-fluorinated) sample. Considering their low water uptake, this strategy has great potential for PEMFC operated under fully humidified condition, as shown in Fig. 40(c). Accordingly, if combined with appropriate structural or morphological design, these types of PEMs may possibly attain high performance.

Multiblock PEMs (cyan triangles in Fig. 40(a)) have relatively high water uptake values among sulfonated hydrocarbon PEMs. In particular, a drastic increase in water uptake can be observed at IEC values of 1.5–1.7 mequiv. $g^{-1}$. As mentioned in Section 1, excessive swelling (i.e., dimensional change under hydrated conditions) in PEMs causes poor mechanical stability and bad adhesion to catalyst layer, resulting in failure of the PEMFC during operation. However, since multiblock PEMs generally exhibit low dimensional swelling despite their high water uptake, because of their well-defined phase-separated morphology (see Section 2.2.3), their high water uptake is a less significant problem. On the other hand, appropriately high water uptake is beneficial and necessary for high proton conductivity. High water affinity can confine water molecules within PEMs enough to maintain water channels for proton transport, even under low humidity conditions, which leads to lower humidity dependence for proton conductivity, as observed in Nafion®. Accordingly, providing dimensional swelling is controlled, high water

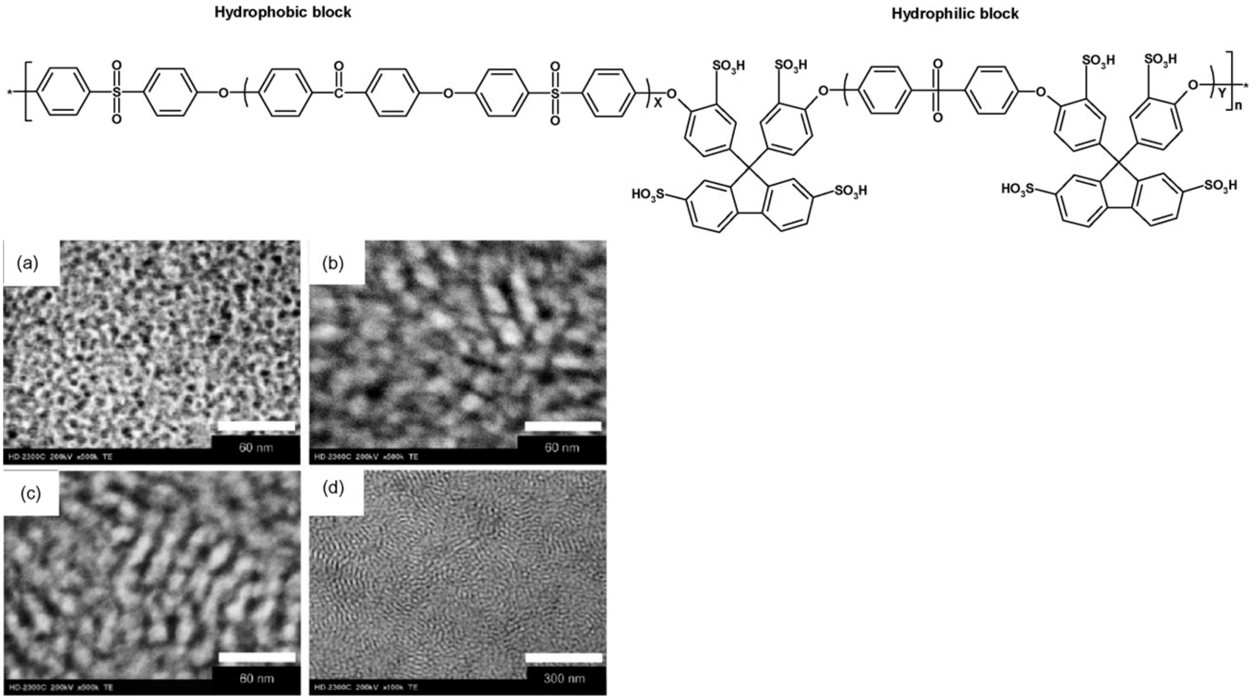

**Fig. 38.** Chemical structure of sulfonated poly(arylene ether sulfone ketone)s having highly sulfonatable fluorenyl groups and their STEM images: (a) Nafion® 112 (IEC = 0.91 mequiv. $g^{-1}$); (b) X60Y8 (IEC = 1.07 mequiv. $g^{-1}$); (c) X30Y8 (IEC = 1.62 mequiv. $g^{-1}$); (d) X30Y8 with large scale [117,118].
[118] Copyright 2010, American Chemical Society.

uptake in sulfonated hydrocarbon multiblock PEMs positively affects PEMFC performance under both reduced and fully humidified conditions. This is also confirmed by proton conductivity data in Fig. 40(b). Sulfonated hydrocarbon multiblock PEMs have comparatively the highest level of proton conductivity (over 0.1–0.3 S $cm^{-1}$ even at low temperatures of 25 °C) of those PEMs discussed in this section. In particular, most have similar or higher proton conductivities than Nafion® for IEC values greater than 1.2 mequiv. $g^{-1}$. The observed high proton conductivities of multiblock copolymers strongly support the discussion in Section 2.2.3 about the effective formation of well-connected proton transport channels via a well-defined and strong phase separation between hydrophobic and hydrophilic segments. Consequently, sulfonated multiblock copolymers are one of the most attractive design strategies for high performance PEMs operated at medium-temperature and low-humidity as well as under fully

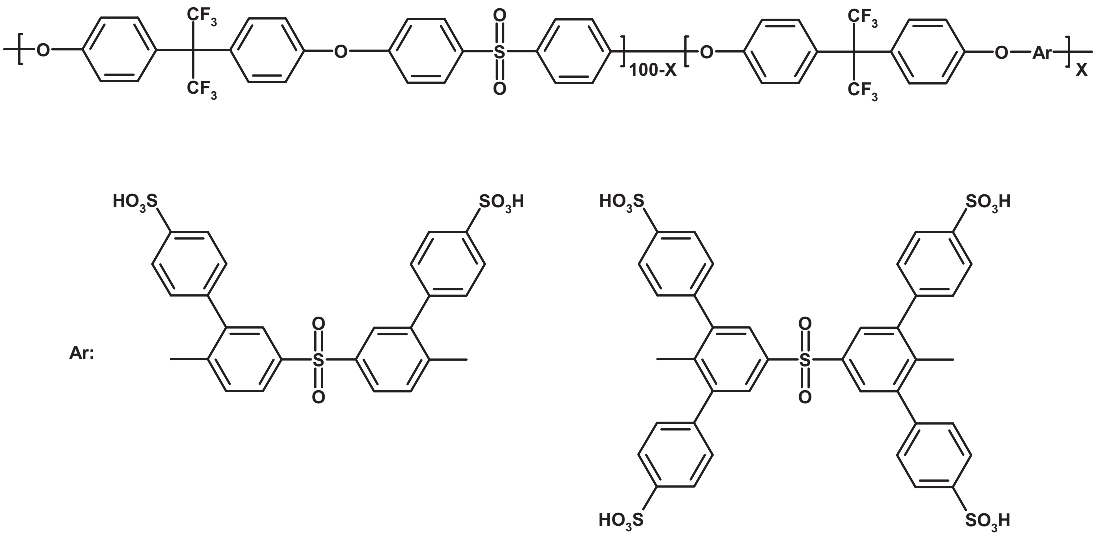

**Fig. 39.** Chemical structure of sulfonated poly(arylene ether sulfone)s with pendent sulfonic acid groups [145].
[145] Copyright 2010, American Chemical Society.

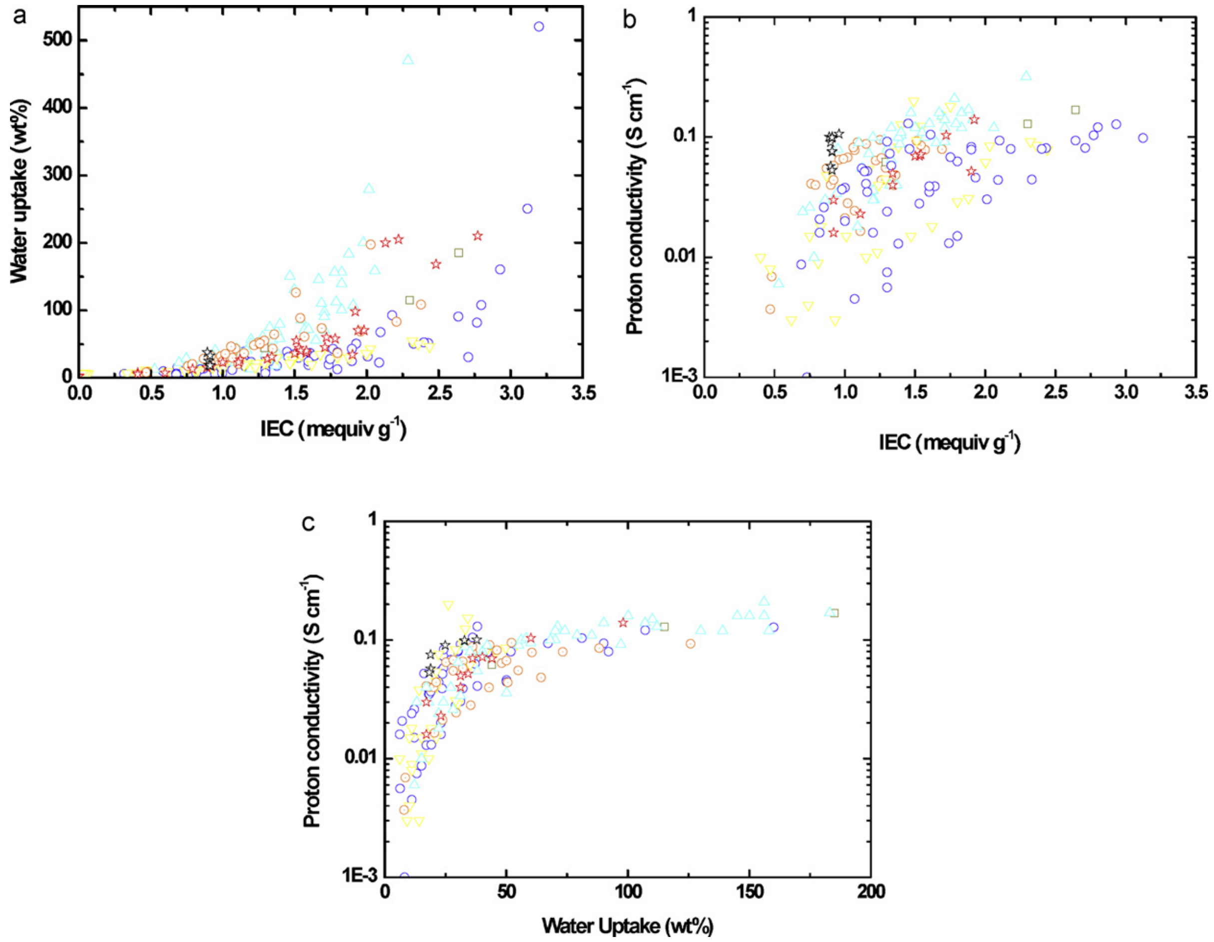

**Fig. 40.** Performance comparison of various types of sulfonated PEMs at around 25 °C: relationship between (a) IEC and water uptake (wt%), (b) IEC and proton conductivity, and (c) water uptake (wt%) and proton conductivity. Here, black stars (Nafion®), red stars (the reference sulfonated hydrocarbon PEMs), blue circles (sulfonated hydrocarbon PEMs with functional groups), cyan triangles (sulfonated hydrocarbon multiblock PEMs), yellow down-triangles (grafted and branched sulfonated hydrocarbon PEMs), dark yellow squares (sulfonated hydrocarbon PEMs with high IEC), and orange dot-center circles (sulfonated hydrocarbon PEMs with highly sulfonatable monomers). (For interpretation of the references to color in this figure legend, the reader is referred to the web version of the article.)

humidified conditions. Despite their high proton conductivities, sulfonated hydrocarbon multiblock PEMs have much higher water uptakes values than other PEMs with similar proton conductivities, as shown in Fig. 40(c). This can be a possible impediment for their application in actual PEMFC systems. For example, in unpublished research, it is known that these PEMs have adhesion problems to the catalyst layer when the MEAs are fabricated by the decal method, due to differences in surface properties between hydrated and non-hydrated conditions. Accordingly, in order to find ways to reduce the water uptake and to increase adhesion with the catalyst layer without sacrificing proton conductivity, it will be helpful to adopt physico-chemical tuning, such as crosslinking, surface fluorination and thermal annealing (which will be discussed in Section 3).

A comparative study of property difference between multiblock and graft PEM architecture was reported by Holdcroft and co-workers [148]. Grafted and branched sulfonated hydrocarbon PEMs are also strong candidates for PEMFC applications operating in the medium-temperature range. As shown in Fig. 40(a), most of these types of PEMs have lower water uptake values (yellow down-triangles) than other hydrocarbon PEMs and are similar to those with functional groups. For IEC values up to 1.3 mequiv. $g^{-1}$, their proton conductivities (yellow down-triangles in Fig. 40(b)) are relatively lower than other PEMs, even including those with functional groups. For IEC value of over 1.3 mequiv. $g^{-1}$, proton conductivities in grafted and branched sulfonated hydrocarbon copolymers drastically increase and then attain very high values (over 0.1–0.2 S $cm^{-1}$ even at 25 °C) despite their persistently low water uptakes. This behavior demonstrates that flexible grafted and branched side chains bearing sulfonic acid groups help the effective formation of water channels for proton transport, even with low water uptake (see Fig. 40(c)), as observed in Nafion® (see Fig. 2). This conclusion is also confirmed by the fact that PEMs with relatively rigid aromatic side chains show much lower proton conductivity values than those with flexible side chain, as shown in Fig. 40(b), because low mobility of rigid side chain hinders aggregation of hydrophilic sulfonic acid groups on the side chains. On the other hand, the low affinity of grafted and branched sulfonated hydrocarbon PEMs to water molecules (i.e., low water uptake values) can be obstacles in PEMFC, particularly for those operated at low humidity, leading to poor proton conductivity at low humidity, and a high humidity dependence for proton conductivity. In fact, many papers dealing with these PEMs reported high humidity dependence for proton conductivity compared with Nafion®, or did not even include proton conductivity data at low humidity. It should be noted that as a grafted PEM, Nafion® has a relatively high water uptake when considering its low IEC value. Consequently, ways to increase hydrophilicity without sacrificing dimensional stability, such as the introduction of hydrophilic inorganic materials (which will be discussed in Section 3), may be a promising approach for PEMFC applications operating at reduced humidity, particularly for hydrocarbon PEMs bearing sulfonic acid groups in grafted or branched side chains. Furthermore, low chemical stability of side chain in these PEMs was frequently reported, particularly for the styrene-based side chains, due to their poor chemical stability against radical species generated in fuel cell operation. Accordingly, molecular design of chemically stable side chains is absolutely necessary for actual PEMFC application of grafted and branched sulfonated hydrocarbon PEM.

In the case of sulfonated hydrocarbon PEMs with very high IEC values, there are only a few water uptake and proton conductivity data at 25 °C because they were originally designed for high temperature PEMFC operation at over 100 °C and at low humidity. These PEMs (dark yellow squares in Fig. 40(a)) have high, but slowly increasing, water uptake, due to the high hydrolytic stability (in the original paper, the authors used this term similarly as 'water insolubility') of sulfone linkage in the backbone. However, proton conductivities of those PEMs, despite their high IEC values, are not so high. High proton conductivities (over 0.1 S $\mathrm{cm}^{-1}$) of those PEMs can be attained even at high IECs of over 2.3 mequiv. $\mathrm{g}^{-1}$, as shown in Fig. 40(b). Accordingly, considering water uptake and proton conductivity in Fig. 40(c), these types of PEMs ostensibly have lower performance than other sulfonated hydrocarbon PEMs. However, this conclusion is not appropriate due to the target condition (over 100 °C and at low humidity) of sulfonated hydrocarbon PEMs with high IEC. Moreover, one of these PEMs show extremely high IECs of 4.3 mequiv. $\mathrm{g}^{-1}$ and seven times higher proton conductivity than Nafion® at high temperature (135 °C) and low humidity (30% RH), which is beyond the scope of discussion in this review.

Sulfonated hydrocarbon PEMs with highly sulfonatable monomer (orange dot-center circles) have distinctive characteristic in water uptake and proton conductivity in Fig. 40. Most of these PEMs have relatively low IEC (below 1.7 mequiv. $\mathrm{g}^{-1}$), whereas their water uptakes and proton conductivities are higher than those of other sulfonated hydrocarbon PEMs and almost similar to those of sulfonated multiblock PEMs, as shown in Fig. 40(a) and (b). In particular, introduction of highly sulfonatable monomer into sulfonated hydrocarbon PEM enables the highest water uptake and proton conductivity of these PEM among the sulfonated hydrocarbon PEMs in the IEC range below 1.1 mequiv. $\mathrm{g}^{-1}$. These high performances are also comparable to Nafion®. The high water uptake and proton conductivity of these types of PEMs may result from the structural characteristics which have both the advantages of multiblock copolymers and grafted/branched PEMs, as discussed in Section 2.2.6. However, these structural characteristics also limit actual PEMFC application. Since most highly sulfonatable monomers have very rigid aromatic structures, the sulfonatable monomer composition should be limited to avoid the brittleness of the final membranes. As a result, it is difficult to obtain high IEC in this type PEMs which enables high proton conductivity (over 0.1 S $\mathrm{cm}^{-1}$), as shown in Fig. 40(b) and (c). In order to solve this problem, some possible ways were suggested: introduction of flexible linkage in highly sulfonatable monomer and block copolymerization with the monomer having less sulfonatable sites.

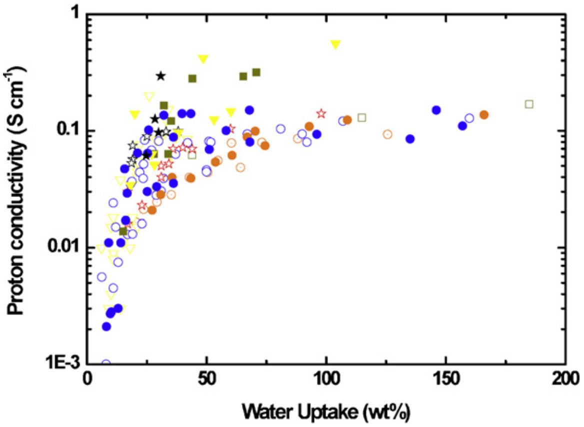

**Fig. 41.** Relationship between water uptake (wt%) and proton conductivity of various types of sulfonated PEMs at around 25 (open marks) and 80 °C (closed marks): Here, black stars (Nafion®), red stars (the reference sulfonated hydrocarbon PEMs), blue circles (sulfonated hydrocarbon PEMs with functional groups), cyan triangles (sulfonated hydrocarbon multiblock PEMs), yellow down-triangles (grafted and branched sulfonated hydrocarbon PEMs), dark yellow squares (sulfonated hydrocarbon PEMs with high IEC), and orange dot-center circles (sulfonated hydrocarbon PEMs with highly sulfonatable monomers). (For interpretation of the references to color in this figure legend, the reader is referred to the web version of the article.)

Fig. 41 shows the relationship between water uptake and proton conductivity at different temperatures (25 °C (open circles) and 80 °C (filled circles)) according to the types of sulfonated hydrocarbon PEMs. There is no significant change in water uptake for Nafion® (back stars), but proton conductivity is much improved by increasing temperature. Among the sulfonated hydrocarbon PEMs, the grafted and branched PEMs (yellow down triangles) and those with high IEC values (dark yellow squares) show relatively low increase in water uptake but exhibit remarkably enhanced proton conductivity. However, it should be noted that the water uptake and proton conductivity data of PEMs with high IECs at 25 and 80 °C are chosen from different research sources (see Table S1 in Appendix). Accordingly, a direct comparison of both data is meaningless, but their high performance at 80 °C demonstrates that these types of PEMs have high potential for medium-temperature PEMFC.

On the other hand, sulfonated hydrocarbon PEMs with highly sulfonatable monomers (orange dot-center circles) exhibit less change in water uptake and proton conductivity in the water uptake range below 75%. After that, water uptake drastically increases but proton conductivities are only slowly improved. In the case of functional group PEMs (blue circles), some performance improvement can be observed at 80 °C, but proton conductivity is typically below 0.1 S cm$^{-1}$. In fact, since most researchers measure water uptakes at 25–30 °C, there are only a few reports on water uptake measured at 80 °C. Accordingly, it should be noted that the data in Fig. 41 are limited and useful only as a reference.

## 3. Physico-chemically tuned sulfonated hydrocarbon PEMs

In this section, methods to physico-chemically tune sulfonated hydrocarbon PEMs will be discussed. Such approaches include crosslinking, thermal annealing, surface modification, and the use of composites and reinforced PEMs. Basic PEM characteristics and electrochemical performance will also be addressed.

### *3.1. Tuned sulfonated hydrocarbon PEMs*

### *3.1.1. Crosslinked PEMs*

Crosslinking PEM materials with high IEC values is one way to overcome excessive water swelling that is often observed in copolymers that have a high DS. Usually, the crosslinking of copolymers with DS values lower than a certain level (e.g., percolation threshold) leads to proton conductivity losses resulting from a reduction in the polymer mobility. Crosslinking the high DS copolymers can improve proton conductivity at the fully hydrated state by improving the ionic density per volume due to reduced water uptake. However, ineffective control of the crosslinking degree (or gel point) can give rise to membrane brittleness and unexpected side effects (e.g., a large reduction in proton conductivity).

*3.1.1.1. Ionic crosslinking.* Ionic crosslinking is effective for reinforcing the mechanical strength of PEM materials [149–152]. Crosslinking is mainly achieved by blending a sulfonated copolymer, particularly in the form of a salt (e.g., $-SO_3^-Na^+$), with a basic polymer (e.g., polybenzimidazole (PBI)). After membrane formation and subsequent acidification, $-SO_3^-$ groups in the sulfonated polymer interact with H–N– groups in the basic polymer, resulting in an acid–base complex. The crosslinking density can be changed by varying both the mixing content and the basicity of the basic polymer. For example, weakly basic polymers (e.g., post-sulfonated orthosulfonediamines) exhibit slightly reduced proton conductivities due to physical crosslinking. In addition, strongly basic PBI is easily protonated by sulfonated polymers. Below the percolation threshold of sulfonated polymers, most of their acid functionality is ionically trapped by PBI groups and thus, proton conduction capability is considerably reduced. At a high DS over the percolation threshold, the water-soluble character of sulfonated polymers is converted into water-insoluble character, which exhibits a certain level of proton conductivity. Despite morphological stability, water swelling is much higher than in other crosslinking systems based on covalent bonds. The strength of physical crosslinking is also not strong sufficient to prevent hydrolysis in water over 80 °C, which lowers the reproducibility of fuel cell performance [153]. However, the use of amphiphilic copolymers, which contain $-SO_3H$ groups in addition to basic functional groups (e.g., PBI) in the polymer backbone, as basic polymer counterparts can compensate for proton conductivity losses and maintain stable fuel cell performance [154].

*3.1.1.2. UV-assisted photo-crosslinking.* Polyphosphazenes (PPhs) are representative inorganic polymers and their substituent sites can be easily functionalized with $-SO_3^-H^+$ groups [155]. The resulting SPPhs have a low $T_g$, which enables photo-crosslinking in their membrane state under UV light [46,47]. For this purpose, SPPh cast solutions should contain a certain concentration of benzophenone photo-initiator. While significant improvements in SPPh dimensional stability have been observed after crosslinking, avoiding proton conductivity loss is difficult. Currently, crosslinked SPPh membranes have been recognized as promising materials for direct methanol fuel cells rather than PEFCs due to their low methanol diffusivity.

*3.1.1.3. Thermally activated crosslinking.* Thermally crosslinked sulfonated copolymers are prepared in a membrane state over a wide temperature range from 90 to ~360 °C. The curing temperature and $-SO_3^-M^+$ form ($M^+ = H^+$, $Na^+$, or $K^+$) of the copolymers during covalent bond formation are mainly determined by the choice of crosslinkers or crosslinkable groups. Thermally crosslinked copolymers are classified into two different categories: polymer-crosslinker systems and self-crosslinkable polymer systems (see Fig. 42).

In the early stages of research, thermal crosslinking was accomplished through condensation between $-SO_3^-H^+$ groups in sulfonated copolymers such as SPEEK, and polyatomic alcohols (e.g., glycerol, ethylene glycol, and meso-erythritol) as crosslinkers through a thermal treatment at 120–150 °C under vacuum [156]. The crosslinking reaction was accompanied by a loss in $-SO_3^-H^+$ content. A major issue in the thermally crosslinked systems is their severely reduced proton conductivity ($<4.6 \times 10^{-2}$ S cm$^{-1}$ in water at 25 °C) that is observed even when highly sulfonated polymers (DS > 78 mol%) are used.

Incorporating crosslinkers, which react with other functional sites (except $-SO_3^-H^+$ groups) in polymer backbones, can be a good approach to minimize the aforementioned proton conductivity losses. Representative crosslinked copolymers are derived from biphenyl-based disulfonated PAES (BPSH) oligomers with phenoxide ($-O^-K^+$) groups at their terminal ends and crosslinkers with different curing temperatures. In previous research, salt form ($-SO_3^-Na^+$ or $-SO_3^-K^+$) BPS oligomers with end-groups were primarily synthesized with controlled molecular weights (>15 kg mol$^{-1}$) via step growth polymerization, which is essential to maximize the end-group concentration and to promote chain mobility for high

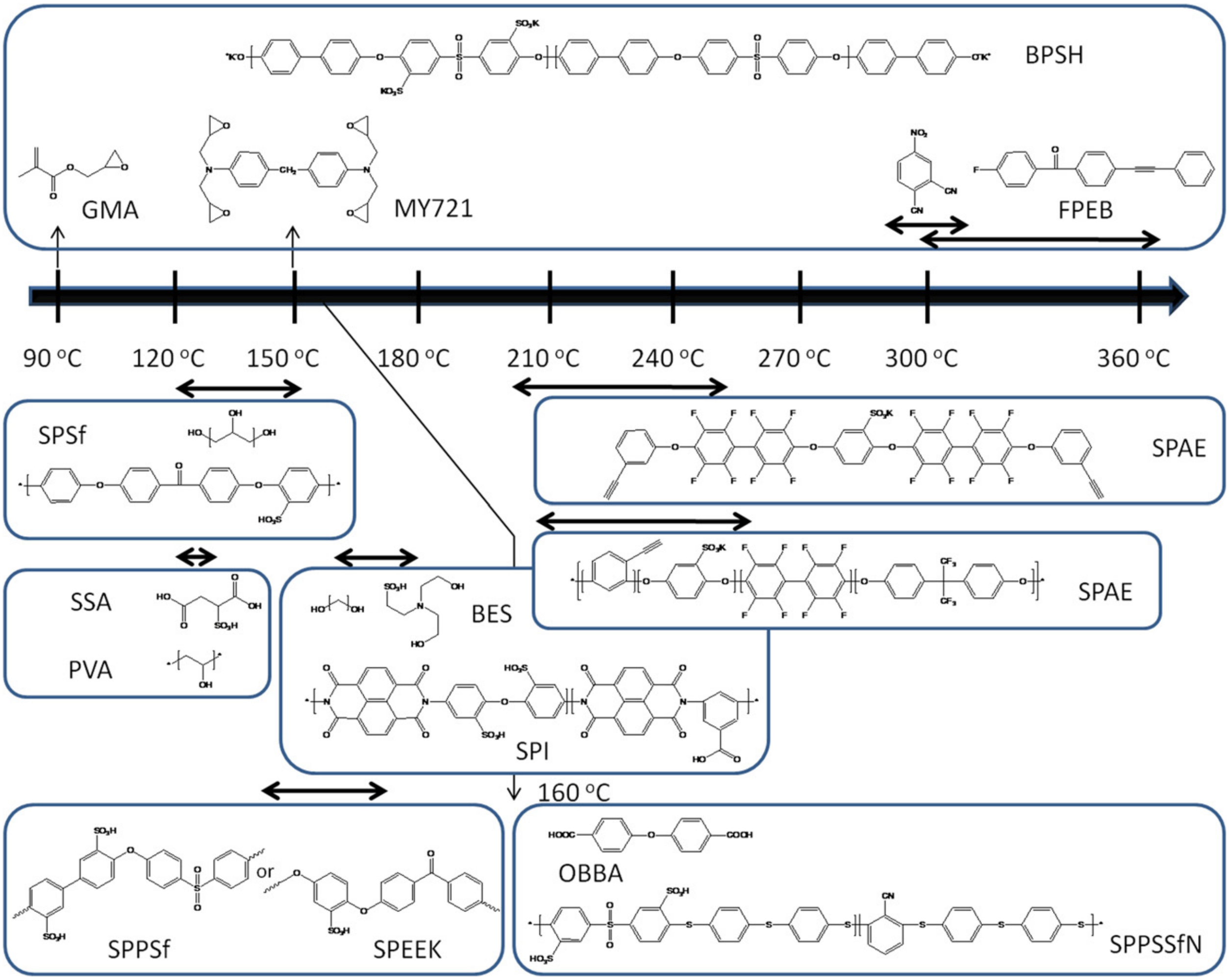

**Fig. 42.** Thermally crosslinked polymer systems with different curing temperature spectra.

conversion. Phenoxide end groups in the oligomers then reacted with the crosslinkers so as to form cured membranes. The resulting membranes were ultimately acidified to achieve high proton conductivity. Glycidyl methacrylate (GMA) is one of the promising crosslinkers in the phenoxide-terminated BPS system. In previous studies, GMA reacted with phenoxide endgroups via nucleophilic substitution. BPS oligomers with crosslinkable GMA endgroups were then obtained. After adding a benzoyl phenoxide initiator, the GMA–BPS system was thermally cured at 90–95 °C [157]. Another available crosslinker is tetraglycidyl bis(p-aminophenyl) methane (MY721 epoxy resin), which is more hydrolytically and thermally stable than GMA with an ester linkage. The phenoxide endgroups in BPS oligomers with a high DS (e.g., BPS-50 with DS = 50 mol%) react with multi-functional epoxide rings in MY721 in the presence of a triphenyl phosphine catalyst around 150 °C to produce a MY721-BPS crosslinked network [158]. A small amount of a high boiling solvent [e.g., N-methyl-2-pyrrolidinone (NMP)] was used to depress the high $T_g$ of the high DS oligomer so as to make vitrification feasible. The gel fraction of the crosslinked copolymer was influenced by the crosslinking time, epoxy concentration, molecular weight, and DS of the BPS oligomers. After crosslinking and acidification, the water uptake of proton ($-SO_3^-H^+$) form BPSH-50 was greatly reduced from 232% to 84%. Such a reduction may induce enhanced proton conductivity by prohibiting the proton concentration per polymer volume from being diluted due to excessive swelling in the hydrated state. Furthermore, 4-nitrophthalonitrile ($T_{curing} > \sim 300\,^\circ C$) [159,160] and 4-fluoro-4-phenylethynyl benzophenone (FPEB) ($T_{curing} > \sim 350\,^\circ C$) are crosslinkers with curing temperatures higher than the $T_g$ of BPS oligomers. After membrane formation, a curing reaction was conducted in the thermally stable salt form ($-SO_3^-M^+$, M = Na or K), since $-SO_3^-H^+$ groups in the BPSH backbone begin to thermally decompose around 250 °C. It may be attractive to use FPEB as a crosslinker since volatile gases are not evolved during the curing reaction. The high curing temperature of FPEB would be a challenge when designing crosslinked structures.

The crosslinking of sulfonated copolymers generally leads to reduced proton conductivity due to a combination of the restricted mobility of the polymer chains and blocked hydrophilic water channels. A plausible way to compensate for such a loss may be to use crosslinkers with a $-SO_3^-H^+$ group [161,162]. One example is the poly(vinyl alcohol) (PVA)–sulfosuccinic acid (SSA) system [162], which was employed as both a sulfonating agent and a crosslinker. After membrane formation at 60 °C, hydroxyl (–OH) groups in the PVA reacted with carboxylic acid (–COOH) groups in the SSA at temperatures in the range of 120–130 °C via a condensation reaction to form thermally cured polymer networks. The proton conductivity trends in the system were highly variable depending on the amount of SSA and the crosslinking temperature. Membranes cured at a relatively high temperature (125–130 °C) exhibited a high degree of crosslinking, which led to a reduced proton conductivity at a low SSA concentration (<17 wt%). Above this concentration, SSA contributed to an improvement in the proton conductivity as a proton conductor. At a relatively low curing temperature, SSA played an important role in transporting protons due to the low degree of crosslinking. Introducing crosslinkers with a $-SO_3^-H^+$ group was more effective in a sulfonated polymer system than in a non-sulfonated polymer system such as PVA. When N,N-bis(2-hydroxyethyl)-2-aminoethanesulfonic acid (BES), a crosslinker containing an $-SO_3^-H^+$ group, was added to DS-controlled SPIs ($1.9 < \mathrm{IEC} < 2.2$ mequiv. g$^{-1}$), the water uptake decreased as in other crosslinked systems but IEC increased to the range of 2.0–2.5 mequiv. g$^{-1}$ [161]. Unlike crosslinked systems composed of sulfonated polymers and fixed-ion free crosslinkers, the proton conductivity of the BES-SPI crosslinked system measured at 30 °C and 90% RH was comparable to Nafion® under the same condition. This result is believed to be due to the additional $-SO_3^-H^+$ group in the aliphatic crosslinker giving rise to improved acidity and/or ionic density. Note that improved ionic density per volume obtained from both reduced water uptake and enhanced $-SO_3^-H^+$ concentration contribute to improved charge carrier concentration [163]. In addition, the proton conductivity of the crosslinked SPI system was higher than that of Nafion® at elevated temperatures, while its activation energy (e.g., 4.5–5.6 kcal mol$^{-1}$ obtained from the proton conductivity measurement in the temperature range of 30–90 °C at 90% RH) is lower than that (7.3 kcal mol$^{-1}$) of Nafion®. It might be due to increased bound water content, in addition to the contribution of charge carrier concentration as mentioned above [163]. Here, bound water arises from the strong interaction between water molecules and the polymer matrix and is affected by the polarity and ionic concentration in the hydrated polymer system. The bound water is thermally durable at elevated temperature (90 °C) where water activity increases and protons can be well dissociated. When compared to a polymer system based on a fixed-ion free crosslinker with a similar aliphatic chain length, the resistance of the membrane to hydrolysis and peroxide radical attack was slightly weakened as a result of the higher IEC value [164]. However, these model systems provide information on how to design crosslinked polymer membranes for mid-temperature and/or low-humidity PEMFC applications.

Most thermal curing processes that proceed in the salt ($-SO_3^-Na^+$ or $-SO_3^-K^+$) form exhibit excellent thermal stability (<~400 °C). Some crosslinking reactions occur in more acidic proton ($-SO_3^-H^+$) form polymers instead of salt form polymers. One example is the sulfonated poly(phenylene sulfide sulfone nitrile) (SPPSSfN)-4,4′-oxybis(benzoic acid) (OBBA) crosslinked system [165]. The carboxylic acid ($-COO^-H^+$) in OBBA underwent Friedel–Craft acylation with nucleophilic phenyl rings in proton form SPPSSfN under vacuum at 160 °C for 10 h. Here, SPPSSfN acted as a solid acidic catalyst in order to activate the condensation reaction. Also, the nitrile (–CN) groups in the SPPSSfN backbone gave rise to a polar–polar interaction, which in turn contributed to both an interface formation that was compatible with Nafion® electrodes and enhanced dimensional stability in the hydrated state. The level of water swelling in highly sulfonated SPPSSfN (DS = 50–60) membranes was too high to evaluate their proton conductivity, particularly at 90 °C. However, the water uptake of the crosslinked system decreased to about 50% of the non-crosslinked system. Interestingly, the proton conductivity after crosslinking was somewhat reduced, but the values were superior to those of Nafion® membranes with a similar activation energy over a wide temperature range from 30 to 90 °C.

Unlike conventional crosslinked systems where crosslinkers are incorporated into as-prepared polymers or oligomer matrices in the solution state and thermally cured in the membrane state, self-crosslinkable polymer systems are composed of homopolymers containing thermally crosslinkable functional groups (e.g., sulfonic acid group and ethynyl group) in the polymer synthesis step. The crosslinkable functional groups in the homopolymers then undergo inter- or intramolecular covalent bond formation with reactive sites in their backbones over certain curing temperature ranges. In addition to the curing time, the curing temperature in self-crosslinkable systems is a critical factor in determining their crosslinking degree. Recently, self-crosslinkable polymers have been reported in the literature [166–169]. Representative examples are SPEEK and SPPSf [166,167] where a portion of the sulfonic acid groups (crosslinking sites) present in the aromatic backbone is sacrificed for thermal conversion into sulfone bridge groups to cure the polymer matrices. The resulting crosslinked polymers exhibit improved hydrolytic, thermal, and mechanical stability. However, the crosslinking reaction is necessarily accompanied by proton conductivity loss owing to their reduced IEC. The use of highly sulfonated polymer matrices (e.g., IEC = 3.57 mequiv. g$^{-1}$ [167]) can be a solution to compensate this unavoidable proton conductivity loss. The self-crosslinkable polymer systems also include SPAEs with ethynyl crosslinkable groups randomly located within the polymer backbone [168] or positioned at their terminal ends [169]. The ethynyl groups in SPAEs were effective in removing the thermal bottleneck observed in the aforementioned BPS–FPEB curing system. This is because the ethynyl groups used in the SPAEs exhibit a relatively high reactivity to a subsequent curing reaction due to their low steric hindrance. As such, the thermal curing temperature was 100 °C lower than that of the BPS–FPEB system.

### *3.1.2. Surface fluorinated PEMs*

A key element that determines electrochemical fuel cell performance is the MEA. A MEA is generally composed of a PEM and electrodes positioned at both sides of the PEM. Some sulfonated hydrocarbon materials used as PEMs show excellent barrier properties to oxygen molecules that are associated with active radical generation on the platinum catalyst in the electrodes [170,171]. Such PEMs have also exhibited proton conductivities that are higher than commercially available PFSA (e.g., Nafion®) under harsh PEMFC operating conditions such as a low humidity (e.g., 50% RH) and a high temperature (>80 °C) [98,148,172,173]. Consequently, their fuel cell performance is superior to that of PFSA over a short period of time. However, the good electrochemical performance of sulfonated hydrocarbon PEMs rapidly declines within several days because of interfacial problems related to the electrodes. A firm understanding of the electrode formula for MEA fabrication is important for the development of high-performance sulfonated hydrocarbon PEM-based MEAs (HC-MEAs). Nafion® ionomers (EW = 1100) have conventionally been added as a catalyst binder in the electrode for the following reasons: (1) to physically support catalyst-adsorbed carbon clusters and (2) to facilitate proton migration from the anode to the PEM and from the PEM to the cathode [174]. Unlike PFSA membrane-based MEA fabrication methods, the use of Nafion® in HC-MEA fabrication processes gives rise to crucial interfacial issues. These issues include a high interfacial resistance between the sulfonated hydrocarbon PEM and the electrodes due to their low compatibility and poor catalyst layer adhesion, which leads to the delamination of catalyst layers from the PEM and rapid electrochemical losses during fuel cell on-off cycles.

Extensive research has been conducted to overcome the above HC-MEA issues. One approach is to use a catalyst binder with the same composition as the PEM [109,175,176]. This method was effective in improving compatibility with the PEM. However, it resulted in low fuel permeability, which caused a mass flux limitation potential drop in the corresponding current–voltage polarization curves. Another approach is to tune the chemical nature of the sulfonated hydrocarbon PEMs via the incorporation of partially or fully fluorinated monomers. Despite the reduced interfacial resistance attained with Nafion® electrodes [103,177,178], the relatively high cost of fluorinated monomers made their use in PEMs less attractive [179].

Surface fluorination (or “post-fluorination”) can be effectively used in preparing sulfonated hydrocarbon PEMs that have a high compatibility with Nafion® electrodes and an excellent single cell lifetime. In surface fluorination, the surface state of sulfonated hydrocarbon PEMs is simply and rapidly converted into one that is analogous to fluorinated membranes. At present, surface fluorination has been utilized in a wide range of applications for automobiles, packaging, food storage and preservation, and coatings. Such diverse usage arises because surface-fluorinated hydrocarbon polymers combine the desirable characteristics of fluoropolymers, such as chemical stability and good gas barrier properties, with the beneficial bulk properties of hydrocarbon polymers (e.g., good processability and excellent mechanical strength) [180–182].

Surface fluorination of sulfonated hydrocarbon membranes [BPSH-40 [183] and PVA–poly(styrene sulfonic acid-co-maleic acid) (PSSA-MA) [184]] has been achieved using a dilute $F_2$ gas (e.g., 500 ppm) in an $F_2/N_2$ mixture under ambient pressure and temperature for a short period of time (5–60 min). Such a process minimizes undesirable side reactions (e.g., chemical degradation) that may arise due to the use of highly reactive $F_2$ gas. Prior to surface fluorination, all sulfonated hydrocarbon membranes were acidified so as to maintain a level of chain mobility that was higher than that of physically crosslinked salt ($-SO_3^-M^+$, $M^+ = Na^+$ or $K^+$) form membranes in the solid state. After the surface treatment, the resulting membranes were acidified again to eliminate the possibility that $-SO_2F$ group formation on the membrane surface would lower their IEC values.

In the above experiments, the fluorine content, which was measured in atomic ratio by X-ray photoelectron spectroscopy, increased as a function of the $F_2$ gas exposure time. Under the same fluorination conditions, the fluorine content was much higher in an aromatic polymer matrix (atomic F content: ~15%) [183] than in an aliphatic matrix (atomic F content: ~5.4%) [184] because the substitution reaction of a C–H bond with a C–F bond in the aromatic rings is the most thermodynamically favorable route. The C–F substitution reaction in BPSH-40 during surface fluorination was expected to occur randomly in its aromatic backbone since such $F_2$ gas reactions have been reported to be governed by a complicated radical chain mechanism [185]. The IEC values of BPSH-40 were independent of the fluorination times. However, surface fluorination extensively altered the surface characteristics of the structures. The formation of C–F bonds resulted in a hydrophobic membrane surface, as demonstrated by increased water contact angles (Fig. 43(a)). In the AFM image of BPSH-40 as a random statistical copolymer (Fig. 43(b)), randomly distributed hydrophilic cluster-like structures (dark region) were observed within a hydrophobic polymer matrix (light region). Surprisingly, the surface treatment transformed the morphology into fairly well-defined hydrophilic–hydrophobic microphase separated morphologies, similar to those of hydrophilic–hydrophobic multiblock copolymers [74]. Hydrophilic domains became interconnected and continuous ionic channels for fast proton transport were created as a result of self-assembly on the partially fluorinated membrane surface. It can be inferred that C–F bonds with a low surface free energy would be formed mainly on the hydrophobic domains rather than the hydrophilic domains of BPSH-40. Similar to multiblock copolymers, surface fluorinated BPSH membranes have exhibited reduced water uptakes and anisotropic swelling behavior in the thickness direction. These peculiar swelling characteristics can lead to dimensional stability of the surface-fluorinated membranes and contribute to an enhancement in the lifetime of the resulting MEAs. In addition, the high electronegativity of fluorine atoms in the C–F bonds improved the acidity of $-SO_3^-H^+$ groups in the aromatic rings containing the bonds. Consequently, the proton conductivity of the surface fluorinated BPSH membranes increased up to a certain fluorination level (e.g., >30 min). Above 30 min, the proton conduction

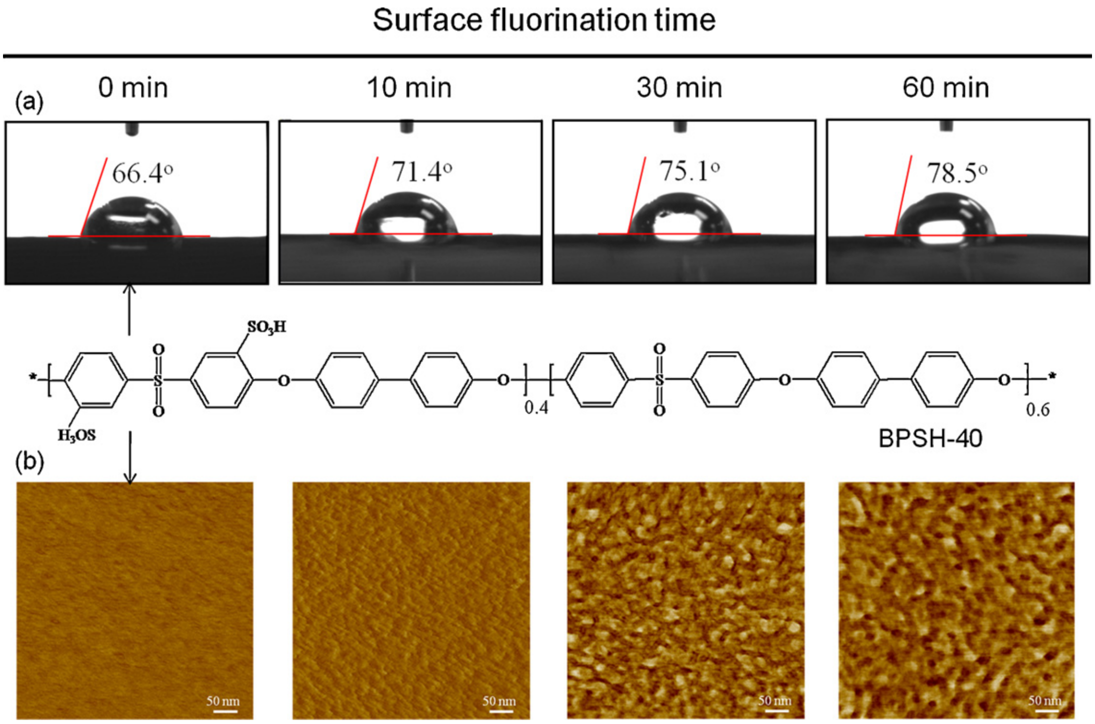

**Fig. 43.** Effects of surface fluorination of BPSH random copolymers on surface hydrophobicity and morphology based on water contact angle measurement and atomic force microscopy (AFM), respectively. In AFM images, the scale bar indicates 50 nm [183].
[183] Copyright 2009, American Chemical Society.

properties of the membranes slightly deteriorated, indicating that chemical deformation may have occurred. It is also interesting to compare the interfacial resistance between a PEM and Nafion® electrodes in terms of the high-frequency resistance (HFR, $\Omega\,cm^2$) of the MEA measured during a long-term direct methanol fuel cell (DMFC) test. Though their electrochemical single cell performances were evaluated under DMFC conditions, similar results can be obtained even in a PEMFC and directly applied to high performance MEA development. Here, HFR is the sum of all resistances in the pathway from the potentiometer to all MEA components. The surface fluorinated membranes exhibited significantly reduced HFR values. In addition, changes in the HFR values were negligibly small even after a few thousand hours of operation. This means that surface-fluorinated surfaces form a stable interface with Nafion® electrodes. The combination of improved proton conductivity and a low interfacial resistance was beneficial in the high performance of single cells and extended the electrochemical MEA lifetime.

Multiblock copolymers exhibit proton conductivities that are much higher than those of corresponding random copolymers with the same IEC and chemical integrity because of their well-defined hydrophilic–hydrophobic phase separated morphologies. For example, a BPSH100–BPS0 multiblock copolymer with an IEC value of ~1.7 mequiv. $g^{-1}$ had a proton conductivity of 0.14 $S\,cm^{-1}$ in liquid water at 30 °C. Meanwhile, the proton conductivity of a corresponding BPSH random copolymer with the same IEC was 0.11 $S\,cm^{-1}$ under the same test conditions. When the surface fluorination technique was applied to the multiblock copolymer, more developed nanophase-separated structures were obtained [186]. The morphological transformation seemed to contribute to an improvement in the proton conductivity in both liquid water and at different RHs. Surface fluorinated multiblock copolymers have exhibited a very slow reduction in their proton conductivity, particularly at a low humidity [30–70% RH, e.g., the proton conductivity of a multiblock copolymer after surface fluorination for 60 min = ~0.087 $S\,cm^{-1}$ at 50% RH versus ~0.020 $S\,cm^{-1}$ for Nafion® 212]. This behavior was more remarkably observed in highly fluorinated multiblock copolymers with higher water retention levels. Therefore, multiblock copolymers are expected to show electrochemical performances that are superior to Nafion® 212 during low humidity PEMFC operation. Despite the effectiveness of surface fluorination, the mechanisms of the process and the correlation of macroscopic membrane properties to the fluorination depth have not been elucidated.

### 3.1.3. *Thermally annealed PEMs*

In addition to the chemical structure, composition, and morphology of PEMs, the membrane preparation condition is one of most important factors to consider in PEM design. Most sulfonated hydrocarbon PEMs are derived from amorphous glassy polymers in the non-equilibrium state. Amorphous glassy polymers generally encompass a free volume that is higher than the minimal free volume, which is obtained from the difference in specific volume when the transition from the liquid to the hypothetical equilibrium glassy state occurs. Thus, the thermal history of glassy polymers can significantly influence the packing density of their polymer chains. A thermal annealing process is a well-known and simple route to stabilize a glassy polymer and induce densification of the polymer matrix. Consequently, polymer chain mobility is restricted and membrane plasticization by absorbed small molecules (e.g., water or solvents) is minimized [187]. It is important to investigate the thermal annealing effect on sulfonated hydrocarbon copolymers since a thermal post-treatment can alter the overall macroscopic characteristics of PEMs with the same chemical structure and composition.

Sulfonated polysulfone membranes have been fabricated via post-sulfonation of Udel® using mixtures of chlorosulfonic acid and chlorotrimethylsilane. The structures were annealed in the proton ($-SO_3^-H^+$) form membrane state at temperatures (60 °C and 150 °C) lower than the $T_g$ of Udel® ($T_g = 185$ °C) [188]. The resulting randomly sulfonated polysulfones (Fig. 44) exhibited a single and broad $T_g$ in the temperature range of 193–225 °C due to the $T_g$ contributions of the hydrophilic and hydrophobic domains. These $T_g$ values increased with increasing DS, similar to what was observed in directly copolymerized sulfonated copolymers based on sulfonated monomers. Prior to annealing, all membranes were kept in deionized water for one day so as to exclude the contribution of the solvent on the $T_g$. Thermal annealing at 150 °C yielded a $T_g$ that was higher than that of the sulfonated polysulfone treated at 60 °C. Both the water uptake and the number of water molecules coordinated per $-SO_3^-$ group ($\lambda$) of the sulfonated polysulfone were reduced after the heat treatment. Such a result may be associated with an increase in the packing density and a reduction in the free volume for the transport of proton and water molecules. The post-sulfonated polysulfones may also undergo inter- or intra-molecular covalent bond formation through a thermally induced conversion from $-SO_3H$ to $-SO_2$ groups, losing a portion of their ionic characters [166,167]. Consequently, proton conductivity was slightly reduced after thermal annealing.

Shown in Fig. 44 is the effect of thermal annealing on the ionic conductivity of randomly sulfonated copolymers fabricated with different sulfonation routes. Directly copolymerized disulfonated polysulfone (BisA) copolymers in the proton form exhibited higher proton conductivities than post-sulfonated polysulfones, even though their proton conductivity measurement was conducted at a relatively low temperature (30 °C). It should be noted that disulfonate ($-SO_3^-M^+$, $M^+ = H^+$ or $K^+$) groups in BisA copolymers are attached in the meta-position of an electron-withdrawing sulfonyl (O=S=O) group in the segmented phenyl rings, while mono-sulfonated ($-SO_3^-H^+$) groups in post-sulfonated polysulfones are randomly located in the ortho-position of an electron-donating ether (–O–) linkage in other phenyl rings. The different location of these functional groups causes an electron density difference, which makes the disulfonated groups in BisA copolymers more acidic [79]. As a result, protons are easily released from the disulfonated groups in BisA copolymers. It is interesting to monitor the changes in BisA copolymer characteristics when a thermal annealing protocol similar to that described above is applied to BisA copolymers with the same Udel® backbone as post-sulfonated polysulfone. Differences with the previous thermal annealing procedure for post-sulfonated polysulfone were that all BisA membranes were annealed at sub-$T_g$ (60 and 150 °C) in the salt ($-SO_3^-K^+$) form membrane state containing a small amount of solvent. The structures were then restored in deionized water so as to completely remove residual solvent. The thermal annealing effects exhibited by BisA copolymers were almost identical to those displayed by post-sulfonated polysulfones, i.e., the water uptake was reduced and the $T_g$ was increased. However, the proton conductivity of the BisA copolymers was greatly improved after the thermal annealing irrespective of whether they were in the proton form or salt form. This peculiar behavior may be associated with a change in the ionic density ($IEC_{v(wet)}$), which is defined as the molar equivalent of $-SO_3^-H^+$ groups per water-swollen polymer volume [146]. In other words, a reduction in the water uptake as a result of a heat treatment can give rise to an improved $IEC_{v(wet)}$. This behavior is believed to be more dominant in a BisA system with two $-SO_3^-H^+$ groups in one hydrophilic moiety than in a post-sulfonated system with one $-SO_3^-H^+$ group in one hydrophilic moiety. As such, the conductivities of thermally annealed BisA copolymers in the salt form with a high IEC were comparable to those of post-sulfonated polysulfones in the proton form.

The thermal annealing temperature plays an important role in determining the proton conductivity of annealed membranes. A high dependency on the annealing temperature is more significantly observed in hydrophilic–hydrophobic multiblock copolymers than in randomly sulfonated copolymers. Multiblock copolymers are generally synthesized via a coupling reaction between phenoxide-terminated disulfonated hydrophilic oligomers and coupling agent (e.g., decafluorobiphenyl)-end-capped hydrophobic oligomers with a controlled molecular weight [121]. Multiblock copolymers have two $T_g$ values: one from the hydrophilic block (high $T_g$) and another from the hydrophobic block (low $T_g$). Up to now, it has been believed that thermal annealing around the $T_g$ of hydrophilic blocks would influence proton conduction because protons are transported through water channels formed by hydrophilic blocks. As shown in Fig. 45, thermal annealing near the $T_g$ of hydrophobic blocks leads to a large change in the proton conductivity, particularly at a low humidity. In BPSH100–PPH0 multiblock copolymers used as an example [189], the $T_g$ values of its hydrophobic and hydrophilic blocks have been found to be approximately 250 °C and over 300 °C, respectively. A heat treatment at around the $T_g$ of the hydrophobic block prevented the absorption of water molecules within the polymer matrices dramatically. Despite the reduced water content in the multiblock copolymer, its proton conductivity in liquid water slightly increased as the annealing temperature was increased. This positive contribution of the thermal annealing process on the proton conductivity was significant at humidities lower than 70% RH. The conventional conductivity drop at low humidities was gradually retarded as the thermal annealing temperature

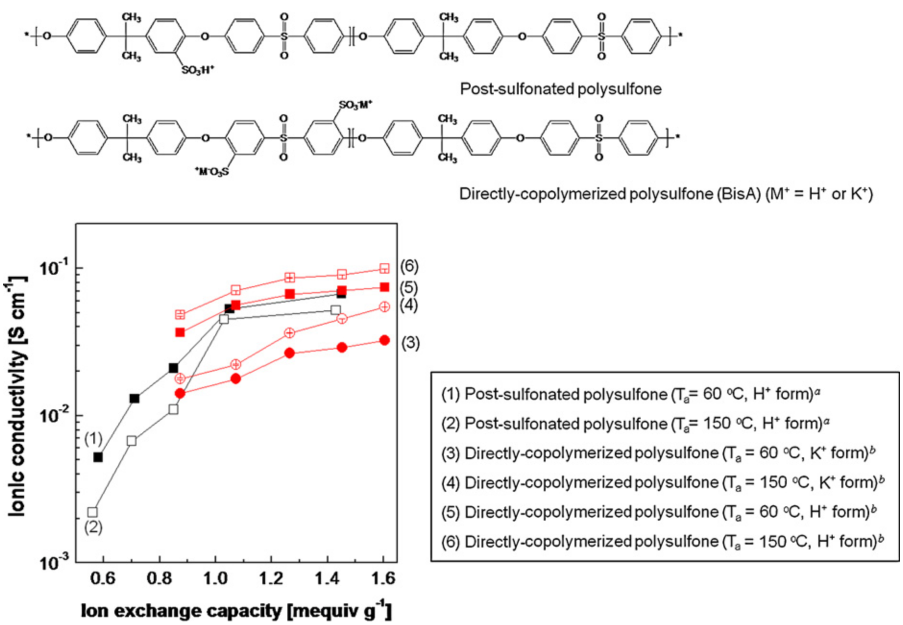

**Fig. 44.** Thermal annealing effect on the ionic conductivity of post-sulfonated and directly copolymerized polysulfone random copolymers. Here, [a]measured at 60 °C and 95% RH [188]; [b]measured at 30 °C in liquid water.

was increased close to the $T_g$ of the hydrophobic block. Simultaneously, the mechanical strength of the multiblock polymer was further improved. Similar behavior was also observed in other hydrophilic–hydrophobic multiblock copolymers with different chemical structures, $T_g$ values, and compositions [190]. This indicates that a thermal treatment at around $T_g$ of the hydrophobic block results in the densification of hydrophobic domains. A thermal treatment also induces $IEC_{V(wet)}$ improvement in the hydrophilic domains of multiblock copolymers due to a decrease in the water uptake level. Furthermore, thermal annealing may change the Flory–Huggins interaction

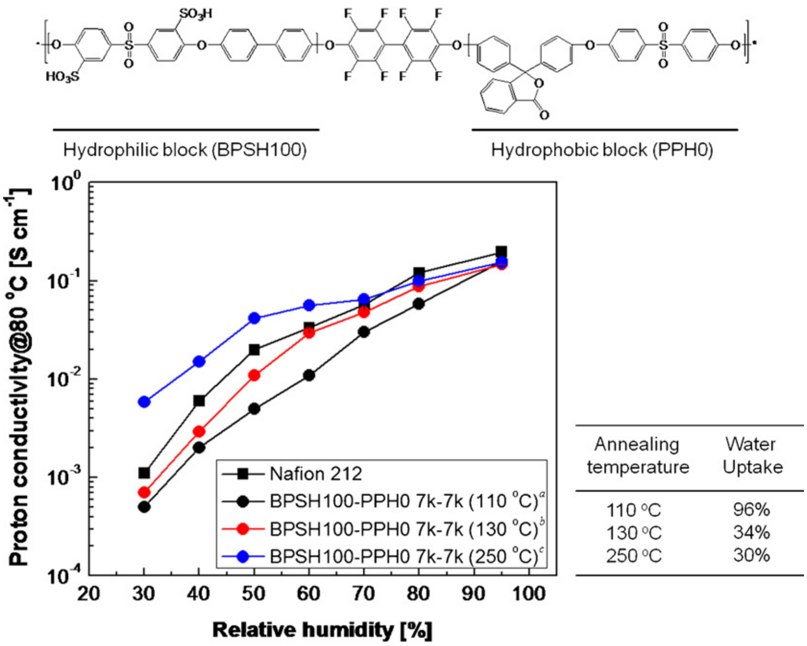

| Annealing temperature | Water Uptake |
|---|---|
| 110 °C | 96% |
| 130 °C | 34% |
| 250 °C | 30% |

**Fig. 45.** Thermal annealing effect on proton conductivity and water uptake of a hydrophilic–hydrophobic multiblock copolymers [189]. Here, [a]initial drying at 45 °C under IR lamp and final drying at 110 °C under vacuum for one day, respectively, [b]initial drying at 75 °C under IR lamp and final drying at 130 °C under vacuum oven for one day, respectively, and [c]initial drying at 75 °C under IR lamp for one day and final drying at 250 °C for 30 min under $N_2$ atmosphere.
[189] Copyright 2010, American Chemical Society.

parameter ($\chi$) of multiblock systems, as the casting solvent and drying temperature do [191]. This implies that increased dissimilarity between the two different blocks may induce a more developed hydrophilic–hydrophobic phase separation. As of yet, a correlation between thermally annealed morphologies and proton conduction at a low humidity has not been clearly investigated. Nevertheless, thermal annealing is definitely a promising route to promote proton conduction under low humidified conditions when considering medium-temperature and/or low-humidity fuel cell operations.

### *3.2. Composite-type PEMs*

A sulfonated polymer-based composite PEM is defined as a polymeric membrane containing at least one inorganic component (organic–inorganic composite) or organic component (polymer composite) in addition to the sulfonated polymer. In the present review, the primary focus is on organic–inorganic composite PEMs with inorganic oxides and heteropolyacids, as well as reinforced sulfonated hydrocarbon PEMs where the pore-filling concept has been adopted.

#### *3.2.1. Organic–inorganic composite PEMs*

The incorporation of inorganic additives into sulfonated copolymers for PEMFC applications has been gaining interest since inorganic additives can improve the thermal, mechanical, chemical, and electrochemical properties of sulfonated hydrocarbon PEMs to a certain degree. Such improvements are due to a combination of the intrinsic properties derived from the polymers themselves when the additives are used appropriately. Representative inorganic candidates include silica [192–194], zeolite [195], titania [196–199], heteropolyacids [200–203], and carbon nanotubes [204]. Inorganic additives commonly have a high surface area and excellent thermal/mechanical stability.

Heteropolyacids are one class of proton-conducting inorganic additives. These additives exhibit intrinsic proton conduction capabilities over a wide range of temperatures and humidities (Fig. 46(a)) [205–214]. Their proton conductivity usually becomes high as the humidity increases. Unlike $-SO_3H$ groups in sulfonated polymer matrices, heteropolyacids exhibit improved proton conduction capabilities even at elevated temperatures (>80 °C), where many sulfonated PEMs, including PFSA membranes, begin to lose their excellent proton conductivity due to the evaporation of water molecules associated with proton transport based on the vehicle mechanism [13,215]. For this reason, heteropolyacids are interesting inorganic additives for medium-temperature and low-humidity PEMFC applications. However, most heteropolyacids composite membranes are prone to leaching-out issues that occur during fuel cell operation.

Another class of proton-conducting inorganic additives are the inorganic oxides containing surface hydroxyl (–OH) groups. Their surface potential is spontaneously changed depending on the pH. The electrochemical behavior of hydrophilic silica ($SiO_2$, Aerosil® 380) as a function of the pH is shown in Fig. 46(b). The –Si–OH groups can take $H^+$ ions at a pH lower than ~2 and make their surface potential positive ($-Si-OH_2^+$, aquo state). Above a pH of 2, hydrophilic silica surface charges become negative due to the adsorption of $OH^-$ ions ($-Si-O^-$, oxo state). The –Si–OH groups on Aerosil® 380 exist in the neutral state at a pH of 2 (isoelectric point (IEP) of Aerosil® 380) [216]. Interestingly, the pH of sulfonated copolymers (0–1 [217]) as solid acids is lower than the IEP of Aerosil® 380. Hence, Aerosil® 380 in sulfonated polymer matrices is always positively charged and appears to act as an additional acid that can selectively take and transport protons, even though Aerosil® is a weaker acid than the $-SO_3H$ groups in the polymer matrices. When a surfactant is absorbed onto Aerosil® 380, its surface potential may be altered by the charge characteristics and content of the surfactant. These pH-dependent amphoteric properties have been reported in a variety of metallic oxides such as tungsten(VI) oxide, vanadium(V) oxide, zirconium(IV) oxide, chromium(III) oxide, and copper(II) oxide [218], but their IEP values are different from each other. It may be used as information to control the proton conduction of the corresponding composite membranes.

Some researchers maintain that performance improvements that are not expected in pure polymeric materials may be accomplished in composite materials with a high inorganic concentration (>15 wt.%) [219]. However, the use of high inorganic contents often gives rise to an uneven distribution and undesirable aggregation of the inorganic additives in polymer matrices. High inorganic concentrations may also cause non-selective cavities at the interface between the additives and the sulfonated polymers, which makes control of PEM characteristics difficult and weakens the mechanical strength of the resulting composite membranes.

The most important issue to consider when preparing organic–inorganic composite membranes is how to distribute the inorganic additives homogenously in the sulfonated polymer matrices, minimizing their self-aggregation that arises due to their physical interaction derived from surface functionalities (e.g., $-SO_3H$, –COOH, –OH, $-CH_3$, etc.). Well-distributed inorganic additives are expected to boost the synergistic effect on macroscopic composite-type PEM properties such as the thermal, mechanical, and chemical stability, as well as the electrochemical characteristics [220]. Improvements in these properties can significantly contribute to excellent fuel cell performance over a long period of time.

*3.2.1.1. Direct mixing of inorganic additives.* The simplest direct mixing method is to directly mix as-prepared inorganic additives in powder form with sulfonated copolymer solutions. For improved dispersion of the additives, sonication is sometimes employed after mixing. Most of the sulfonated polymer matrices used in this approach have a proton conductivity that is sufficiently high for PEMFC applications, but their excessive water swelling and high fuel permeability ($H_2$ and $O_2$) must be reduced via a combination with inorganic additives [205–214]. Unfortunately, it is very hard to avoid heterogeneity in both the size of the inorganic agglomerates and the dispersion state with the direct mixing method. This in turn prevents the PEM properties from being reproducible [210,214].

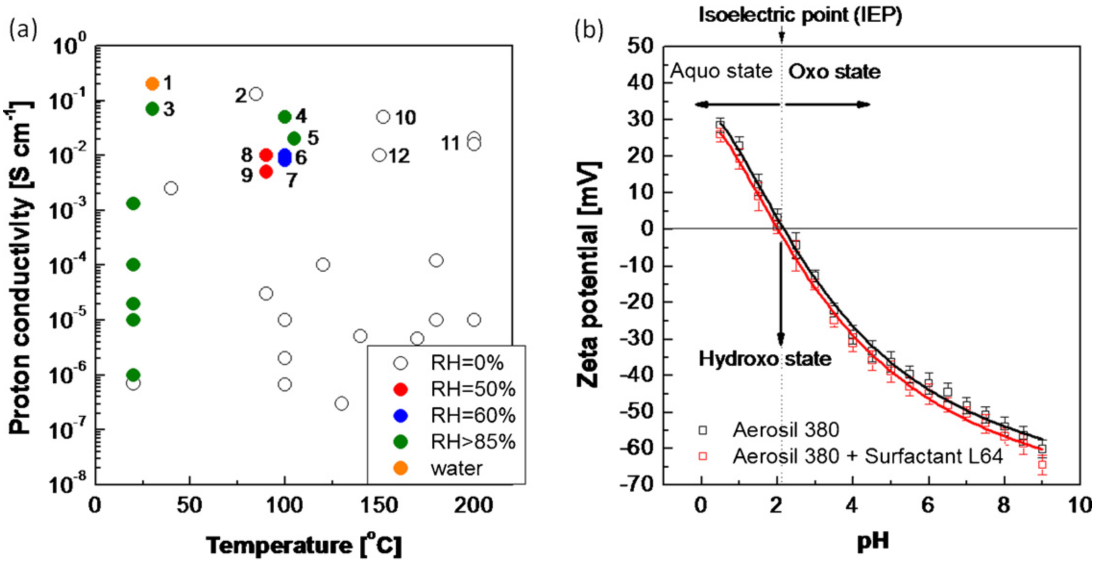

**Fig. 46.** (a) Inorganic fillers with proton conductivity at a specific temperature and humidity (1: tungstophosphoric acid ($H_3PW_{12}O_{40}{\cdot}xH_2O$) [214]; 2: $Ti(HPO_4)_{0.25}(O_3PC_6H_5)_{0.12}(O_3PC_6H_4SO_3H)_{1.63}$ [213]; 3: $BPO_4$ [210]; 4: $\gamma$-$Zr(PO_4)(H_2PO_4)_{0.54}(HO_3PC_6H_4SO_3H)_{0.46}{\cdot}nH_2O$ [205]; 5: $\alpha$-$Zr(O_3PC_6H_4SO_3H){\cdot}3.6H_2O$ [213]; 6: $Zr(O_3PCH_2OH)_{1.27}Y_{0.73}{\cdot}nH_2O$ [206]; 7: $\alpha$-$Zr(O_3PCH_2OH)_{1.27}(O_3PC_6H_4SO_3H)_{0.73}{\cdot}nH_2O$ [207]; 8: $(P_2O_5)_4(ZrO_2)_3$ glass [208]; 9: $P_2O_5$–$ZrO_2$–$SiO_2$ glass [211]; 10: $CsDSO_4$ [209]; 11 and 12: $CsHSO_4$ [212]) and (b) hydrophilic fumed silica (Aerosil® 380) with pH-dependent electrochemical properties [216].

A plausible approach to achieve good inorganic dispersion is to use surface-functionalized inorganic additives on the nano-scale. In particular, hydrophilic additives are relatively compatible with sulfonated copolymer matrices. The hydrophilic functional groups on their surface can physically interact with polymer matrices via ionic or hydrogen bonds. For example, –OH group-functionalized silica ($SiO_2$) was readily mixed with Nafion® [221–223] and sulfonated polystyrenes [224] dispersed or suspended in hydrophilic alcohols (e.g., methanol, ethanol, iso-propanol, and butanol) through sonication or homogenization. The well-distributed $SiO_2$ nanoparticles were effective in improving the level of water retention to temperatures lower than 155 °C and reducing fuel permeation through the resulting composite membranes. Here, improved water retention capability was validated by measuring water gains obtained when cooling the composite membranes dried at a high temperature via thermogravimetric analysis [222] or comparing both specific resistances and single cell performances of the composite membranes with those of Nafion® membrane under the same non-humidifying conditions [221,224]. However, a high inorganic concentration induced the formation of inorganic agglomerates, which weakened the mechanical strength of the resulting composites and sometimes led to undesirable fuel leakage/water flooding phenomena through their non-selective cavities.

Given the above issue, perhaps the best strategy for directly mixing inorganic additives is to maximize the effects of the inorganic additives while minimizing their usage. The use of amphiphilic surfactants in previous research was helpful in demonstrating this strategy [109,183,193,201,216,225–227]. A representative amphiphilic surfactant is a sort of non-ionic triblock copolymer (ABA block, A = poly(ethylene oxide) (PEO) and B = poly(propylene oxide) (PPO), e.g., Pluronics®) that has a good balance of hydrophilicity and hydrophobicity so as to distribute the surface-functionalized inorganic additives. When the surfactant exists in polar solvents (such as water) over its critical micelle concentration, it creates a peculiar micelle structure composed of a hydrophobic PPO core and a hydrophilic PEO shell [216,226–230]. After the addition of nano-sized inorganic additives (e.g., hydrophilic $SiO_2$, Aerosil® 380 with an average diameter of 7 nm), the surfactant was absorbed on the inorganic surface and the micelle diameter became larger than that of the surfactant as a result of the incorporation of inorganic additives within the surfactant micelle (Fig. 47(a)). When the surfactant-$SiO_2$ micelles were incorporated into sulfonated copolymer matrices, EO units in the surfactants formed strong complexes via ion–dipole interactions with sulfonated groups in the polymers (Fig. 47(b) [216,231]). It made functionalized $SiO_2$ particles positioned at the hydrophilic domains, which control water/proton transport in the copolymer systems [193,216,227]. The agglomeration of $SiO_2$ nanoparticles was simultaneously minimized, maintaining the individual particle size. Interestingly, even a small amount (1–5 wt%) of homogenously distributed $SiO_2$ nanoparticles was sufficient to significantly alter PEM properties. The corresponding nanocomposite PEMs exhibited improved proton conductivity, particularly at elevated temperatures, because well-dispersed $SiO_2$ nanoparticles act as additional solid acids in the sulfonated medium and contribute to an increase in the bound water content. This trend was significant at a high $SiO_2$ content (max. $SiO_2$ content = 10 wt%). Similar results were also observed in other sulfonated polymer matrices (i.e., SPI [109,193] and

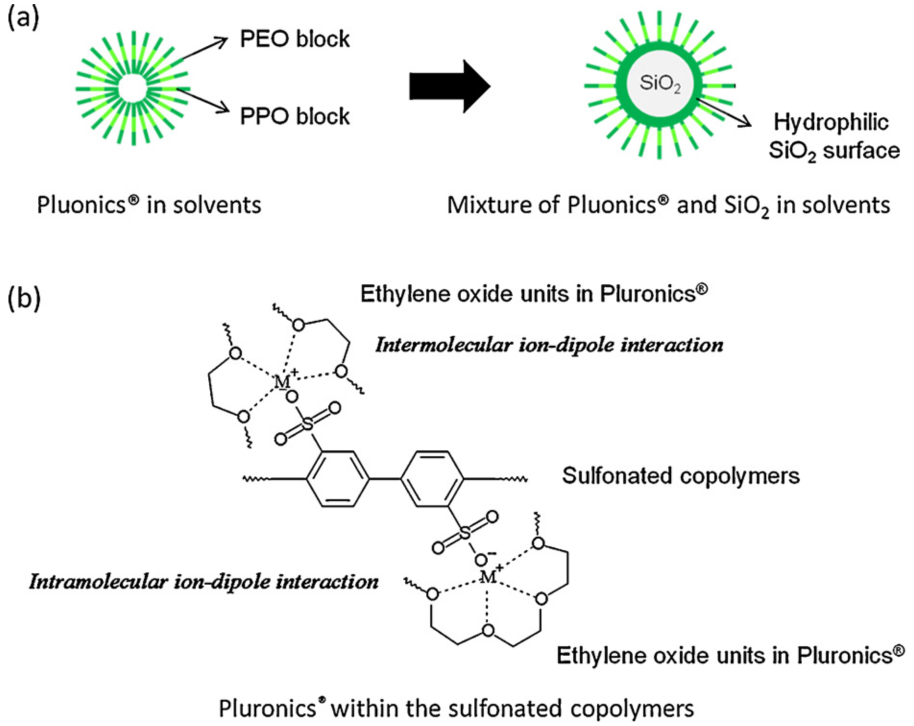

**Fig. 47.** (a) Micelle structure of Pluronics® dispersant in solvents [193] and (b) strong interaction between ethylene oxide (EO) units and sulfonated groups in the dispersants and sulfonated copolymers, respectively [231].
[231] Copyright 2011, American Chemical Society.

BPSH [183,216,227]). In the case of SPI–$SiO_2$ nanocomposites, well-dispersed $SiO_2$ nanoparticles greatly extended the lifetime of SPI matrices which are easily decomposed under hydrolysis conditions [193]. Consequently, the nanocomposites exhibited electrochemical single cell performances that were higher than or comparable to Nafion® even under the same PEMFC acceleration test conditions (Pt loading content = 0.3 mg $cm^{-2}$, operating temperature = 90 °C, relative humidity = 25%, $O_2/H_2$ feed rate = 200 mL $min^{-1}$/200 mL $min^{-1}$).

The characteristics of inorganic additives and surfactants play important roles in controlling the PEM properties of nanocomposite membranes. For example, when hydrophilic $SiO_2$ nanoparticles with different average diameters (7, 12, and 14 nm) and surface areas (150, 200, 300, and 380 $m^2\,g^{-1}$) were added to a BPSH-40 (DS = 40) random copolymer at the same concentration, both inorganic characteristics contributed to the transport behavior of small molecules (e.g., water) and/or ions (e.g., proton) through corresponding BPSH-40 $SiO_2$ nanocomposite membranes [227]. The smallest $SiO_2$ particles (7 nm) with the largest surface area (380 $m^2\,g^{-1}$) had the highest Si–OH concentration per unit gram, which gave rise to a considerable increase in the bound water content. Thus, the resulting nanocomposite membranes exhibited a proton conductivity (e.g., $\sigma = 0.24\,S\,cm^{-1}$ at 90 °C in liquid water) that was higher than other BPSH-40 $SiO_2$ nanocomposite membranes ($\sigma = 0.18–0.22\,S\,cm^{-1}$) and BPSH-40 membranes ($\sigma = 0.15\,S\,cm^{-1}$) even at elevated temperatures.

PEM properties can be affected by surface hydrophilicity of inorganic oxides in corresponding composites. Under a fully hydrated condition, sulfonated $ZrO_2$ nanoparticles exhibited proton conductivity of 0.01 S $cm^{-1}$ at 120 °C. Since its proton conductivity was higher than that of Nafion® at 120 °C and 70% RH, the resulting composite is expected to show improved low humidity PEMFC performances [232]. Also, the use of hydrophobic fluoroalkylated silica afforded the formation of composite membranes with remarkable mechanical and thermal stability, and good proton conductivity [233].

The nature of a surfactant is likely to determine its compatibility with polymer matrices and thus, the status of the inorganic dispersion. In highly fluorinated hydrocarbon polymer matrices, fluorosurfactants may be more effective than hydrocarbon surfactants like Pluronics® in preparing high-performance nanocomposite membranes due to their similar fluorine chemistry. In fact, fluorosurfactants (Zonyl® FSP: $[F(CF_2CF_2)_lCH_2CH_2O]_mP(O)(ONH_4)_n$; Zonyl® TBS: $F(CF_2CF_2)_xCH_2CH_2SO_3H$) with different ionic functionalities (phosphoric acid; sulfonic acid characteristics) positively contributed to $SiO_2$ distribution within a perfluorinated Nafion® matrix and greatly improved the proton conduction capability over a wide temperature range (25–90 °C) when compared to pure Nafion® and Nafion®-$SiO_2$ composites without surfactants [36,234]. For example, Nafion®-hydrophilic $SiO_2$ nanocomposite membranes, in which Zonyl® TBS was used as a dispersant, exhibited PEFC performances (ca. 1600 mA $cm^{-2}$ at 0.6 V, temperature = 80 °C, $O_2/H_2$ flow rate = 200/200 mL $min^{-1}$, and catalyst loading = 0.3 mg Pt $cm^{-2}$) that were higher than those of Nafion® recast membranes (ca. 1000 mA $cm^{-2}$ at 0.6 V) with the same fabrication history [234].

When PEO–PPO-based surfactants with two vinyl (–C=CH) groups at the terminal ends of the PPO are used (Fig. 48), the surfactants can act as dispersants for the distribution of inorganic additives and simultaneously produce characteristic chemical structures and morphologies according to the chemistry of the polymer matrices. For example, the vinyl groups in PEO–PPO-based surfactants can be polymerized using 2,2′-azxobisisobutyronitrile (AIBN) initiator and produce IPN structures (red line). In addition, the hydroxyl groups in the surfactants can produce crosslinked structures through the formation of covalent bonds with other functional groups (e.g., $-SO_3H$ or –COOH) in the polymer matrices [226,235]. The resulting polymer–$SiO_2$ nanocomposites have exhibited excellent chemical durability and mechanical strength, as well as improved proton conductivity when compared to a corresponding pure copolymer due to the synergistic effect of well-dispersed $SiO_2$ and tuned polymer structures.

*3.2.1.2. In situ inorganic formation.* Inorganic components can be grown within sulfonated polymer matrices in both (1) the membrane state and (2) the solution state via the sol–gel transition of inorganic precursors. Sol–gel transition in the membrane state is based on the *in situ* local growth of inorganic sub-lattices that occurs within the hydrophilic domains of sulfonated copolymers. Initially, sulfonated copolymers were soaked in aqueous solutions containing precursors such as silicon oxide, titanium oxide, aluminum oxide, zirconium oxide [e.g. tetrabutylzirconate ($Zr(OBu)_4$, TBZ)] [236,237], and a mixture of zirconium chloride octahydrate and phosphoric acid [238]. After permeation or ion-exchange of the precursors, successive precipitation or hydrolysis, aging, and drying processes followed. Here, the hydrophilic domains consisting of $-SO_3H$ groups were used as acidic nanoreactors for the sol–gel transition [236–239]. Consequently, inorganic components were preferentially incorporated in the hydrophilic domains of the sulfonated copolymers. The concentration of inorganic precursors was relatively high on the membrane surface, which induced a compositional inorganic concentration profile according to the membrane thickness. Inorganic components in the resulting hybrid membrane were asymmetrically distributed. Membrane properties, including the morphology, were highly influenced by various factors such as the temperature, reaction time, precursor concentration, permeation properties of the precursors through the copolymer matrices, and the IEC of the sulfonated copolymers. The proton conductivity of the hybrid membrane was generally superior to that of pure copolymer membranes. However, its fuel permeability was comparable to that of sulfonated copolymers due to the non-selective and porous inorganic (e.g., $SiO_2$) network that is produced from the sol–gel reaction. Furthermore, the inorganic content in the hybrid membranes was restricted by both its IEC value and its precursor permeability. In sulfonated SPEEK–zirconium phosphate (ZrP) composites, the ZrP content was limited to 30 wt% at an IEC of 1.3 mequiv. $g^{-1}$ [239].

The above limitation on the inorganic content can be eliminated through inorganic growth in the polymer solution state. Theoretically, corresponding membrane characteristics can be varied from pure organic to pure inorganic as the inorganic content is increased. Up to now, many polymers have been used as polymeric matrices for this sol–gel transition. These include various sulfonated polymers such as Nafion® [240], SPSs [241], and SPEEKs [242]. The sol–gel transition is conducted via (1) the hydrolysis of alkoxide precursors and (2) alcohol/water condensation [243] (Fig. 49(a)). The physico-chemical properties of hybrid membranes are affected by a variety of reaction factors including the ratio of water to alkoxide precursors, pH, temperature and pressure of the reaction medium, solvents, and monomer stoichiometry. For example, when Nafion®-$SiO_2$ hybrid membranes with different $SiO_2$ contents (6–54 wt%) were prepared using two different alkoxide precursors (TEOS and TMDES in Fig. 49(b)), the resulting inorganic network morphology was significantly influenced by the $SiO_2$ content and the type of alkoxide used in the hybrid formation. TEOS induced a bank-like structure, which was aligned in the solvent evaporation direction at a low $SiO_2$ content (~6.5 wt%). Meanwhile, a laminar structure was obtained when TEOS was replaced with TMDES at a high $SiO_2$ content (>10 wt%) [240]. In most hybrid membranes, these inorganic networks failed to have a positive impact on proton conductivity. Even in SPEEK with a high DS of 87%, a small amount of inorganic oxide (e.g., 2.5 wt% of $ZrO_2$) severely depressed the proton conductivity of the hybrid membrane. At 12.5 wt%, the hybrid membrane exhibited an extremely high resistance to proton transport [242].

The reduction in proton conductivity after hybrid formation can be compensated for by adding doping acids (e.g., tungstophosphoric acid [241] and 4-dodecylbenzene sulfonic acid (DBSA) [244]) into the inorganic oxide network. Particularly, the combination of $SiO_2$ and tungstophosphoric acid contributed to a high level of water retention and excellent proton conductivity ($<6.2 \times 10^{-1}$ S $cm^{-1}$) in the resulting SPS-$SiO_2$ hybrid membranes at 120 °C and 87% RH.

### 3.2.2. Reinforced sulfonated hydrocarbon PEMs

The polymer reinforcement concept that involves the use of mechanically durable, porous non-sulfonated polymer substrates to impregnate highly sulfonated polymers has been studied. The resulting reinforced sulfonated hydrocarbon PEMs are classified into pore-filling membranes [173,245–249] and sulfonated polymer-impregnated electrospun composite membranes [250,251] according to the substrate characteristics.

Pore-filling membranes are comprised of an organic or inorganic substrate with interconnected pores that have an average size smaller than 500 nm and a gel-type or branched sulfonated hydrocarbon copolymer filling the pores of the substrate (Fig. 50). The porous substrate should be thermally stable and inert to fuel gases or liquids ($H_2$, $O_2$, CO, $CO_2$, water, and methanol) that come into contact with during fuel cell operations. The substrate must

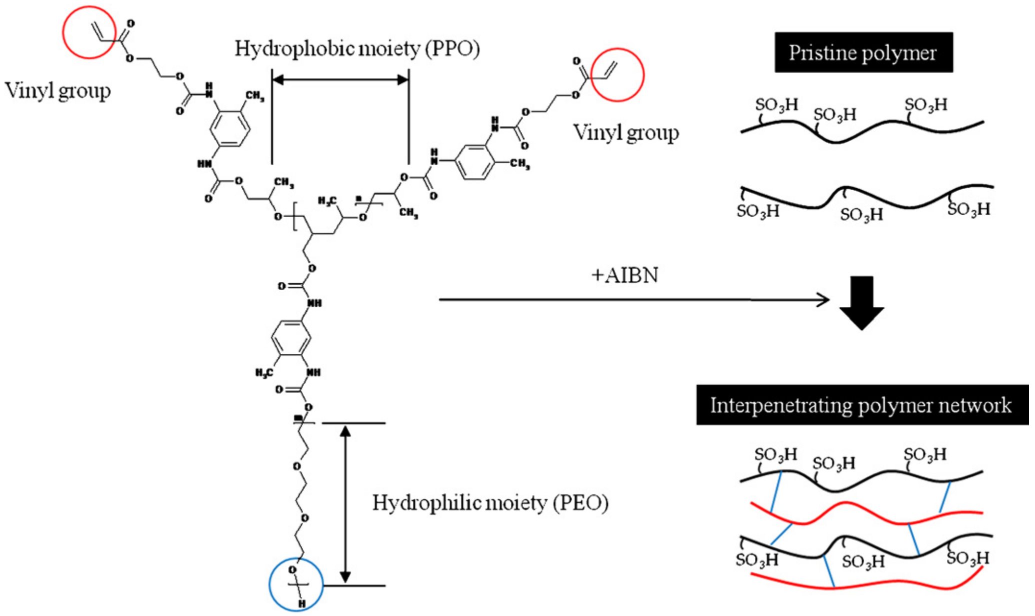

**Fig. 48.** Chemical structure of PEO–PPO based surfactants with vinyl groups at their terminal ends (left) and interpenetrating polymer network obtained from the surfactant (right) [226,235].

simultaneously be mechanically strong enough to endure the swelling of sulfonated copolymers filling the pores in the fully hydrated state. In the early stages of pore-filling research, porous silica (e.g., $SiO_2$ gel) on a carbon support was used as a substrate [245]. Despite its thermal stability, $SiO_2$ gel was fragile and cannot form a self-supporting film structure. Meanwhile, some porous polymeric substrates [e.g., polytetrafluoroethylene (PTFE) [247], cross-linked high-density polyethylene substrate (CLPE) [246,248,249], and PI [173,246]] satisfy the substrate requirements mentioned above.

The proton conductivity of pore-filling membranes is determined by the pore-filling ratio and, more commonly, by the acidity of the filling polymers. Among the filling polymers used for pore-filling membrane formation, poly(acrylic acid) (PAA) is a weak acid and

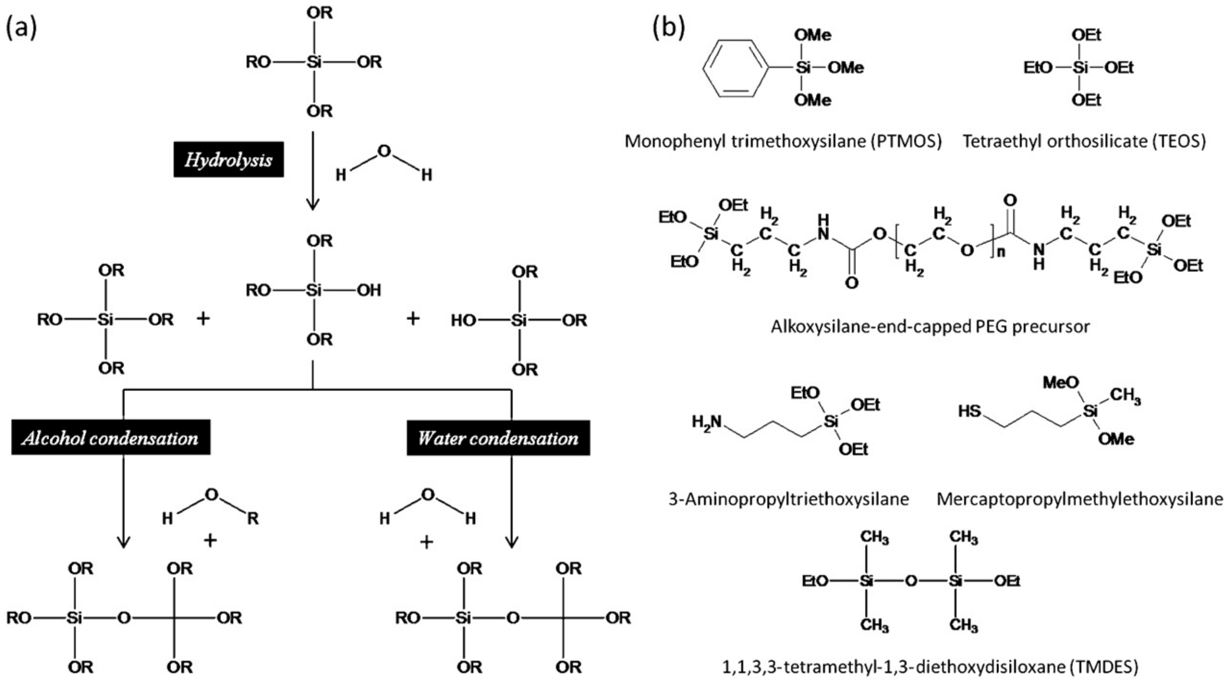

**Fig. 49.** (a) Synthetic scheme of sol–gel process and (b) representative alkoxide precursors.

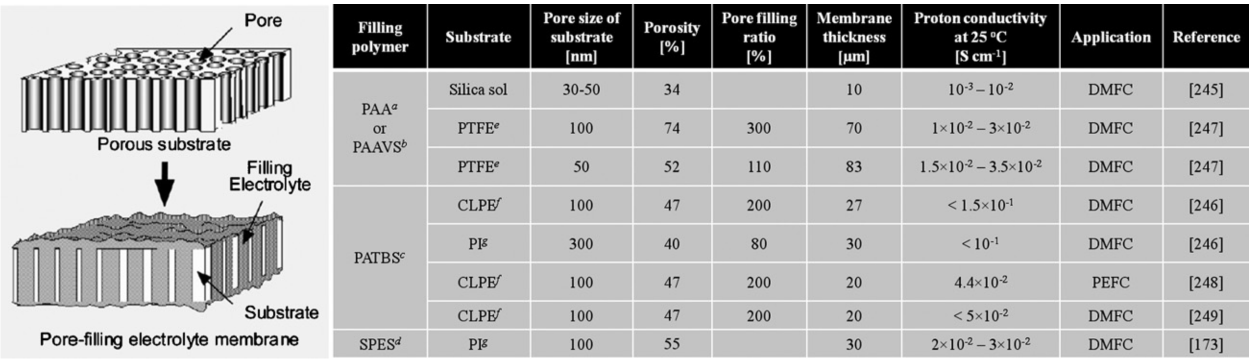

| Filling polymer | Substrate | Pore size of substrate [nm] | Porosity [%] | Pore filling ratio [%] | Membrane thickness [μm] | Proton conductivity at 25 °C [S cm⁻¹] | Application | Reference |
|---|---|---|---|---|---|---|---|---|
| PAA[a] or PAAVS[b] | Silica sol | 30-50 | 34 | | 10 | $10^{-3} – 10^{-2}$ | DMFC | [245] |
| | PTFE[e] | 100 | 74 | 300 | 70 | $1\times10^{-2} – 3\times10^{-2}$ | DMFC | [247] |
| | PTFE[e] | 50 | 52 | 110 | 83 | $1.5\times10^{-2} – 3.5\times10^{-2}$ | DMFC | [247] |
| PATBS[c] | CLPE[f] | 100 | 47 | 200 | 27 | $< 1.5\times10^{-1}$ | DMFC | [246] |
| | PI[g] | 300 | 40 | 80 | 30 | $< 10^{-1}$ | DMFC | [246] |
| | CLPE[f] | 100 | 47 | 200 | 20 | $4.4\times10^{-2}$ | PEFC | [248] |
| | CLPE[f] | 100 | 47 | 200 | 20 | $< 5\times10^{-2}$ | DMFC | [249] |
| SPES[d] | PI[g] | 100 | 55 | | 30 | $2\times10^{-2} – 3\times10^{-2}$ | DMFC | [173] |

**Fig. 50.** Basic concept of pore-filling membranes [173] and their characteristics summary. [a]Poly(acrylic acid), [b]poly(acrylic acid-*co*-vinylsulfonic acid), [c]poly(acrylamide-*tert*-butylsulfonic acid), [d]crosslinked sulfonated poly(ether sulfone), [e]poly(tetrafluoroethylene), [f]porous crosslinked high-density polyethylene, and [g]porous polyimide.
[173] Copyright 2007, Wiley–VCH Verlag GmbH & Co.

poly(acrylic acid-*co*-vinylsulfonic acid) (PAAVS) copolymer has a low IEC value (0.7 mequiv. $g^{-1}$). The corresponding pore-filling membranes [245,247] exhibited proton conductivities that were much lower than that of Nafion® 117 ($\sigma = 8 \times 10^{-2}$ S $cm^{-1}$) under the same measurement conditions (25 °C and humid state). On the other hand, poly(acrylamide-*tert*-butylsulfonic acid) (PATBS) has one $-SO_3H$ group per monomer unit (IEC = 4.5 mequiv. $g^{-1}$). PATBS-CLPE and PATBS-PI pore-filling membranes were prepared via monomer impregnation into pores and a subsequent polymerization process. Gelation of PATBS was achieved with a methylene-bis-acrylamide crosslinker [247–249]. The proton conductivity increased with the pore-filling ratio, regardless of the substrate type, and was superior to that of Nafion® 117 and other pore-filling membranes. Under PEFC operating conditions, a PATBS-CLPE pore-filling membrane ($\sigma = 4.4 \times 10^{-2}$ S $cm^{-1}$) exhibited a single cell performance (power density = 1000 mW $cm^{-2}$ and current density = 2000 mA $cm^{-2}$ at 0.5 V and 60 °C) that was comparable to that of Nafion® 112 [252]. Such behavior could be observed because a thin (20 μm) layer of PATBS-CLPE resulted in a membrane conductance (in S $cm^{-2}$) that was similar to that of thick Nafion® 112 (58 μm) while maintaining good $H_2$ barrier characteristics.

Most pore-filling membranes were designed for DMFCs, where the mechanical restriction of the substrates to membrane swelling was helpful in lowering methanol crossover while maintaining water uptake for proton migration. Previous gel-type pore-filling polymers failed to show excellent methanol barrier properties. However, the combination of a tough and rigid SPES crosslinked copolymer and a thermo-chemically durable PI substrate allowed the resulting SPES-PI pore-filling membranes to have greatly reduced methanol permeability [173]. The pore-filling membranes were fabricated via *in situ* polycondensation of sulfonated 4,4′-dichlorodiphenylsulfone (SDCDPS)/non-sulfonated [DCDPS and diphenol (DP)] monomers and a crosslinking agent (1,1,1-trihydroxy phenylethane) inside the pores of the PI substrate. After the polycondensation process, the total membrane thickness did not significantly change (~30 μm). In addition, swelling of the pore-filling membranes in the fully hydrated state was negligibly small (0–1%) when compared to Nafion® 117 (25%). The greatly reduced level of methanol permeation and the thin membrane thickness of SPES-PI pore-filling membranes are expected to compensate for its low proton conductivity ($\sigma = 2 \times 10^{-2}$–$3 \times 10^{-2}$ S $cm^{-1}$). This is demonstrated in PATBS-CLPE pore-filling membranes, which exhibited single cell performances that were higher than Nafion® 117 at a high methanol concentration (>16 wt%). Such a concept is expected to be directly applied to PEMFC systems.

Recently, there have been approaches aimed at impregnating sulfonated polymers into electrospun membranes instead of polymer substrates with sub-micrometer scale pores [248,250]. One example is Nafion®-impregnated polyvinylidene fluoride (PVdF) composites [250]. Even after composite formation, a tortuous framework structure was maintained. The peculiar three-dimensional network structure of PVdF led to reduced liquid fuel (e.g., methanol) permeability. However, the proton conductivity of the membrane was one order of magnitude lower than Nafion® 115 at almost the same membrane thickness. While a limited amount of electrochemical information derived from the composite membranes was reported, their significant advantages in single cell performance and the theoretical background supporting them have not yet been clearly revealed.

## 4. Conclusions and outlook

Sulfonated hydrocarbon PEMs have been reviewed as promising electrolytes for medium-temperature and low relative humidity PEMFC applications. Sulfonated hydrocarbon PEMs require excellent membrane durability to chemicals and hydrolysis and a high proton conductivity under harsh conditions. Considering practical PEMFC operation, the current DOE target (proton conductivity >0.1 S $cm^{-1}$ at 80 °C and 50% RH) is still challenging.

It was explained that new sulfonated aromatic hydrocarbon membranes have been synthesized so as to form effective water channels within wider hydrophilic domains. This was achieved by fabricating multiblock copolymers, comb-type graft copolymers, highly sulfonatable polymers with aromatic and/or aliphatic side chains, high free volume polymers, etc. These polymers usually form a micro-phase separated structure, as evidenced by AFM and TEM images. In order to increase the membrane durability, sulfonic acid groups must be located apart from the polymer backbone. Well-connected nanoscale hydrophilic domains in sulfonated aromatic hydrocarbons that mimic the Nafion® structure should be formed.

To improve PEM properties further, physico-chemical tuning may accompany the architectural design of PEMs. These approaches include crosslinking, surface fluorination, thermal annealing, the use of organic–inorganic composites, and the polymer reinforcement concept. Such combinational methods are expected to be new strategies in the rational design of next-generation PEM materials with high electrochemical PEMFC performances over a long period of time.

## Acknowledgements

This research was supported by the WCU (World Class University) program through the National Research Foundation funded by the Ministry of Education, Science and Technology (R31-10092) and by the International Research & Development Program of the National Research Foundation of Korea (NRF) funded by the Ministry of Education, Science and Technology (MEST) of Korea (Grant number: K20701010356-07A0100-10610).

## Appendix A. Supplementary data

Supplementary data associated with this article can be found, in the online version, at doi:10.1016/j.progpolymsci.2011.06.001.

## References

[1] Maugeri L. Understanding oil price behavior through an analysis of a crisis. Rev Environ Econ Policy 2009;3:147–66.
[2] Cook J. Next stop for oil prices: $100 or $150? Washington: EIA Office of Oil and Gas DOE; 2008.
[3] Anonymous. Petroleum marketing annual 2008. Washington: EIA Office of Oil and Gas DOE; 2009.
[4] Appleby AJ, Foules FR. Fuel cell handbook. New York: Van Nostrand Reinhold; 1989.
[5] Savadogo O. Emerging membranes for electrochemical systems. I. Solid polymer electrolyte membranes for fuel cell systems. J New Mater Electrochem Syst 1998;1:47–66.
[6] Steele BCH, Heinzel A. Materials for fuel-cell technologies. Nature 2001;414:345–52.
[7] Hamnett A. Introduction to fuel-cell types. In: Vielstich W, Lamm A, Gasteiger HA, editors. Handbook of fuel cells-fundamentals, technology and applications. Chichester, UK: John Wiley & Sons Ltd.; 2003. p. 36–43.
[8] Doyle M, Rajendran G. Perfluorinated membranes. In: VielstichW, Lamm A, Gasteiger HA, editors. Handbook of fuel cells-fundamentals, technology and applications. Chichester, UK: John Wiley & Sons Ltd.; 2003. p. 351–95.
[9] Li Q, Jensen JO, Savinell RF, Bjerrum NJ. High temperature proton exchange membranes based on polybenzimidazoles for fuel cells. Prog Polym Sci 2009;34:449–77.
[10] Anonymous. Multi-year research, development and demonstration plan: planned program activities for 2005–2015. Washington: EIA Office of Oil and Gas DOE; 2007.
[11] Kreuer KD, Rabenau A, Weppner W. Vehicle mechanism, a new model for the interpretation of the conductivity of fast proton conductors. Angew Chem Int Ed 1982;21:208–9.
[12] Kreuer KD. Proton conductivity: materials and applications. Chem Mater 1996;8:610–41.
[13] Eikerling M, Kornyshev AA, Kuznetsov AM, Ulstrup J, Walbran S. Mechanisms of proton conductance in polymer electrolyte membranes. J Phys Chem B 2001;105:3646–62.
[14] Kreuer K-D, Paddison SJ, Spohr E, Schuster M. Transport in proton conductors for fuel-cell applications: simulations, elementary reactions, and phenomenology. Chem Rev 2004;104:4637–78.
[15] Cukierman S. Et tu, Grotthuss! and other unfinished stories. Biochim Biophys Acta 2006;1757:876–85.
[16] Kreuer KD. On the development of proton conducting polymer membranes for hydrogen and methanol fuel cells. J Membr Sci 2001;185:29–39.
[17] Agmon N. The Grotthuss mechanism. Chem Phys Lett 1995;244:456–62.
[18] Tuckerman M, Laasonen K, Sprik M, Parrinello M. Ab initio molecular dynamics simulation of the solvation and transport of hydronium and hydroxyl ions in water. J Chem Phys 1995;103:150–61.
[19] Tuckerman M, Laasonen K, Sprik M, Parrinello M. Ab initio molecular dynamics simulation of the solvation and transport of $H_3O^+$ and $OH^-$ ions in water. J Phys Chem 1995;99:5749–52.
[20] Dippel T, Kreuer KD, Lassègues JC, Rodriguez D. Proton conductivity in fused phosphoric acid: a $^1H/^{31}P$ PFG-NMR and QNS study. Solid State Ionics 1993;61:41–6.
[21] Schuster M, Kreuer KD, Steininger H, Maier J. Proton conductivity and diffusion study of molten phosphonic acid $H_3PO_3$. Solid State Ionics 2008;179:523–8.
[22] Münch W, Kreuer KD, Silvestri W, Maier J, Seifert G. The diffusion mechanism of an excess proton in imidazole molecule chains: first results of an ab initio molecular dynamics study. Solid State Ionics 2001;145:437–43.
[23] Bureekaew S, Horike S, Higuchi M, Mizuno M, Kawamura T, Tanaka D, Yanai N, Kitagawa S. One-dimensional imidazole aggregate in aluminium porous coordination polymers with high proton conductivity. Nat Mater 2009;8:831–6.
[24] Maier G, Meier-Haack J. Sulfonated aromatic polymers for fuel cell membranes. In: Scherer GG, editor. Fuel cells II. Berlin/Heidelberg: Springer; 2008. p. 1–62.
[25] Meier-Haack J, Taeger A, Vogel C, Schlenstedt K, Lenk W, Lehmann D. Membranes from sulfonated block copolymers for use in fuel cells. Sep Purif Technol 2005;41:207–20.
[26] Yin Y, Yamada O, Tanaka K, Okamoto KI. On the development of naphthalene-based sulfonated polyimide membranes for fuel cell applications. Polym J 2006;38:197–219.
[27] Hickner MA, Ghassemi H, Kim YS, Einsla BR, McGrath JE. Alternative polymer systems for proton exchange membranes (PEMs). Chem Rev 2004;104:4587–612.
[28] Rikukawa M, Sanui K. Proton-conducting polymer electrolyte membranes based on hydrocarbon polymers. Prog Polym Sci 2000;25:1463–502.
[29] Smitha B, Sridhar S, Khan AA. Synthesis and characterization of proton conducting polymer membranes for fuel cells. J Membr Sci 2003;225:63–76.
[30] Miyatake K, Hay AS. New poly(arylene ether)s with pendant phosphonic acid groups. J Polym Sci Part A Polym Chem 2001;39:3770–9.
[31] Meng YZ, Tjong SC, Hay AS, Wang SJ. Proton-exchange membrane electrolytes derived from phosphonic acid containing poly(arylene ether)s. Eur Polym J 2003;39:627–31.
[32] Savett SC, Atkins JR, Sides CR, Harris JL, Thomas BH, Creager SE, Pennington WT, DesMarteau DD. A comparison of bis[(perfluoroalkyl)sulfonyl]imide ionomers and perfluorosulfonic acid ionomers for applications in PEM fuel-cell technology. J Electrochem Soc 2002;149:A1527–32.
[33] Hofmann MA, Ambler CM, Maher AE, Chalkova E, Zhou XY, Lvov SN, Allcock HR. Synthesis of polyphosphazenes with sulfonimide side groups. Macromolecules 2002;35:6490–3.
[34] Liu B, Kim DS, Guiver MD, Kim YS, Pivovar BS. Sulfonated poly(arylene ether)-type polymers as proton exchange membranes: synthesis and performance. In: Peinemann K-V, Nunes SP, editors. Membranes for energy conversion. Weinheim: Wiley–VCH Verlag GmbH & Co. KgaA; 2008. p. 1–45.
[35] Hornback JM. Organic chemistry. 2nd ed. Belmont: Thomson Brooks/Cole; 2005.
[36] Park CH, Kim HK, Lee CH, Park HB, Lee YM. Nafion® nanocomposite membranes: effect of fluorosurfactants on hydrophobic silica nanoparticle dispersion and direct methanol fuel cell performance. J Power Sources 2009;194:646–54.
[37] Souzy R, Ameduri B. Functional fluoropolymers for fuel cell membranes. Prog Polym Sci 2005;30:644–87.

[38] Park CH, Lee CH, Sohn JY, Park HB, Guiver MD, Lee YM. Phase separation and water channel formation in sulfonated block copolyimide. J Phys Chem B 2010;114:12036–45.
[39] Mauritz KA, Moore RB. State of understanding of Nafion. Chem Rev 2004;104:4535–85.
[40] Takimoto N, Wu L, Ohira A, Takeoka Y, Rikukawa M. Hydration behavior of perfluorinated and hydrocarbon-type proton exchange membranes: relationship between morphology and proton conduction. Polymer 2009;50:534–40.
[41] Schmidt-Rohr K, Chen Q. Parallel cylindrical water nanochannels in Nafion fuel-cell membranes. Nat Mater 2008;7:75–83.
[42] Xie T. Tunable polymer multi-shape memory effect. Nature 2010;464:267–70.
[43] Kreuer KD. Hydrocarbon membranes. In: Vielstich W, Lamm A, Gasteiger HA, editors. Handbook of fuel cells-fundamentals, technology and applications. Chichester, UK: John Wiley & Sons Ltd.; 2003. p. 420–35.
[44] Roziére J, Jones DJ. Non-fluorinated polymer materials for proton exchange membrane fuel cells. Annu Rev Mater Res 2003;33:503–55.
[45] Kobayashi T, Rikukawa M, Sanui K, Ogata N. Proton-conducting polymers derived from poly(ether-etherketone) and poly(4-phenoxybenzoyl-1,4-phenylene). Solid State Ionics 1998;106:219–25.
[46] Guo Q, Pintauro N, Tang P, O'Connor HS. Sulfonated and crosslinked polyphosphazene-based proton-exchange membranes. J Membr Sci 1999;154:175–81.
[47] Wycisk R, Pintauro PN, Wang W, O'Connor S. Polyphosphazene membranes. I. Solid-state photocrosslinking of poly[(4-ethylphenoxy)-(phenoxy)phosphazene]. J Appl Polym Sci 1996;59:1607–17.
[48] Bauman WC, Skidmore JR, Osmun RH. Dowex 50. Ind Eng Chem 1948;40:1350–5.
[49] Genova-Dimitrova P, Baradie B, Foscallo D, Poinsignon C, Sanchez JY. Ionomeric membranes for proton exchange membrane fuel cell (PEMFC): sulfonated polysulfone associated with phosphatoantimonic acid. J Membr Sci 2001;185:59–71.
[50] Serpico JM, Ehrenberg SG, Fontanella JJ, Jiao X, Perahia D, McGrady KA, Sanders EH, Kellogg GE, Wnek GE. Transport and structural studies of sulfonated styrene–ethylene copolymer membranes. Macromolecules 2002;35:5916–21.
[51] Kim J, Kim B, Jung B. Proton conductivities and methanol permeabilities of membranes made from partially sulfonated polystyrene-block-poly(ethylene-ran-butylene)-block-polystyrene copolymers. J Membr Sci 2002;207:129–37.
[52] Hodgdon RB. Polyelectrolytes prepared from perfluoroalkylaryl macromolecules. J Polym Sci 1968;6:171–91.
[53] Ding J, Chuy C, Holdcroft S. Solid polymer electrolytes based on ionic graft polymers: effect of graft chain length on nano-structured ionic networks. Adv Funct Mater 2002;12:389–94.
[54] Norsten TB, Guiver MD, Murphy J, Astill T, Navessin T, Holdcroft S, Frankamp BL, Rotello VM, Ding J. Highly fluorinated comb-shaped copolymers as Proton Exchange Membranes (PEMs): improving PEM properties through rational design. Adv Funct Mater 2006;16:1814–22.
[55] Noshay A, Robeson LM. Sulfonated polysulfone. J Appl Polym Sci 1976;20:1885–903.
[56] Bishop MT, Karasz FE, Russo PS, Langley KH. Solubility and properties of a poly(aryl ether ketone) in strong acids. Macromolecules 1985;18:86–93.
[57] Alberti G, Casciola M, Massinelli L, Bauer B. Polymeric proton conducting membranes for medium temperature fuel cells (110–160 °C). J Membr Sci 2001;185:73–81.
[58] Xing P, Robertson GP, Guiver MD, Mikhailenko SD, Wang K, Kaliaguine S. Synthesis and characterization of sulfonated poly(ether ether ketone) for proton exchange membranes. J Membr Sci 2004;229:95–106.
[59] Liu B, Robertson GP, Kim DS, Guiver MD, Hu W, Jiang Z. Aromatic poly(ether ketone)s with pendant sulfonic acid phenyl groups prepared by a mild sulfonation method for proton exchange membranes. Macromolecules 2007;40:1934–44.
[60] Miyatake K, Hay AS. Synthesis and properties of poly(arylene ether)s bearing sulfonic acid groups on pendant phenyl rings. J Polym Sci Part A Polym Chem 2001;39:3211–7.
[61] Miyatake K, Oyaizu K, Tsuchida E, Hay AS. Synthesis and properties of novel sulfonated arylene ether/fluorinated alkane copolymers. Macromolecules 2001;34:2065–71.
[62] Kerres J, Cui W, Reichle S. New sulfonated engineering polymers via the metalation route. I. Sulfonated poly(ethersulfone) PSU Udel® via metalation–sulfination–oxidation. J Polym Sci Part A Polym Chem 1996;34:2421–38.
[63] Schuster M, Kreuer KD, Andersen HT, Maier J. Sulfonated poly(phenylene sulfone) polymers as hydrolytically and thermooxidatively stable proton conducting ionomers. Macromolecules 2007;40:598–607.
[64] Guiver MD, ApSimon JW, Kutowy O. Modification of polysulfone by metalation. J Polym Sci Part C Polym Lett 1988;16:123–7.
[65] Guiver MD, Robertson GP, Yoshikawa M, Tam CM. Functionalized polysulfones: methods for chemical modification and membrane applications. ACS Symp Ser 1999;744:137–61.
[66] Lafitte B, Karlsson LE, Jannasch P. Sulfophenylation of polysulfones for proton-conducting fuel cell membranes. Macromol Rapid Commun 2002;23:896–900.
[67] Lafitte B, Puchner M, Jannasch P. Proton conducting polysulfone ionomers carrying sulfoaryloxybenzoyl side chains. Macromol Rapid Commun 2005;26:1464–8.
[68] Zhao L, Ding J, Robertson GP, Guiver MD. A novel bisphenol monomer with grafting capability and the resulting poly(arylene ether sulfone)s. Macromolecules 2006;39:6990–6.
[69] Wang JL, Lee MH, Yang J. Synthesis and characterization of sulphonated polymer derived from 6FDA-ODA polyimide. Polym Bull 2005;55:357–65.
[70] Deligöz H, Vatansever S, Öksüzömer F, Koç SN, Özgümüş S, Gürkaynak MA. Preparation and characterization of sulfonated polyimide ionomers via post-sulfonation method for fuel cell applications. Polym Adv Technol 2008;19:1126–32.
[71] Kim YS, Wang F, Hickner M, McCartney S, Hong YT, Harrison W, Zawodzinski TA, McGrath JE. Effect of acidification treatment and morphological stability of sulfonated poly(arylene ether sulfone) copolymer proton-exchange membranes for fuel-cell use above 100 °C. J Polym Sci Part B Polym Phys 2003;41: 2816–28.
[72] Vallejo E, Pourcelly G, Gavach C, Mercier R, Pineri M. Sulfonated polyimides as proton conductor exchange membranes. Physicochemical properties and separation $H^+/M(z^+)$ by electrodialysis comparison with a perfluorosulfonic membrane. J Membr Sci 1999;160:127–37.
[73] Ghassemi H, McGrath JE, Zawodzinski Jr TA. Multiblock sulfonated-fluorinated poly(arylene ether)s for a proton exchange membrane fuel cell. Polymer 2006;47:4132–9.
[74] Lee H-S, Badami AS, Roy A, McGrath JE. Segmented sulfonated poly(arylene ether sulfone)-b-polyimide copolymers for proton exchange membrane fuel cells. I. Copolymer synthesis and fundamental properties. J Polym Sci Part A Polym Chem 2007;45:4879–90.
[75] Cornet N, Diat O, Gebel G, Jousse F, Marsacq D, Mercier R, Pineri M. Sulfonated polyimide membranes: a new type of ion-conducting membrane for electrochemical applications. J New Mater Electrochem Syst 2000;3:33–42.
[76] Robeson LM, Matzner M. Poly(arylene ether)s-directcopolymerization-first sulfonated monomer patent-flame retarding properties. US 4,380,598; 1983.
[77] Ueda M, Toyota H, Ouchi T, Sugiyama J-I, Yonetake K, Masuko T, Teramoto T. Synthesis and characterization of aromatic poly(ether sulfone)s containing pendant sodium sulfonate groups. J Polym Sci Part A Polym Chem 1993;31:853–8.
[78] Wang F, Chen T, Xu J. Sodium sulfonate-functionalized poly(ether ether ketone)s. Macromol Chem Phys 1998;199:1421–6.
[79] Wang F, Hickner M, Ji Q, Harrison W, Mecham J, Zawodzinski TA, McGrath JE. Synthesis of highly sulfonated poly(arylene ether sulfone) random (statistical) copolymers via direct polymerization. Macromol Symp 2001;175:387–96.
[80] Wang F, Hickner M, Kim YS, Zawodzinski TA, McGrath JE. Direct polymerization of sulfonated poly(arylene ether sulfone) random (statistical) copolymers: candidates for new proton exchange membranes. J Membr Sci 2002;197:231–42.
[81] Harrison WL, Wang F, Mecham JB, Bhanu VA, Hill M, Kim YS, McGrath JE. Influence of the bisphenol structure on the direct synthesis of sulfonated poly(arylene ether) copolymers. I. J Polym Sci Part A Polym Chem 2003;41:2264–76.
[82] Harrison WL, Hickner MA, Kim YS, McGrath JE. Poly(arylene ether sulfone) copolymers and related systems from disulfonated monomer building blocks: synthesis, characterization, and performance—a topical review. Fuel Cells 2005;5:201–12.
[83] Kim YS, Einsla B, Sankir M, Harrison W, Pivovar BS. Structure–property–performance relationships of sulfonated poly(arylene ether sulfone)s as a polymer electrolyte for fuel cell applications. Polymer 2006;47:4026–35.

[84] Hickner MA, Pivovar BS. The chemical and structural nature of proton exchange membrane fuel cell properties. Fuel Cells 2005;5:213–29.
[85] Li X, Na H, Lu H. Novel sulfonated poly(ether ether ketone ketone) derived from bisphenol S. J Appl Polym Sci 2004;94:1569–74.
[86] Li X, Liu C, Lu H, Zhao C, Wang Z, Xing W, Na H. Preparation and characterization of sulfonated poly(ether ether ketone ketone) proton exchange membranes for fuel cell application. J Membr Sci 2005;255:149–55.
[87] Gao Y, Robertson GP, Guiver MD, Mikhailenko SD, Li X, Kaliaguine S. Synthesis of poly(arylene ether ether ketone ketone) copolymers containing pendant sulfonic acid groups bonded to naphthalene as proton exchange membrane materials. Macromolecules 2004;37:6748–54.
[88] Gao Y, Robertson GP, Guiver MD, Mikhailenko SD, Li X, Kaliaguine S. Synthesis of copoly(aryl ether ether nitrile)s containing sulfonic acid groups for PEM application. Macromolecules 2005;38:3237–45.
[89] Gao Y, Robertson GP, Guiver MD, Mikhailenko SD, Li X, Kaliaguine S. Low-swelling proton-conducting copoly(aryl ether nitrile)s containing naphthalene structure with sulfonic acid groups meta to the ether linkage. Polymer 2006;47:808–16.
[90] Gao Y, Robertson GP, Kim DS, Guiver MD, Mikhailenko SD, Li X, Kaliaguine S. Comparison of PEM properties of copoly(aryl ether ether nitrile)s containing sulfonic acid bonded to naphthalene in structurally different ways. Macromolecules 2007;40:1512–20.
[91] Detallante V, Langevin D, Chappey C, Metayer M, Mercier R, Pineri M. Kinetics of water vapor sorption in sulfonated polyimide membranes. Desalination 2002;148:333–9.
[92] Genies C, Mercier R, Sillion B, Cornet N, Gebel G, Pineri M. Soluble sulfonated naphthalenic polyimides as materials for proton exchange membranes. Polymer 2001;42:359–73.
[93] Genies C, Mercier R, Sillion B, Petiaud R, Cornet N, Gebel G, Pineri M. Stability study of sulfonated phthalic and naphthalenic polyimide structures in aqueous medium. Polymer 2001;42: 5097–105.
[94] Fang J, Guo X, Harada S, Watari T, Tanaka K, Kita H, Okamoto KI. Novel sulfonated polyimides as polyelectrolytes for fuel cell application. 1. Synthesis, proton conductivity, and water stability of polyimides from 4,4′-diaminodiphenyl ether-2,2′-disulfonic acid. Macromolecules 2002;35:9022–8.
[95] Guo X, Fang J, Watari T, Tanaka K, Kita H, Okamoto KI. Novel sulfonated polyimides as polyelectrolytes for fuel cell application. 2. Synthesis and proton conductivity of polyimides from 9,9-bis(4-aminophenyl)fluorene-2,7-disulfonic acid. Macromolecules 2002;35:6707–13.
[96] Yin Y, Fang J, Watari T, Tanaka K, Kita H, Okamoto KI. Synthesis and properties of highly sulfonated proton conducting polyimides from bis(3-sulfopropoxy)benzidine diamines. J Mater Chem 2004;14:1062–70.
[97] Yin Y, Fanga J, Cui Y, Tanaka K, Kita H, Okamoto KI. Synthesis, proton conductivity and methanol permeability of a novel sulfonated polyimide from 3-(2′,4′-diaminophenoxy)propane sulfonic acid. Polymer 2003;44:4509–18.
[98] Asano N, Aoki M, Suzuki S, Miyatake K, Uchida H, Watanabe M. Aliphatic/aromatic polyimide ionomers as a proton conductive membrane for fuel cell applications. J Am Chem Soc 2006;128:1762–9.
[99] Einsla BR, Hong YT, Kim YS, Wang F, Gunduz N, McGrath JE. Sulfonated naphthalene dianhydride based polyimide copolymers for proton-exchange-membrane fuel cells. I. Monomer and copolymer synthesis. J Polym Sci Part A Polym Chem 2004;42:862–74.
[100] Einsla BR, Kim YS, Hickner MA, Hong Y-T, Hill ML, Pivovar BS, McGrath JE. Sulfonated naphthalene dianhydride based polyimide copolymers for proton-exchange-membrane fuel cells. II. Membrane properties and fuel cell performance. J Membr Sci 2005;255:141–8.
[101] Li N, Cui Z, Zhang S, Li S. Synthesis and properties of novel polyimides from sulfonated binaphthalene dianhydride for proton exchange membranes. J Polym Sci Part A Polym Chem 2008;46:2820–32.
[102] Sumner MJ, Harrison WL, Weyers RM, Kim YS, McGrath JE, Riffle JS, Brink A, Brink MH. Novel proton conducting sulfonated poly(arylene ether) copolymers containing aromatic nitriles. J Membr Sci 2004;239:199–211.
[103] Kim YS, Sumner MJ, Harrison WL, Riffle JS, McGrath JE, Pivovar BS. Direct methanol fuel cell performance of disulfonated poly(arylene ether benzonitrile) copolymers. J Electrochem Soc 2004;151:A2150–6.
[104] Xing P, Robertson GP, Guiver MD, Mikhailenko SD, Kaliaguine S. Sulfonated poly(aryl ether ketone)s containing the hexafluoroisopropylidene diphenyl moiety prepared by direct copolymerization as proton exchange membranes for fuel cell application. Macromolecules 2004;37:7960–7.
[105] Xing P, Robertson GP, Guiver MD, Mikhailenko SD, Kaliaguine S. Synthesis and characterization of poly(aryl ether ketone) copolymers containing (hexafluoroisopropylidene)-diphenol moiety as proton exchange membrane materials. Polymer 2005;46:3257–63.
[106] Kim YS, Kim DS, Liu B, Guiver MD, Pivovar BS. Copoly(arylene ether nitrile)s–high-performance polymer electrolytes for direct methanol fuel cells. J Electrochem Soc 2008;155:B21–6.
[107] Kim DS, Kim YS, Guiver MD, Pivovar BS. High performance nitrile copolymers for polymer electrolyte membrane fuel cells. J Membr Sci 2008;321:199–208.
[108] Kim DS, Robertson GP, Kim YS, Guiver MD. Copoly(arylene ether)s containing pendant sulfonic acid groups as proton exchange membranes. Macromolecules 2009;42:957–63.
[109] Lee CH, Lee SY, Lee YM, McGrath JE. Chemically tuned anode with tailored aqueous hydrocarbon binder for direct methanol fuel cells. Langmuir 2009;25:8217–25.
[110] Zhang Y, Litt M, Savinell RF, Wainright JS. Molecular design considerations in the synthesis of high conductivity PEMs for fuel cells. Polym Prepr Am Chem Soc Div Polym Chem 1999;40(2):480–1.
[111] Zhang Y, Litt M, Savinell RF, Wainright JS, Vendramini J. Molecular design of polyimides toward high proton conducting materials. Polym Prepr Am Chem Soc Div Polym Chem 2000;41(2):1561–2.
[112] Miyatake K, Zhou H, Uchida H, Watanabe M. Highly proton conductive polyimide electrolytes containing fluorenyl groups. Chem Commun 2003;2003:368–9.
[113] Miyatake K, Chikashige Y, Watanabe M. Novel sulfonated poly(arylene ether): a proton conductive polymer electrolyte designed for fuel cells. Macromolecules 2003;36:9691–3.
[114] Chikashige Y, Chikyu Y, Miyatake K, Watanabe M. Poly(arylene ether) Ionomers containing sulfofluorenyl groups for fuel cell applications. Macromolecules 2005;38:7121–6.
[115] Miyatake K, Chikashige Y, Higuchi E, Watanabe M. Tuned polymer electrolyte membranes based on aromatic polyethers for fuel cell applications. J Am Chem Soc 2007;129:3879–87.
[116] Bae B, Miyatake K, Watanabe M. Synthesis and properties of sulfonated block copolymers having fluorenyl groups for fuel-cell applications. ACS Appl Mater Interfaces 2009;1: 1279–86.
[117] Bae B, Yoda T, Miyatake K, Uchida H, Watanabe M. Proton-conductive aromatic ionomers containing highly sulfonated blocks for high-temperature-operable fuel cells. Angew Chem Int Ed 2009;49:317–20.
[118] Bae B, Miyatake K, Watanabe M. Sulfonated poly(arylene ether sulfone ketone) multiblock copolymers with highly sulfonated block. Synthesis and properties. Macromolecules 2010;43:2684–91.
[119] Ghassemi H, Ndip G, McGrath JE. New multiblock copolymers of sulfonated poly(4′-phenyl-2,5-benzophenone) and poly(arylene ether sulfone) for proton exchange membranes. II. Polymer 2004;45:5855–62.
[120] Roy A, Hickner MA, Yu X, Li Y, Glass TE, McGrath JE. Influence of chemical composition and sequence length on the transport properties of proton exchange membranes. J Polym Sci Part B Polym Phys 2006;44:2226–39.
[121] Lee H-S, Roy A, Lane O, Dunn S, McGrath JE. Hydrophilic–hydrophobic multiblock copolymers based on poly(arylene ether sulfone) via low-temperature coupling reactions for proton exchange membrane fuel cells. Polymer 2008;49:715–23.
[122] Badami AS, Lane O, Lee HS, Roy A, McGrath JE. Fundamental investigations of the effect of the linkage group on the behavior of hydrophilic–hydrophobic poly(arylene ether sulfone) multiblock copolymers for proton exchange membrane fuel cells. J Membr Sci 2009;333:1–11.
[123] Lee HS, Lane O, McGrath JE. Development of multiblock copolymers with novel hydroquinone-based hydrophilic blocks for proton exchange membrane (PEM) applications. J Power Sources 2010;195:1772–8.
[124] Einsla ML, Kim YS, Hawley M, Lee HS, McGrath JE, Liu B, Guiver MD, Pivovar BS. Toward improved conductivity of sulfonated aromatic proton exchange membranes at low relative humidity. Chem Mater 2008;20:5636–42.
[125] Nakabayashi K, Matsumoto K, Ueda M. Synthesis and properties of sulfonated multiblock copoly(ether sulfone)s by a chain extender. J Polym Sci Part A Polym Chem 2008;46:3947–57.

[126] Nakabayashi K, Matsumoto K, Higashihara T, Ueda M. Influence of adjusted hydrophilic–hydrophobic lengths in sulfonated multiblock copoly(ether sulfone) membranes for fuel cell application. J Polym Sci Part A Polym Chem 2008;46:7332–41.

[127] Kim DS, Kim YS, Guiver MD, Ding J, Pivovar BS. Highly fluorinated comb-shaped copolymer as proton exchange membranes (PEMs): fuel cell performance. J Power Sources 2008;182:100–5.

[128] Kim DS, Robertson GP, Guiver MD. Comb-shaped poly(arylene ether sulfone)s as proton exchange membranes. Macromolecules 2008;41:2126–34.

[129] Matsumoto K, Higashihara T, Ueda M. Star-shaped sulfonated block copoly(ether ketone)s as proton exchange membranes. Macromolecules 2008;41:7560–5.

[130] Lee CH, Park CH, Lee YM. Sulfonated polyimide membranes grafted with sulfoalkylated side chains for proton exchange membrane fuel cell (PEMFC) applications. J Membr Sci 2008;313:199–206.

[131] Schuster M, De Araujo CC, Atanasov V, Andersen HT, Kreuer KD, Maier J. Highly sulfonated poly(phenylene sulfone): preparation and stability issues. Macromolecules 2009;42:3129–37.

[132] De Araujo CC, Kreuer KD, Schuster M, Portale G, Mendil-Jakani H, Gebel G, Maier J. Poly(p-phenylene sulfone)s with high ion exchange capacity: ionomers with unique microstructural and transport features. Phys Chem Chem Phys 2009;11:3305–12.

[133] Nakabayashi K, Higashihara T, Ueda M. Highly sulfonated multiblock copoly(ether sulfone)s for fuel cell membranes. J Polym Sci Part A Polym Chem 2010;48:2757–64.

[134] Nakabayashi K, Higashihara T, Ueda M. Polymer electrolyte membranes based on cross-linked highly sulfonated multiblock copoly(ether sulfone)s. Macromolecules 2010;43:5756–61.

[135] Nakagawa T, Nakabayashi K, Higashihara T, Ueda M. A high performance polymer electrolyte membrane based on sulfonated poly(ether sulfone) with binaphthyl units. J Mater Chem 2010;20:6662–7.

[136] Matsumura S, Hlil AR, Lepiller C, Gaudet J, Guay D, Hay AS. Ionomers for proton exchange membrane fuel cells with sulfonic acid groups on the end groups: novel linear aromatic poly(sulfide-ketone)s. Macromolecules 2008;41:277–80.

[137] Matsumura S, Hlil AR, Lepiller C, Gaudet J, Guay D, Zhiqing S, Holdcroft S, Hay AS. Ionomers for proton exchange membrane fuel cells with sulfonic acid groups on the end groups: novel branched poly(ether-ketone)s. Macromolecules 2008;41:281–4.

[138] Matsumura S, Hlil AR, Du N, Lepiller C, Gaudet J, Guay D, Shi Z, Holdcroft S, Hay AS. Ionomers for proton exchange membrane fuel cells with sulfonic acid groups on the end-groups: novel branched poly(ether-ketone)s with 3,6-ditrityl-9h-carbazole end-groups. J Polym Sci Part A Polym Chem 2008;46:3860–8.

[139] Matsumura S, Hlil AR, Hay AS. Synthesis, properties, and sulfonation of novel dendritic multiblock copoly(ether-sulfone). J Polym Sci Part A Polym Chem 2008;46:6365–75.

[140] Matsumura S, Hlil AR, Al-Souz MAK, Gaudet J, Guay D, Hay AS. Ionomers for proton exchange membrane fuel cells by sulfonation of novel dendritic multiblock copoly(ether-sulfone)s. J Polym Sci Part A Polym Chem 2009;47:5461–73.

[141] Tian S, Meng Y, Hay AS. Membranes from poly(aryl ether)-based ionomers containing randomly distributed nanoclusters of 6 or 12 sulfonic acid groups. Macromolecules 2009;42:1153–60.

[142] Tian S, Meng Y, Hay AS. Membranes from poly(aryl ether)-based Ionomers containing multiblock segments of randomly distributed nanoclusters of 18 sulfonic acid groups. J Polym Sci Part A Polym Chem 2009;47:4762–73.

[143] Matsumoto K, Higashihara T, Ueda M. Locally and densely sulfonated poly(ether sulfone)s as proton exchange membrane. Macromolecules 2009;42:1161–6.

[144] Matsumoto K, Higashihara T, Ueda M. Locally sulfonated poly(ether sulfone)s with highly sulfonated units as proton exchange membrane. J Polym Sci Part A Polym Chem 2009;47:3444–53.

[145] Li N, Shin DW, Hwang DS, Lee YM, Guiver MD. Polymer electrolyte membranes derived from new sulfone monomers with pendent sulfonic acid groups. Macromolecules 2010;43:9810–20.

[146] Kim YS, Pivovar BS. Moving beyond mass-based parameters for conductivity analysis of sulfonated polymers. Annu Rev Chem Biomol Eng 2010;1:123–48.

[147] Kim DS, Guiver M, McGrath J, Pivovar B, Kim YS. Molecular design aspect of sulfonated polymers for direct methanol fuel cells. ECS Trans 2010;33:711–7.

[148] Tsang EMW, Zhang Z, Shi Z, Soboleva T, Holdcroft S. Considerations of macromolecular structure in the design of proton conducting polymer membranes: graft versus diblock polyelectrolytes. J Am Chem Soc 2007;129:15106–7.

[149] Bouzek K, Moravcova S, Samec Z, Schauer J. $H^+$ and $Na^+$ ion transport properties of sulfonated poly(2,6-dimethyl-1,4-phenyleneoxide) membranes. J Electrochem Soc 2003;150:E329–36.

[150] Hasiotis C, Deimede V, Kontoyannis C. New polymer electrolytes based on blends of sulfonated polysulfones with polybenzimidazole. Electrochim Acta 2001;46:2401–6.

[151] Kerres J, Ullrich A, Meier F, Häring T. Synthesis and characterization of novel acid–base polymer blends for application in membrane fuel cells. Solid State Ionics 1999;125:243–9.

[152] Kosmala B, Schauer J. Ion-exchange membranes prepared by blending sulfonated poly(2,6-dimethyl-1,4-phenylene oxide) with polybenzimidazole. J Appl Polym Sci 2002;85:1118–27.

[153] Kreuer KD. Handbook of fuel cell-fundamental technology and applications. Chichester, UK: John Wiley & Sons Ltd.; 2003.

[154] Hong YT, Lee CH, Park HS, Min KA, Kim HJ, Nam SY, Lee YM. Improvement of electrochemical performances of sulfonated poly(arylene ether sulfone) via incorporation of sulfonated poly(arylene ether benzimidazole). J Power Sources 2008;175:724–31.

[155] Allcock HR, Fitzpatrick RJ, Salvati L. Sulfonation of (aryloxy)- and (arylamino)phosphazenes: small-molecule compounds, polymers, and surfaces. Chem Mater 1991;3:1120–32.

[156] Mikhailenko SD, Wang K, Kaliaguine S, Xing P, Robertson GP, Guiver MD. Proton conducting membranes based on cross-linked sulfonated poly(ether ether ketone) (SPEEK). J Membr Sci 2004;233:93–9.

[157] Paul M, Roy A, Riffle J, McGrath JEE. Crosslinked sulfonated poly(arylene ether sulfone) membranes as candidate for PEMs. ECS Trans 2008;6:9–16.

[158] Paul M, Park HB, Freeman BD, Roy A, McGrath JE, Riffle JS. Synthesis and crosslinking of partially disulfonated poly(arylene ether sulfone) random copolymers as candidates for chlorine resistant reverse osmosis membranes. Polymer 2008;49:2243–52.

[159] Sastri SB, Keller TM. Phthalonitrile cure reaction with aromatic diamines. J Polym Sci Part A Polym Chem 1998;36:1885–90.

[160] Sastri SBA, Armistead JP, Keller TM, Sorathia U. Phthalonitrile-glass fabric composites. Polym Compos 1997;18:48.

[161] Lee CH, Park HB, Chung YS, Lee YM, Freeman BD. Water sorption, proton conduction, and methanol permeation properties of sulfonated polyimide membranes cross-linked with N,N-bis(2-hydroxyethyl)-2-aminoethanesulfonic acid (BES). Macromolecules 2005;39:755–64.

[162] Rhim JW, Park HB, Lee CS, Jun JH, Kim DS, Lee YM. Crosslinked poly(vinyl alcohol) membranes containing sulfonic acid group: proton and methanol transport through membranes. J Membr Sci 2004;238:143–51.

[163] Telfah A, Majer G, Kreuer KD, Schuster M, Maier J. Formation and mobility of protonic charge carriers in methyl sulfonic acid–water mixtures: a model for sulfonic acid based ionomers at low degree of hydration. Solid State Ionics 2010;181:461–5.

[164] Park HB, Lee CH, Sohn JY, Lee YM, Freeman BD, Kim HJ. Effect of crosslinked chain length in sulfonated polyimide membranes on water sorption, proton conduction, and methanol permeation properties. J Membr Sci 2006;285:432–43.

[165] Phu DS, Lee CH, Park CH, Lee SY, Lee YM. Synthesis of crosslinked sulfonated poly(phenylene sulfide sulfone nitrile) for direct methanol fuel cell applications. Macromol Rapid Commun 2009;30:64–8.

[166] Di Vona ML, Sgreccia E, Licoccia S, Alberti G, Tortet L, Knauth P. Analysis of temperature-promoted and solvent-assisted cross-linking in sulfonated poly(ether ether ketone) (SPEEK) proton-conducting membranes. J Phys Chem B 2009;113:7505–12.

[167] Di Vona ML, Sgreccia E, Tamilvanan M, Khadhraoui M, Chassigneux C, Knauth P. High ionic exchange capacity polyphenylsulfone (SPPSU) and polyethersulfone (SPES) cross-linked by annealing treatment: thermal stability, hydration level and mechanical properties. J Membr Sci 2010;354:134–41.

[168] Jeong MH, Lee KS, Lee JS. Cross-linking density effect of fluorinated aromatic polyethers on transport properties. Macromolecules 2009;42:1652–8.

[169] Lee KS, Jeong MH, Lee JP, Lee JS. End-group cross-linked poly(arylene ether) for proton exchange membranes. Macromolecules 2009;42:584–90.

[170] Assink RA, Arnold Jr C, Hollandsworth RP. Preparation of oxidatively stable cation-exchange membranes by the elimination of tertiary hydrogens. J Membr Sci 1991;56:143–51.

[171] Bernardi DM, Verbrugge MW. A mathematical model of the solid-polymer-electrolyte fuel cell. J Electrochem Soc 1992;139:2477–91.

[172] Li Y, Roy A, Badami AS, Hill M, Yang J, Dunn S, McGrath JE. Synthesis and characterization of partially fluorinated hydrophobic–hydrophilic multiblock copolymers containing sulfonate groups for proton exchange membrane. J Power Sources 2007;172:30–8.

[173] Yamaguchi T, Zhou H, Nakazawa S, Hara N. An extremely low methanol crossover and highly durable aromatic pore-filling electrolyte membrane for direct methanol fuel cells. Adv Mater 2007;19:592–6.

[174] Borup R, Meyers J, Pivovar B, Kim YS, Mukundan R, Garland N, Myers D, Wilson M, Garzon F, Wood D, Zelenay P, More K, Stroh K, Zawodzinski T, Boncella J, McGrath JE, Inaba M, Miyatake K, Hori M, Ota K, Ogumi Z, Miyata S, Nishikata A, Siroma Z, Uchimoto Y, Yasuda K, Kimijima KI, Iwashita N. Scientific aspects of polymer electrolyte fuel cell durability and degradation. Chem Rev 2007;107:3904–51.

[175] Jung HY, Cho KY, Sung KA, Kim WK, Park JK. The effect of sulfonated poly(ether ether ketone) as an electrode binder for direct methanol fuel cell (DMFC). J Power Sources 2006;163:56–9.

[176] Lee JK, Li W, Manthiram A. Sulfonated poly(ether ether ketone) as an ionomer for direct methanol fuel cell electrodes. J Power Sources 2008;180:56–62.

[177] Sankir M, Kim YS, Pivovar BS, McGrath JE. Proton exchange membrane for DMFC and $H_2$/air fuel cells: synthesis and characterization of partially fluorinated disulfonated poly(arylene ether benzonitrile) copolymers. J Membr Sci 2007;299:8–18.

[178] Wiles KB, de Diego CM, de Abajo J, McGrath JE. Directly copolymerized partially fluorinated disulfonated poly(arylene ether sulfone) random copolymers for PEM fuel cell systems: synthesis, fabrication and characterization of membranes and membrane–electrode assemblies for fuel cell applications. J Membr Sci 2007;294:22–9.

[179] Nieh MP, Guiver MD, Kim DS, Ding J, Norsten T. Morphology of comb-shaped proton exchange membrane copolymers based on a neutron scattering study. Macromolecules 2008;41:6176–82.

[180] Anand M, Hobbs JP, Brass IJ. Organofluorine chemistry: principles and applications. New York: Plenum Press; 1994.

[181] Hobbs JP, Anand M, Campion BA. Fluorinated high-density polyethylene barrier containers. ACS Symp Ser 1990;423:280–94.

[182] Mohr JM, Paul DR, Pinnau I, Koros WJ. Surface fluorination of polysulfone asymmetric membranes and films. J Membr Sci 1991;56:77–98.

[183] Lee CH, Lee SY, Lee YM, Lee SY, Rhim JW, Lane O, McGrath JE. Surface-fluorinated proton-exchange membrane with high electrochemical durability for direct methanol fuel cells. ACS Appl Mater Interfaces 2009;1:1113–21.

[184] Kim DS, Cho HI, Kim DH, Lee BS, Lee BS, Yoon SW, Kim YS, Moon GY, Byun H, Rhim JW. Surface fluorinated poly(vinyl alcohol)/poly(styrene sulfonic acid-co-maleic acid) membrane for polymer electrolyte membrane fuel cells. J Membr Sci 2009;342:138–44.

[185] Barsamyan G, Sokolov VB. Fluoropolymers. I. Synthesis. New York: Plenum Press; 1999.

[186] Lee CH, Lee KS, Lee SY, Lane O, Zhang M, Moore RB, Madsen LA, Wi SS, McGrath JE, Lee YM. Morphological transformation in solid state via post-fluorination. Angew Chem Int Ed, submitted for publication.

[187] Ismail AF, Lorna W. Suppression of plasticization in polysulfone membranes for gas separations by heat-treatment technique. Sep Purif Technol 2003;30:37–46.

[188] Park HB, Shin HS, Lee YM, Rhim JW. Annealing effect of sulfonated polysulfone ionomer membranes on proton conductivity and methanol transport. J Membr Sci 2005;247:103–10.

[189] Guo R, Lane O, VanHouten D, Lee CH, McGrath JE. Synthesis and characterization of phenolphthalein-based poly(arylene ether sulfone) hydrophilic–hydrophobic multiblock copolymers for proton exchange membranes. Ind Eng Chem Res 2010;49:12125–34.

[190] Chen Y, Guo R, Lee CH, Lee MB, McGrath JE. Partly fluorinated poly(arylene ether ketone sulfone) hydrophilic–hydrophobic multiblock copolymers for fuel cell membranes. Int J Hydrogen Energy, submitted for publication.

[191] Lee M, Park JK, Lee HS, Lane O, Moore RB, McGrath JE, Baird DG. Effects of block length and solution-casting conditions on the final morphology and properties of disulfonated poly(arylene ether sulfone) multiblock copolymer films for proton exchange membranes. Polymer 2009;50:6129–38.

[192] Chen SL, Xu KQ, Dong P. Preparation of three-dimensionally ordered inorganic/organic bi-continuous composite proton conducting membranes. Chem Mater 2005;17:5880–3.

[193] Lee CH, Park HB, Park CH, Lee SY, Kim JY, McGrath JE, Lee YM. Preparation of high-performance polymer electrolyte nanocomposites through nanoscale silica particle dispersion. J Power Sources 2010;195:1325–32.

[194] Li H, Nogami M. Pore-controlled proton conducting silica films. Adv Mater 2002;14:912–4.

[195] McKeen JC, Yan YS, Davis ME. Proton conductivity in sulfonic acid-functionalized zeolite beta: effect of hydroxyl group. Chem Mater 2008;20:3791–3.

[196] Chalkova E, Pague MB, Fedkin MV, Wesolowski DJ, Lvov SN. Nafion/$TiO_2$ proton conductive composite membranes for PEMFCs operating at elevated temperature and reduced relative humidity. J Electrochem Soc 2005;152:A1035–40.

[197] Chalkova E, Fedkin MV, Wesolowski DJ, Lvov SN. Effect of $TiO_2$ surface properties on performance of Nafion-based composite membranes in high temperature and low relative humidity PEM fuel cells. J Electrochem Soc 2005;152:A1742–7.

[198] Di Noto V, Gliubizzi R, Negro E, Vittadello M, Pace G. Hybrid inorganic–organic proton conducting membranes based on Nafion and 5 wt.% of MxOy (M = Ti, Zr, Hf, Ta and W). Part I. Synthesis properties and vibrational studies. Electrochim Acta 2007;53:1618–27.

[199] Di Noto V, Piga M, Lavina S, Negro E, Yoshida K, Ito R, Furukawa T. Structure properties and proton conductivity of Nafion/$[(TiO_2)(WO_3)_{0.148}]_{\psi TiO2}$ nanocomposite membranes. Electrochim Acta 2010;55:1431–44.

[200] Staiti P, Aricò A, Baglio V, Lufrano F, Passalacqua E, Antonucci V. Hybrid Nafion-silica membranes doped with heteropolyacids for application in direct methanol fuel cells. Solid State Ionics 2001;145:101–7.

[201] Kim YS, Wang F, Hickner M, Zawodzinski TA, McGrath JE. Fabrication and characterization of heteropolyacid ($H_3PW_{12}O_{40}$)/directly polymerized sulfonated poly(arylene ether sulfone) copolymer composite membranes for higher temperature fuel cell applications. J Membr Sci 2003;212:263–82.

[202] Ponce ML, Prado L, Ruffmann B, Richau K, Mohr R, Nunes SP. Reduction of methanol permeability in polyetherketone-heteropolyacid membranes. J Membr Sci 2003;217:5–15.

[203] Vernon DR, Meng F, Dec SF, Williamson DL, Turner JA, Herring AM. Synthesis, characterization, and conductivity measurements of hybrid membranes containing a mono-lacunary heteropolyacid for PEM fuel cell applications. J Power Sources 2005;139:141–51.

[204] Kannan R, Kakade B, Pillai V. Polymer electrolyte fuel cells using Nafion-based composite membranes with functionalized carbon nanotubes. Angew Chem Int Ed 2008;47:2653–6.

[205] Alberti G, Boccali L, Casciola M, Massinelli L, Montoneri E. Protonic conductivity of layered zirconium phosphonates containing $-SO_3H$ groups. III. Preparation and characterization of [gamma]-zirconium sulfoaryl phosphonates. Solid State Ionics 1996;84:97–104.

[206] Alberti G, Casciola M. Layered metalIV phosphonates, a large class of inorgano-organic proton conductors. Solid State Ionics 1997;97:177–86.

[207] Alberti G, Casciola M, Costantino U, Peraio A, Montoneri E. Protonic conductivity of layered zirconium phosphonates containing $-SO_3H$ groups. I. Preparation and characterization of a mixed zirconium phosphonate of composition $Zr(O_3PR)_{0.73}(O_3PR')_{1.27}\cdot nH_2O$, with $R = -C_6H_4-SO_3H$ and $R' = -CH_2-OH$. Solid State Ionics 1992;50:315–22.

[208] Grot WG, Rajendran G. Membranes containing inorganic fillers and membrane and electrode assemblies and electrochemical cells employing same. US 5,919,583; 1999.

[209] Kirpichnikova L, Polomska M, Wolak J, Hilczer B. Polarized light study of the $CsHSO_4$ and $CsDSO_4$ superprotonic crystals. Solid State Ionics 1997;97:135–9.

[210] Mikhailenko SD, Zaidi SMJ, Kaliaguine S. Sulfonated polyether ether ketone based composite polymer electrolyte membranes. Catal Today 2001;67:225–36.

[211] Nogami M, Miyamura K, Abe Y. Fast protonic conductors of water-containing $P_2O_5-ZrO_2-SiO_2$ glasses. J Electrochem Soc 1997;144:2175–8.

[212] Pawowski A, Pawlaczyk C, Hilczer B. Electric conductivity in crystal group $Me_3H(SeO_4)_2$ (Me: $NH^{4+}$, $Rb^+$, $Cs^+$). Solid State Ionics 1990;44:17–9.

[213] Stein EW, Clearfield A, Subramanian MA. Conductivity of group IV metal sulfophosphonates and a new class of interstratified metal amine-sulfophosphonates. Solid State Ionics 1996;83:113–24.

[214] Zaidi SMJ, Mikhailenko SD, Robertson GP, Guiver MD, Kaliaguine S. Proton conducting composite membranes from polyether ether ketone and heteropolyacids for fuel cell applications. J Membr Sci 2000;173:17–34.

[215] Day TJF, Schmitt UW, Voth GA. The mechanism of hydrated proton transport in water. J Am Chem Soc 2000;122:12027–8.

[216] Lee CH, Xie W, VanHouten D, McGrath JE, Freeman BD, Spano J, Wi SS, Park CH, Lee YM. Nanodispersed hydrophilic silica additives for disulfonated poly(arylene ether sulfone) random copolymer membranes. J Membr Sci, submitted for publication.

[217] Binks PB, Lumsdon OS. Stability of oil-in-water emulsions stabilised by silica particles. Phys Chem Chem Phys 1999;1:3007–16.

[218] Kosmulski K. Chemical properties of material surfaces. New York: Mercel Dekker; 2001.

[219] Koros WJ. Evolving beyond the thermal age of separation processes: membranes can lead the way. AlChE J 2004;50:2326–34.

[220] Zou H, Wu S, Shen J. Polymer/silica nanocomposites: preparation characterization. Properties and applications. Chem Rev 2008;108:3893–957.

[221] Watanabe M, Uchida H, Seki Y, Emori M, Stonehart P. Self-humidifying polymer electrolyte membranes for fuel cells. J Electrochem Soc 1996;143:3847–52.

[222] Aricò A. Influence of the acid–base characteristics of inorganic fillers on the high temperature performance of composite membranes in direct methanol fuel cells. Solid State Ionics 2003;161:251–65.

[223] Adjemian KT, Dominey RD, Krishnan L, Ota H, Majsztrik P, Zhang T, Mann J, Kirby B, Gatto L, Velo-Simpson M, Leahy J, Srinivasan S, Benziger J, Bocarsly AB. Function and charaterization of metal oxide-Nafion composite membranes for elevated-temperature $H_2/O_2$ PEM fuel cells. Chem Mater 2006;18:2238–48.

[224] Stonehart P, Watanabe M. Polymer solid-electrolyte composition and electrochemical cell using the composition. US 5,523,181; 1996.

[225] Kim JY, Mulmi S, Lee CH, Lee YM, Ihn KJ. Synthesis of microphase-separated poly(styrene-co-sodium styrene sulfonate) membranes using amphiphilic urethane acrylate nonionomers as an reactive compatibilizer. J Appl Polym Sci 2008;107:2150–8.

[226] Lee CH, Hwang SY, Sohn JY, Park HB, Kim JY, Lee YM. Water-stable crosslinked sulfonated polyimide-silica nanocomposite containing interpenetrating polymer network. J Power Sources 2006;163:339–48.

[227] Lee CH, Min KA, Park HB, Hong YT, Jung BO, Lee YM. Sulfonated poly(arylene ether sulfone)-silica nanocomposite membrane for direct methanol fuel cell (DMFC). J Membr Sci 2007;303:258–66.

[228] Alexandridis P, Alan Hatton T. Poly(ethylene oxide)–poly(propylene oxide)–poly(ethylene oxide) block copolymer surfactants in aqueous solutions and at interfaces: thermodynamics structure dynamics and modeling. Colloids Surf A 1995;96:1–46.

[229] Mata JP, Majhi PR, Guo C, Liu HZ, Bahadur P. Concentration temperature and salt-induced micellization of a triblock copolymer Pluronic L64 in aqueous media. J Colloid Interface Sci 2005;292: 548–56.

[230] Yang L, Alexandridis P, Steytler DC, Kositza MJ, Holzwarth JF. Small-angle neutron scattering investigation of the temperature-dependent aggregation behavior of the block copolymer Pluronic L64 in aqueous solution. Langmuir 2000;16:8555–61.

[231] Lee CH, VanHouten D, Lane O, McGrath JE, Hou J, Madsen LA, Spano J, Wi S, Cook J, Xie W, Oh HJ, Geise GM, Freeman BD. Disulfonated poly(arylene ether sulfone) random copolymer blends tuned for rapid water permeation via cation complexation with poly(ethylene glycol) oligomers. Chem Mater 2011;23:1039–49.

[232] Wang C, Chalkova E, Lute CD, Fedkin MV, Komarneni S, Chung TCM, Lvov SN. Proton conductive inorganic materials for temperatures up to 120 °C and relative humidity down to 5%. J Electrochem Soc 2010;157:B1634–42.

[233] Di Noto V, Boaretto N, Negro E, Pace G. New inorganic–organic proton conducting membranes based on Nafion and hydrophobic fluoroalkylated silica nanoparticles. J Power Sources 2010;195:7734–42.

[234] Mulmi S, Park CH, Kim HK, Lee CH, Park HB, Lee YM. Surfactant-assisted polymer electrolyte nanocomposite membranes for fuel cells. J Membr Sci 2009;344:288–96.

[235] Kim JY, Mulmi S, Lee CH, Park HB, Chung YS, Lee YM. Preparation of organic–inorganic nanocomposite membrane using a reactive polymeric dispersant and compatibilizer: proton and methanol transport with respect to nano-phase separated structure. J Membr Sci 2006;283:172–81.

[236] Gummaraju RV, Moore RB, Mauritz KA. Asymmetric [Nafion®]/[silicon oxide] hybrid membranes via the in situ sol–gel reaction for tetraethoxysilane. J Polym Sci Part B Polym Phys 1996;34:2383–92.

[237] Mauritz KA. Organic–inorganic hybrid materials: perfluorinated ionomers as sol–gel polymerization templates for inorganic alkoxides. Mater Sci Eng C 1998;6:121–33.

[238] Tripathi BP, Shahi VK. SPEEK–zirconium hydrogen phosphate composite membranes with low methanol permeability prepared by electro-migration and in situ precipitation. J Colloid Interface Sci 2007;316:612–21.

[239] Jones DJ, Rozière J. Recent advances in the functionalisation of polybenzimidazole and polyetherketone for fuel cell applications. J Membr Sci 2001;185:41–58.

[240] Zoppi RA, Yoshida IVP, Nunes SP. Hybrids of perfluorosulfonic acid ionomer and silicon oxide by sol–gel reaction from solution: morphology and thermal analysis. Polymer 1998;39:1309–15.

[241] Aparicio M, Castro Y, Duran A. Synthesis and characterisation of proton conducting styrene-co-methacrylate-silica sol–gel membranes containing tungstophosphoric acid. Solid State Ionics 2005;176:333–40.

[242] Silva VS, Ruffmann B, Silva H, Gallego YA, Mendes A, Madeira LM, Nunes SP. Proton electrolyte membrane properties and direct methanol fuel cell performance. I. Characterization of hybrid sulfonated poly(ether ether ketone)/zirconium oxide membranes. J Power Sources 2005;140:34–40.

[243] Cornelius CJ, Marand E. Hybrid inorganic-organic materials based on a 6FDA-6FpDA-DABA polyimide and silica: physical characterization studies. Polymer 2002;43:2385–400.

[244] Chang HY, Lin CW. Proton conducting membranes based on $PEG/SiO_2$ nanocomposites for direct methanol fuel cells. J Membr Sci 2003;218:295–306.

[245] Yamaguchi T, Ibe M, Nair BN, Nakao S-i. A pore-filling electrolyte membrane-electrode integrated system for a direct methanol fuel cell application. J Electrochem Soc 2002;149:A1448–53.

[246] Yamaguchi T, Miyata F, Nakao S. Polymer electrolyte membranes with a pore-filling structure for a direct methanol fuel cell. Adv Mater 2003;15:1198–201.

[247] Yamaguchi T, Miyata F, Nakao S-i. Pore-filling type polymer electrolyte membranes for a direct methanol fuel cell. J Membr Sci 2003;214:283–92.

[248] Nishimura H, Yamaguchi T. Performance of a pore-filling electrolyte membrane in hydrogen–oxygen PEFC. Electrochem Solid State Lett 2004;7:A385–8.

[249] Yamaguchi T, Kuroki H, Miyata F. DMFC performances using a pore-filling polymer electrolyte membrane for portable usages. Electrochem Commun 2005;7:730–4.

[250] Choi SW, Fu YZ, Ahn YR, Jo SM, Manthiram A. Nafion-impregnated electrospun polyvinylidene fluoride composite membranes for direct methanol fuel cells. J Power Sources 2008;180:167–71.

[251] Takemori R, Kawakami H. Electrospun nanofibrous blend membranes for fuel cell electrolytes. J Power Sources 2010;195:5957–61.

[252] Slade S, Campbell SA, Ralph TR, Walsh FC. Ionic conductivity of an extruded Nafion 1100 EW series of membranes. J Electrochem Soc 2002;149:A1556–64.